Enhancement of Properties of Carbon-Fiber-Reinforced TGDDM/DDS Epoxy Composites Containing Nanoclay

Yuan Xu

A Thesis

in

The Department

of

Mechanical and Industrial Engineering

Presented in Partial Fulfillment of the Requirements

for the Degree of Master of Applied Science(Mechanical Engineering) at

Concordia University

Montreal, Quebec, Canada

September 2006

Your file Votre référence
ISBN: 978-0-494-20767-3
Our file Notre référence
ISBN: 978-0-494-20767-3

ABSTRACT

Enhancement of Properties of Carbon-Fiber-Reinforced TGDDM/DDS Epoxy Composites Containing Nanoclay

Yuan Xu

This thesis was based on the research on the nanocomposites fabricated from TGDDM/DDS epoxy system, carbon fiber reinforcement, and montmorillonite nanoclay modifier. The viscosity and gel time of nanoclay-filled composites with different nanoclay contents were measured. The influence of nanoclay on curing process was investigated by DSC testing.

High quality carbon fiber-reinforced nanocomposites were manufactured through lay-up plus autoclave process. The nanocomposites had uniform fiber volume fraction, fewer dry spots, and fewer resin-rich areas. The plain-strain fracture toughness of nanoclay-filled epoxy composite was measured by single-edge-notch bending testing. The testing results indicated that both the critical-stress-intensity and the critical strain energy release rate were dramatically augmented owing to the introduction of nanoclay. The interlaminar fracture toughness of carbon fiber-reinforced composites was evidently increased with the introduction of nanoclay. The fracture surface of nanoclay-filled samples exhibited relatively rougher feature, compared to the featureless fracture surface of pristine epoxy system. Small amount of nanoclay (2 phr) can significantly enhance the flexural strength and modulus of the composites.

The fire resistance of epoxy composites was enhanced due to the addition of nanoclay via the limiting oxygen index experiment and TGA testing. An evident augmentation of thermal shock resistance was obtained with the addition of nanoclay.

Acknowledgements

I am very grateful to my supervisor, Dr. Suong Van Hoa, for his continuous support in my M.A.Sc program. Dr. Hoa was always there to listen and to offer advice; he enlightened me how to handle research problems and find solutions. Without his constant guidance and encouragement, I could not have finished this thesis. Dr. Hoa has been making CONCOM a wonderful place for all the members working there. In the creative atmosphere of CONCOM, everybody's academic skill has been significantly strengthened.

Special thanks are due to Dr. Ming Xie, who has been helping me with his expertise and experience. My colleagues and friends, Weiping Liu, Lixin Wu, Heng Wang, Khassan Mourtazov, Mourat Mourtazov, and Hasan Salek definitely deserve thanks for their indispensable help, interesting discussions and being fun to be with.

Thanks are due to machine shop supervisor, Brian Cooper for his passionate help with respect to tool making. Thank also goes to Éric Duchesne from L'École Polytechnique de Montréal for the help in SEM test.

I can never sufficiently thank my parents, for giving me life and endless love; my sister, Lan, and my wife, Cherry, for unconditional support and encouragement.

Table of Contents

List of Figures

List of Tables

Chapter 1 Introduction

Over the past few decades, composite materials have been extensively applied to the areas of aerospace, aircraft, sports and military industries. Advanced composite materials have progressed from a laboratory curiosity to a production reality. Composites have demonstrated weight savings for aircraft structures and outstanding corrosion and fatigue-damage resistance. Commercial aircraft applications have ranged from small flight-control surfaces to primary structures [1]. In the automobile industry, composite components are being used. A sports car Carrera GT with first-ever all-carbon chassis has been produced by Porsche AG [2].

However, people have reached the limits of optimizing composite properties made of traditional micrometer-scale fillers, because the properties achieved usually involve compromises. Stiffness is traded for toughness, or toughness is obtained at the cost of optical clarity. In addition, macroscopic defects due to regions of high or low volume fraction of filler often lead to breakdown or failure.

Nanomaterials (NMs) and nanocomposites (NCs) have become one of the most exciting and fashionable research fields. NCs are materials that comprise a dispersion of nanometer-size particles in a matrix. In this work, the matrix material is a polymeric material. Correspondently, the abbreviation of polymeric nanocomposite is given as PNC. It seems that anything with 'nano' attached to it has nearly a magic effect [3]. As a member of NCs family, clay-containing polymeric nanocomposite (CPNC) offers several

advantages over the matrix polymer or classical composites. The main improvements are in: modulus, impact strength, heat resistance, dimensional stability, barrier properties, flame retardance, optical properties, ion conductivity, thermal stability, etc [3]. In the research depicted in reference [4], plain-strain fracture toughness epoxy matrix NC was dramatically enhanced by adding nanoclay.

Carbon fiber is widely used in composite field as it possesses many excellent characteristics. In fact, carbon fiber reinforced epoxy matrix composite has been applied in aircraft and automobile industries.

As mentioned above, epoxy, carbon fiber, and nanoclay all possess specific characteristics respectively, which are significant in composites. It is reasonable to predict that a combination of these three basic constituents should form a specific nanocomposite. We can take advantage of those characteristics and develop novel processes to manufacture functional and reliable advanced nanocomposites.

1.1 Selection and Determination of Research Objectives

In principle, composites can be constructed of any combination of two or more materials, whether metallic, organic, or inorganic. Major constituent forms used in composite materials are fibers, particles, laminae, layers, flakes, fillers and matrices. The matrix is the body constituent, serving to enclose the composite and give it its bulk form. The fibers, particles, laminae, layers, flakes, fillers are the structural constituents.

To manufacture composites, the first step should be selecting the objects, ie

determining the appropriate matrices, curing agents, reinforcements, and fillers. In this project, our focus is epoxy-based system.

1.1.1 Matrix Material and Curing Agent

Epoxy resins have been commercially available for about 60 years and today have many major industrial applications. Epoxies are the most common matrix material for high-performance composites and adhesives. They have an excellent combination of strength, adhesion, low shrinkage and processing versatility [5]. One of the most commonly used formulations of high-temperature-cure systems is tetraglycidyl 4, 4'-diaminodiphenylmethane (TGDDM) that contains four functionalities providing highly cross-linked structures that exhibit high strength, rigidity and elevated temperature resistance. Epoxy is one of the most widely used matrices for carbon-fiber-reinforced composite materials by virtue of its good impregnation and adhesion to carbon fiber. Typical epoxy resins, among the various epoxy resins, are cured at 66°C, 121°C, and 177°C. The cure temperature of an epoxy determines the use temperature of final composites. Thus, epoxy systems with higher cure temperatures are necessary for the development of epoxy-based composites with higher service temperatures and better mechanical properties. The development of 177°C-cured epoxy system can provide composite materials for primary structural applications in aircraft [6].

In order to convert epoxy resin into hard, infusible thermoset networks, it is necessary to use curing agents. 4,4'-diaminodiphenylsulfone (DDS) has principle advantage over other aromatic amines in providing the highest heat resistance. It has become the standard

curing agent in some high temperature tooling, high performance military and aerospace laminating applications [7].

Tetraglycidyl 4, 4'-diaminodiphenylmethane (TGDDM), cured with 4,4'-diaminodiphenylsulfone (DDS), shows a high glass transition temperature due to the presence of polar sulfone groups that favor hydrogen bonding and the regular packing of the polymer chains. Furthermore, the tetrafunctionality of TGDDM leads to a high density crosslinked network on curing, giving a very tough polymer. These characteristics have promoted the use of the TGDDM/DDS system as a binder for high-performance light-weight composites.

1.1.2 Fiber

Compared to glass fiber and aramid fiber, carbon fiber is the most prevalent fiber form in high-performance composite structure. It generally exhibits superior tensile strength, possesses high modulus, excellent fatigue characteristic and does not corrode. The ideal engineering materials should have high strength, high stiffness, high toughness and low weight.

Carbon fibers combined with polymer matrices meet these criteria more closely than any other materials. Carbon fibers are elastic to failure at normal temperature, creep resistant, strong, chemically inert, except in strong oxidizing environments or in contact with certain molten metals, and have excellent damping characteristics. Some disadvantages of carbon fibers are: they are brittle and have low impact resistance; they have low strains to failure; their compressive strengths are less than their tensile strengths;

and they are relatively expensive compared to glass fiber [5]. Normally, carbon fibers are provided in untwisted bundles of filaments called "tows.' As the tow size decreases, the strength and cost increases. For aerospace applications, normal tow sizes are 3k, 6k and 12k. 3k and 6k are most prevalent for woven cloth; 12k is prevalent for unidirectional stitched cloth. Reinforcing carbon fibers can be supplied in dry unimpregnated forms or as prepregs ready for lay-up.

1.1.3 Clays

In the last decade, many researchers have attempted to improve the properties of epoxy composites via adding nanoclay [8]. Clays are composed of extremely fine crystals, usually plate-shaped, less than 2 μm in diameter and less than 10 nm thick. They are mostly phyllosilicates and other elements, having at least one small dimension and large aspect ratio and specific surface areas [3].

Layered nanoparticles can be exfoliated into a dispersion of individual platelets. In industry, the mineral and synthetic clays are in a dominant position. The preferred layered material is montmorillonite (MMT), which is a high aspect ratio material. The aim of using MMT is to exfoliate the platelets, but frequently doublets and tactoids may be present. MMT is abundant and inexpensive, but its main drawback is that it is a mineral with variable composition, which is impossible to totally purify.

The essential nanoclay raw material is montmorillonite, a 2:1 layered smectite clay mineral with a plate structure, meaning that it has 2 tetrahedral sheets sandwiching a central octahedral sheet. Individual platelet thicknesses are just one nanometer, but

surface dimensions are generally 300 to more than 600 nanometers, resulting in an unusually high aspect ratio. The specific surface area of montmorillonite is 750-800 m^2/g (theoretical value is 834 m^2/g). Montmorillonite is a very soft phyllosilicate mineral that typically forms in microscopic crystals, forming a clay. The particles are plate-shaped with an average diameter of approximately 1 micrometer. The particle thickness is extremely small (~ 1 nm). Montmorillonite (MMT) is the most common phyllosilicate used for the production of clay-containing nanocomposites and the member of the smectite clay family. Montmorillonite is generally referred to as "nanoclay". It is also the most common material used in polymer nanocomposites.

Naturally occurring montmorillonite is hydrophilic. Since polymers are generally organophilic, unmodified nanoclay disperses in polymers with great difficulty. Through clay surface modification, montmorillonite can be made organophilic and, therefore, compatible with conventional organic polymers. Surface compatibilization is also known as "intercalation". Compatibilized nanoclays disperse readily in polymers.

Nanomer® I.30E nanoclay is a surface modified montmorillonite mineral which can be dispersed down to a combination of both exfoliated and intercalated clays in epoxy resin systems. The dispersion creates a near-molecular blend commonly known as a nanocomposite. This new type of composite exhibits enhanced strength, thermal and barrier properties. I.30E is supplied as a white fine powder.

1.2 Determination of Research Methods and Technical Processes

The primary objective of our project is combining epoxy, carbon fiber, and nanoclay to manufacture advanced nanocomposites, and then testing the various properties of the composites. Therefore, mixing up nanoclay and epoxy to obtain well-dispersed systems becomes the first issue that should be taken into account. The second step should be combining epoxy systems bearing nanoclay with carbon fiber and making laminates. How to test the laminates to get our final composites is the last step. Simply, this project is principally composed of nanoclay dispersion, carbon fiber impregnation, and laminate testing. The test items include fundamental characteristics test (viscosity, gel time, degree of cure etc), mechanical properties test, thermal properties test, and flammability test.

1.2.1 Dispersion of Nanoclay

A uniform dispersion of nanoclay particles into epoxy system is the prerequisite to make nanocomposite. Some of dispersion methods include *in situ* polymerization, mechanical stirring, ultrasonic mixing, three-roll mill machine etc.

In this project, a patented method called High-pressure Mixing Method (HPMM) was used to guarantee well-dispersed system [9,10]. The process will be summarized in Chapters 3 and 4.

1.2.2 Laminates Manufacturing and Testing

Commonly, carbon fiber/epoxy prepreg is commercially used in aircraft and auto industries. In this project, there is no specific commercial prepreg available. Therefore, we have to find a reliable and feasible method to bond epoxy/clay system with carbon fiber. Considering our labs facilities, wet hand lay-up was chosen as the main method to

bond epoxy with carbon fiber.

To manufacture composite, there are many processes available, such as filament wilding, pultrusion, RTM, VARTM, autoclave etc. Due to the high viscosity of the TGDDM epoxy systems, RTM and VARTM processes are definitely not practical to this research. Thus, hot melt lay-up plus autoclave process, as a primary method, was chosen to manufacture composite laminates. Besides, solution lay-up and Resin Film Infusion (RFI) were also attempted for comparison.

1.3 Prospective Achievements

Based on previous research results [4], the properties of fiber-reinforced nanocomposite are possibly improved by adding nanoclay after being treated through appropriate processes. Particularly, plain strain fracture toughness, interlaminar fracture toughness, and thermal stability are predicted to improve. In the meantime, fire resistance of nanocomposite is predicted to increase. In addition, corresponding technological parameters can be determined for specific systems.

1.4 Potential Challenges

Owing to the high viscosity of TGDDM epoxy at room temperature, potential challenges do exist. Main challenges are listed as follows:

- ✧ Dispersion of nanoclay into epoxy
- ✧ Epoxy-nanoclay system degassing
- ✧ Wetting of carbon fiber sheet with epoxy-nanoclay system

- ✧ Requirement of hand lay-up skills
- ✧ Determination of technological parameters (curing cycle, lay-up temperature etc)

1.5 Main Frame of Thesis

The main structure of this thesis is illustrated in Figure 1.1.

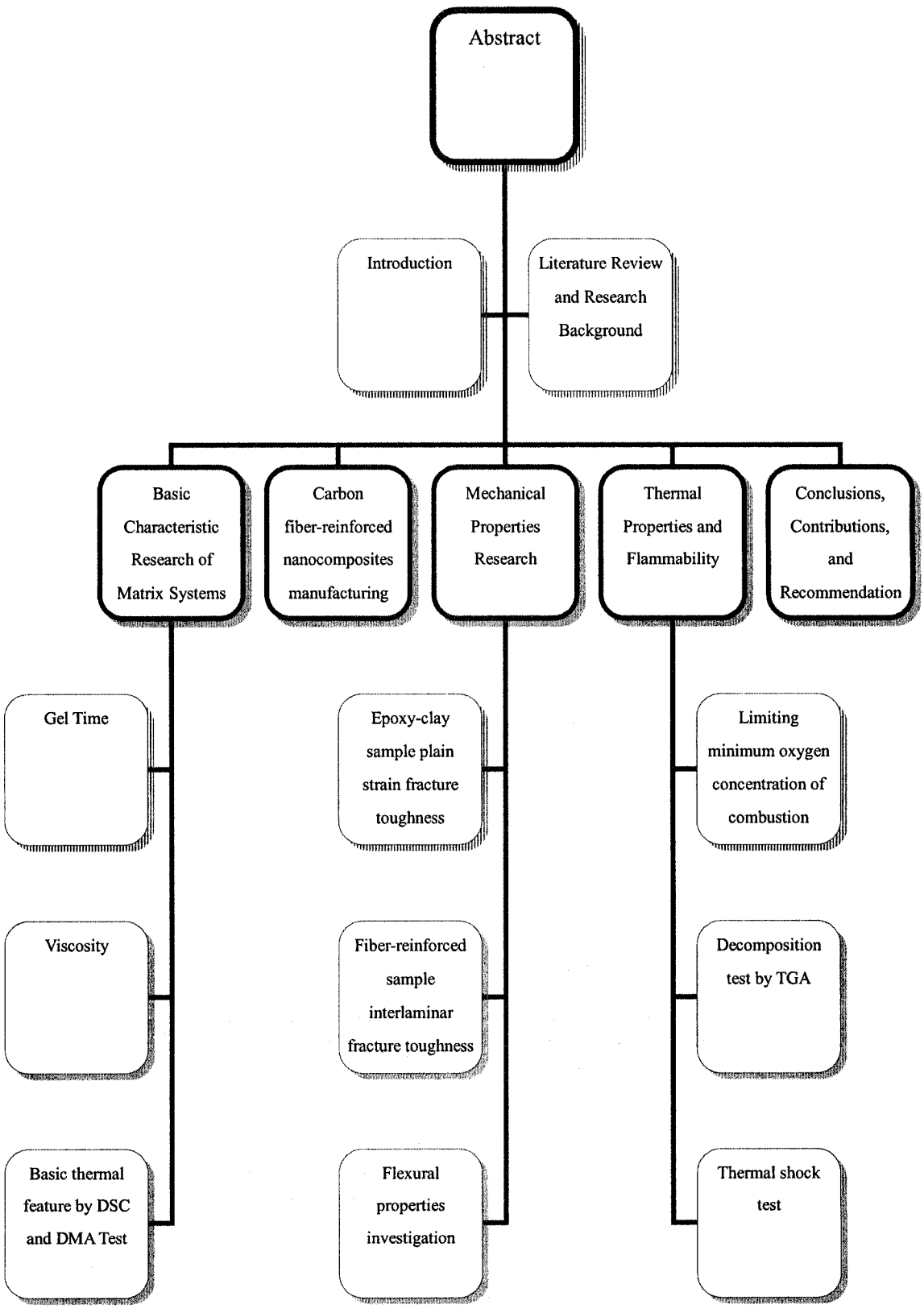

Figure 1. 1. Main Structure of Thesis

Chapter 2 Literature Review and Research Background

Nanomaterials can be defined as those whose characteristic length scale lies within the nanometric range, i.e. in the range between one and several hundreds of nanometers. Within this length scale, the properties of matter are sufficiently different from individual atoms or molecules and from bulk materials, that their study has been recognized as Nanoscience and Nanotechnology.

Among all the potential nanocomposite precursors, those based on clay and layered silicates have been more widely investigated probably because the starting clay materials are easily available and because their interaction chemistry has been studied for a long time. Owing to the nanometer-size particles obtained by dispersion, these nanocomposites exhibit markedly improved mechanical, thermal, optical and physico-chemical properties when compared with pure polymer and conventional (microscale) composites [11].

Montmorillonite (MMT) clay is one of the most widely used nanoclay for nanocomposites synthesis owing to its superior nano-dispersible character. In most research work, the MMT clay is organo-modified clay.

This chapter aims at presenting some very recent developments in sytheses, properties and future applications of nanoclay-filled composites.

2.1 Synthesis of Nanoclay Composites

Montmorillonite, hectorite and saponite are the most commonly used layered silicates. Their chemical formulae are shown in Table 2.1and their structure is given in Figure 2.1.

Table 2. 1. Chemical Formulae of Commonly Used 2:1 Phyllosilicates[a] [11]

2:1 Phyllosilicate	General formula
Montmorillonite	$M_x(Al_{4-x}Mg_x)Si_8O_{20}(OH)_4$
Hectorite	$M_x(Mg_{6-x}Li_x)Si_8O_{20}(OH)_4$
Saponite	$M_xMg_6(Si_{8-x}Al_x)O_{20}(OH)_4$

[a] M=monovalent cation; x=degree of isomorphous substitution (between 0.5 and 1.3).

The montmorillonite (MMT) clay used in nanocomposites belongs to the structure family known as the 2:1 phyllosilicate (Figure 2.1). Their crystal lattice consists of two-dimensional layers where a central octahedral sheet of alumina or magnesia is fused to two external silica tetrahedron by the tip so that the oxygen ions of the octahedral sheet do also belong to the tetrahedral sheets. The layer thickness is around 1 nm and the lateral dimensions of these layers may vary from 300 Å to several microns and even larger depending on the particular silicate.

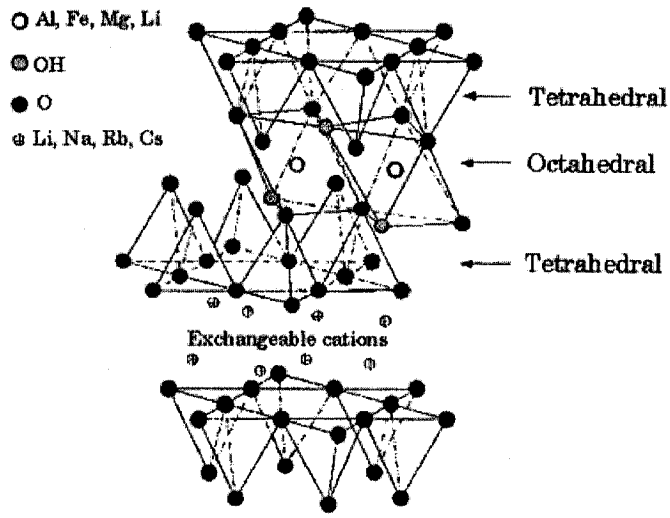

Figure 2. 1. Structure of 2:1 Phyllosilicates [11].

This type of clay is characterized by a moderate negative surface charge. The charge of the layer is not locally constant as it varies from layer to layer and must rather be considered as an average value over the whole crystal. Proportionally, even if a small part of the charge balancing cations is located on the external crystallite surface, the majority of these exchangeable cations are located inside the galleries. When the hydrated cations are ion-exchanged with organic cations such as alkyammoniums, it usually results in a larger interlayer spacing.

Depending on the nature of the components used and the method of preparation, three main types of composites may be obtained when layered clay is associated with a polymer (Figure 2.2). When the polymer is unable to intercalate between the silicate sheets, a phase separated composite is obtained, whose properties stay in the same range as traditional microcomposites. Beyond this classical family of composites, two other types of nanocomposites can be obtained. Intercalated structure in which extended

polymer chains are intercalated between the silicate layers resulting in a well ordered multilayer morphology built up with alternating polymeric and inorganic layers. When the silicate layers are completely and uniformly dispersed in a continuous polymer matrix, an exfoliated structure is obtained (Figures 2.2 and 2.3).

Polymers filled with montmorillonite (MMT) have attracted significant interest in the past decade. A large number of significant works in this field has been done. Usually, to disperse nanoclay into polymers is the first main step of nanocomposites syntheses. Depending on the physical state of the polymer, some different processing methods are used, such as *in situ* polymerization, high shear mixing, three-roll milling, and twin screw extrusion [12]. Mohan et al [13] investigated rheology and curing characteristics

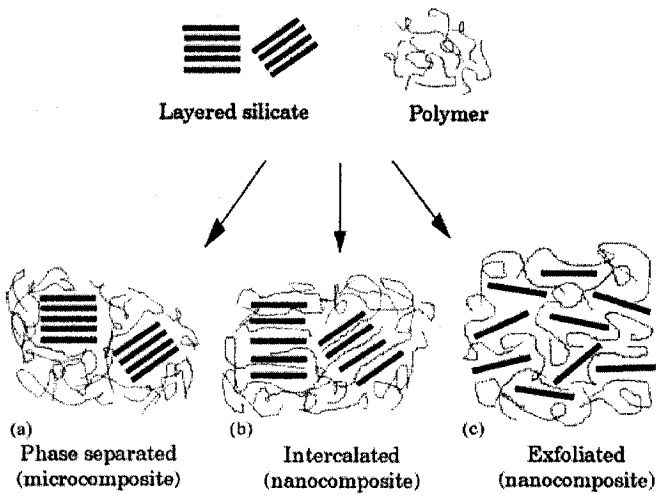

Figure 2. 2. Scheme of Different Types of Composite Arising from the Interaction of Layered Silicates and Polymers [11].

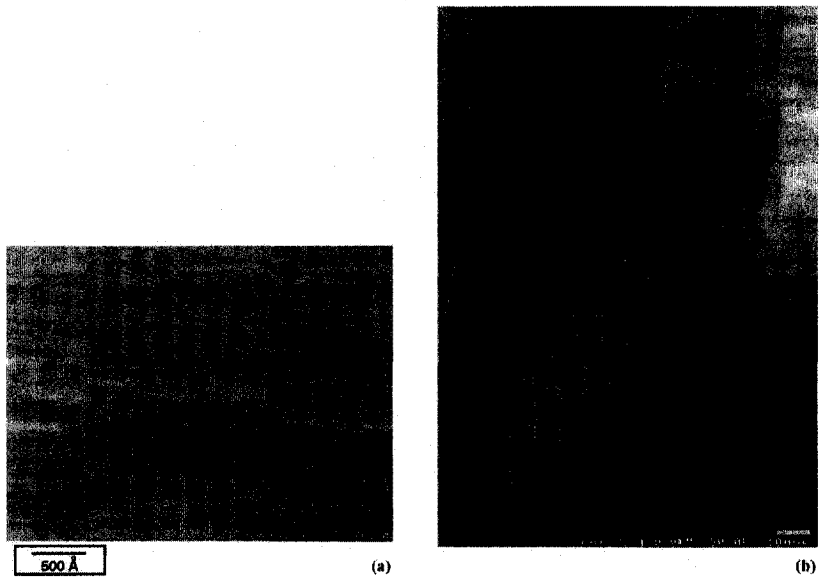

Figure 2. 3. TEM Micrographs of Polystyrene-based Naocomposites: (a) Intercalated Nanocomposite, (b) Exfoliated Nanocomposite [11].

of epoxy-clay nanocomposites. They mixed MMT into diglycidyl ether of bisphenol-A (DGEBA) epoxy resin by mechanical shear. Their results show that the epoxy has penetrated into the gallery region and form the intercalated structure with increase in the clay interlayer. From the literatures [12,14–18], mechanical stirring and sonication processes are used to obtain well-dispersed nanoclay composites. Some of them obtained intercalated structure; the others obtained exfoliated or intercalated /exfoliated mixture structure. A "slurry-compounding" approach has been developed for epoxy/nanoclay composites synthesis by Wang et al [19]. In this process, MMT was first exfoliated and suspended in water; this suspension was further treated with acetone to form a clay-acetone slurry followed by chemical modification using silane. The modified slurry was then mixed extensively with epoxy to form an epoxy/nanoclay composite exhibiting

a high degree of clay exfoliation.

More interestingly, a novel dispersion method for nanoclay into epoxy has been developed by Hoa et al at Concordia University Composites Center (CONCOM) [4,9,20]. An MMT/acetone suspension was treated under extremely high pressure (100 ~ 138 MPa) to form a cream-like nanoclay paste. The paste was then mixed with epoxy by mechanical stirring followed by vacuum degassing. Relevant tests have proved that this method is an effective way to get well-dispersed epoxy/nanoclay system.

2.2 Property Improvement of Nanoclay Composites

The introduction of nanoclay particles increases the mechanical (tensile strength and modulus), physical (permeability and barrier resistance), and thermal (decomposition and mass loss) properties of the polymer composites [13]. The following sections will give a few examples of the investigation in nanocomposite field. For fiber-reinforced composites, the addition of nanoclay also produced evident improvement in the properties of composites.

Advanced carbon fiber-reinforced composites manufacturing processes have been comprehensively introduced in references [21-32]. Depending on different raw materials, new processes are used for composite manufacturing [33–38].

2.2.1 Mechanical Properties Improvement

In Mohan et al's research [13], tensile modulus was significantly increased from 1.10 GPa to 3.59 GPa at 3 wt% nanoclay; tensile strength was increased from 61.1 MPa to

66.3 MPa. Zhou et al's work [17] indicates that tensile modulus and strength improved 80% and 64% respectively with 5wt% MMT nanoclay. Ratna et al's work [39] shows that impact strength of nanocomposite was increased from 0.7 kJ m^{-1} to 1.1 kJ m^{-1} with a clay content of 5%.

In Liu et al's work [9], compressive yield strength of nanocompsoite was slightly increased with a clay content less than 3 phr. However, compressive modulus was increased over 20% at 9 phr nanoclay content. In addition, critical stress intensity factor (K_{Ic}) and critical strain energy release rate (G_{Ic}) were increased by 2.2 and 5.8 times at 4.5 phr nanoclay loading, respectively [8].

Fracture toughness has been one of the most interesting properties to be investigated [40–47]. In reference [48], Mode I interlaminar fracture toughness of carbon-fiber/epoxy composite without clay was tested; the results show that the G_{Ic} values fluctuate between 160 J/m^2 and 240 J/m^2. Chen et al [49] investigated the fracture properties of nanoclay-filled polypropylene; the results indicate that tensile strength and modulus increased steadily with the increase in clay loading. However, the J-integral fracture resistance decreased with an increase in the clay content. However, the influence of nanoclay on the interlaminar fracture toughness was not widely investigated, especially for the TGDDM epoxy.

2.2.2 Flammability and Thermal Properties

In reference [50] and [51], thermal decomposition, combustion and flame-retardancy of

epoxy resins were reviewed in detail. The thermal stability of cured epoxy resins is strongly affected by the curing agent used; the combustion performance of epoxy resins is strongly affected by the crosslinking density; the flame-retardancy of epoxy can be improved by using special epoxy monomers containing highly aromatic bisphenols; phosphorous-containing fire-retardants are particularly effective in epoxy.

Morgan's work indicates that MMT nanoclay has not only the unique advantage of reduced flammability, but also improved mechanical properties [52]. The most important result from this paper is the formation of a clay-reinforced carbonaceous char during combustion of nanocomposites, which lowers Heat Release Rate (HRR). The conclusion of reference [53] indicates that a nano-structure enables to achieve better fire performance than a micro-structure in term of the decrease of HRR and PHRR (Peak of Heat Release Rate). Zhang [54] discovered that the PHRR of nanoclay-filled composites showed 30 ~ 40% reduction, compared to pure polyethylene.

In Timmerman et al's work [55], it was found that nanoclay can be easily used to modify traditional fiber-reinforced composites and enhance their resistance to thermal cycling induced stresses in terms of lower microcrack density.

Chapter 3 Fundamental Characteristics of Matrix Materials Used

In this project, the nanocomposites are composed of epoxy matrix, nanoclay and carbon fiber. Among these components, epoxy is the one that we are mainly concerned about. Therefore, investigation of the basic properties of matrix systems is a prerequisite of our research.

The prime goal of this project is to make fiber-reinforced nanoclay-containing epoxy matrix composites. The work is involved in mixing of epoxy and clay, bonding between epoxy and fiber, curing cycles including temperature, pressure and vacuum degree. Based on what was mentioned above, the primary research in this chapter will focus on viscosity test, gel time test, and curing degree test.

3.1 Materials

3.1.1 Matrix Materials

TGDDM epoxy used in this project is provided by Huntsman Corporation, whose commercial name is Araldite® MY720. Araldite® MY720 is a tetrafunctional epoxy resin suitable for high performance composites applications. It can be cured at 120 -177°C. Araldite® MY720 provides outstanding performance characteristics at elevated temperatures. When post-cured at 200°C, the system exhibits properties in excess of 220°C. The chemical description of Araldite® MY720 is N,N,N',N'-Tetraglycidyl-4,4'-methylenebisbenzenamine. Its chemical structure is shown in Figure 3.1. Typical properties of Araldite® MY720 are shown in Table 3.1.

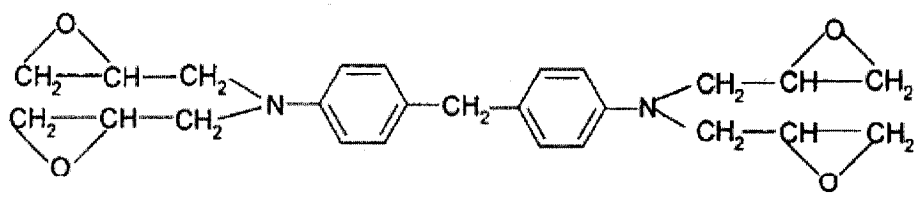

Figure 3. 1. Chemical Structure of Araldite® MY720

Araldite® MY720 possesses many advantages such as, excellent radiation stability, excellent chemical resistance, extraordinary good long-term high temperature performance, high mechanical strength retention, outstanding heat resistance and deflection temperature, and extremely low shrinkage. Araldite® MY720 is mostly applied in high energy radiation resistance components, structural laminating, advanced

composites structures, and high performance structural adhesives.

Table 3. 1. Typical properties of Araldite® MY720 (Vantico Data Sheet)

Visual Appearance	Clear, brown, semi-solid
Epoxy Value, eq/kg	7.5-8.5
Epoxy Equivalent, g/eq	117-134
Viscosity at 50 °C, mPa.s	8000-18000
Density at 25°C, g/cm^3	1.15-1.18
Flash Point, °C	>149

3.1.2 Curing Agent

The curing agent applied in this project is Aradur™ 976-1, which is provided by Vantico Corporation. It belongs to aromatic amine family. Aradur™ 976-1 is also referred to as DDS, which is a high performance hardener used with Araldite® epoxy resins. Its chemical description is 4,4'-Diaminodiphenyl sulfone; its chemical structure is shown in Figure 3.2.

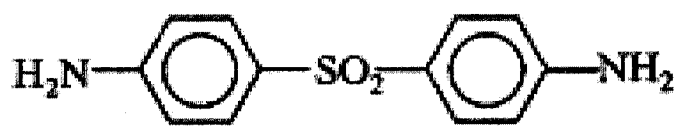

DDS

Figure 3. 2. Chemical Structure of Aradur™ 976-1

The advantages of Aradur™ 976-1 include excellent high temperature properties, outstanding chemical resistance, and excellent stability. It is widely used in high performance coating, advanced composites, high temperature laminates, prepreg manufacturing, printed circuit board laminates, adhesives, and casting applications. The typical properties of Aradur™ 976-1 are shown in Table 3.2.

Table 3. 2. Typical properties of Aradur™ 976-1 (Vantico Data Sheet)

Visual Appearance	White or off-white powder
Assay, %	>99
Melting Point, °C	174-178

3.1.3 Clay

The clay used in this project is from the smectite family. Smectites have a unique morphology, featuring one dimension in the nanometer range. The most common member of the smectite clay family is montmorillonite, which is generally referred to as "nanoclay". It is also the most common material used in polymer nanocomposites. The nanoclay used in this project, Nanomer®I.30E with appearance of white powder, is supplied by Nanocor Inc. Nanomer®I.30E nanoclay is a surface modified montmorillonite mineral which can be dispersed to nanoscale in epoxy resin system.

Table 3.3 shows the properties of Nanocor I.30E.

Table 3. 3. Physical Properties of Nanocor I.30E (Nanocor Data Sheet)

Appearnce	White Powder
Mean Dry Particle Size	8-10 μm
Density	1.71 g/cm^3
Bulk Density	0.41 g/cm^3
Moisture	3%
Mineral Purity	98.5%

3.2 Viscosity Measurement

Viscosity is a measure of the resistance of a fluid to deformation under shear stress. It is commonly perceived as "thickness", or resistance to pouring (see Fig. 3.3). Viscosity describes a fluid's internal resistance to flow and may be thought of as a measure of fluid friction [56].

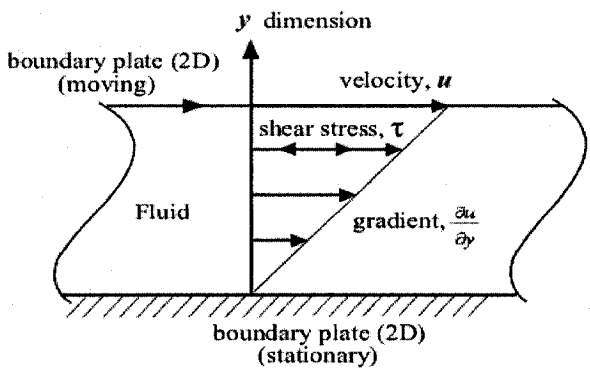

Figure 3. 3. Principle of Viscosity Definition [57]

For the control of the processing of epoxy resin, the information on its rheological properties is absolutely required. Typically, the process requirements depend on viscosity; the lower is the viscosity, the easier it is to process and the better is the wetability of the resin to fiber.

3.2.1 Sample Preparation and Experiment

The samples used for viscosity test were prepared by directly mechanical stirring. Before mixing, nanoclay (I.30E) was dried at 120°C for 2 hours to remove moisture.

Epoxy resin was heated to 120°C ~ 130°C. A desired amount of nanoclay was added to epoxy resin. The epoxy-clay mixture was mechanically stirred at a speed of 1000 RPM at 120°C ~ 130°C for 60 minutes. The mixture was transferred into a vacuum oven for degassing at 130°C for 20 minutes. The degassed system was then cooled down to room temperature for the viscosity test.

Viscosity was measured by Brookfield CAP2000+ Viscometer. The systems tested consist of different nanoclay content of 0, 2, 4, 6, 8, and 10 phr.

The tests were performed by appropriate spindles at 50°C and 75°C respectively. In the course of the tests, thermal equilibrium of the sample and of the spindle must be considered for best measurement results. Upon powering up the viscometer or after changing the temperature set point, sufficient time (>10 minutes) should be allowed for the plate to reach the desired temperature. It is necessary to have the spindle to be in contact with the plate prior to introducing the sample material to ensure that the spindle

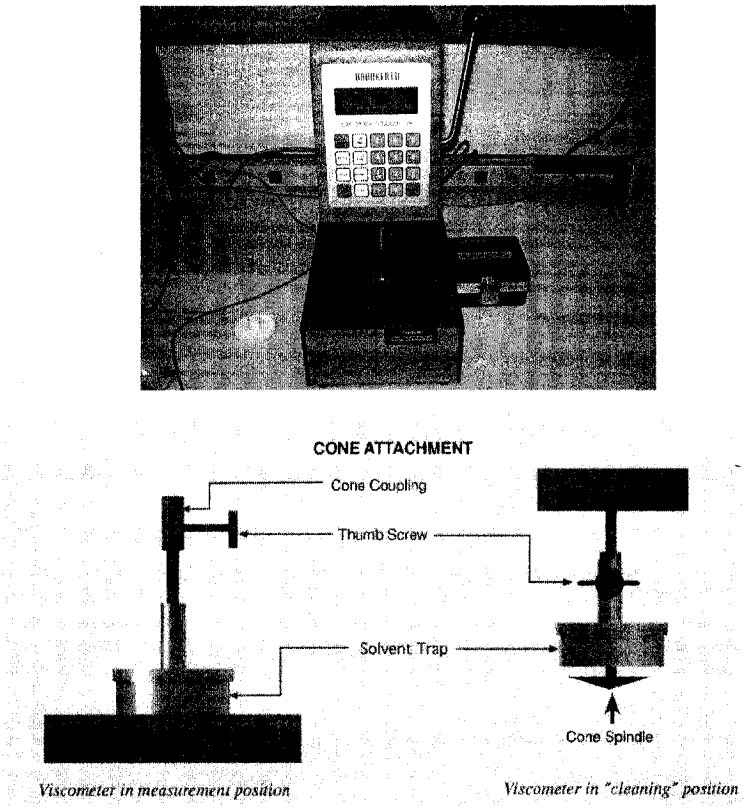

Figure 3. 4. Brookfield CAP2000+ Viscometer and Cone Attachment at CONCOM

is also at the temperature of the test. In addition, a solvent trap was used in order to prevent the test result from being influenced by the environment.

For Brookfield CAP2000+ Viscometer (see Figure 3.4), viscosity is calculated by the following equation.

$$Viscosity(poise) = \frac{FSR \times (\%FSR)}{100}$$

FSR—Full Scale Viscosity Range (provided by the manufacturer)

%FSR—Percentage of FSR (obtained from tests)

Shear rate is calculated by the equation

$$\text{Shear Rate} = \frac{\omega}{\sin\theta}$$

ω = Cone Speed (rad/sec) = $(\frac{2\pi}{60}) \times N$

N = RPM (Rotational Speed)

θ = Cone Angle (degree)

r = Radius of Cone Spindle

3.2.2 Test Results and Discussions

The viscosity of pure resin and resin-clay systems measured at 50°C and 75°C are shown in Figure 3.5 and 3.6 respectively. The test result indicates that the viscosity of the systems decreases when shear rate increases. More importantly, with the increase of nanoclay loading, viscosity of systems changed evidently.

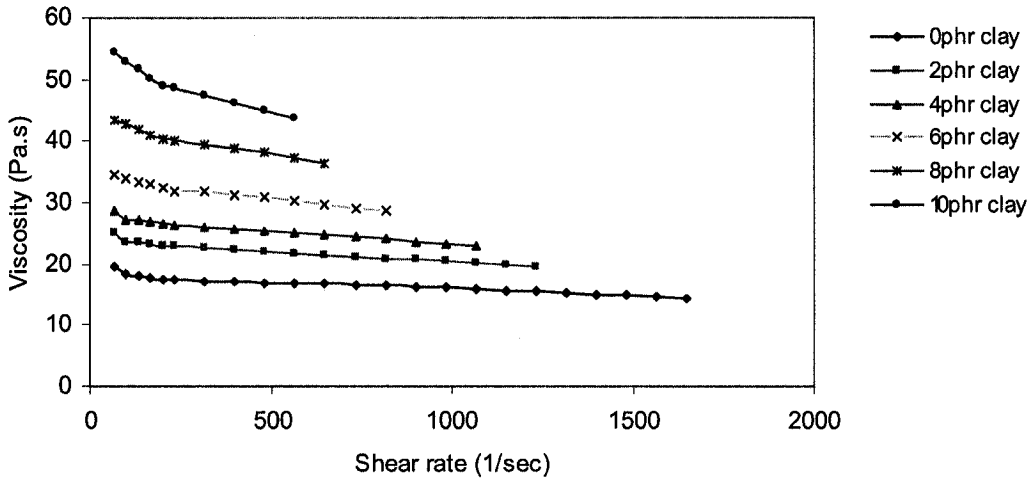

Figure 3. 5. Viscosity with Shear Rate and Nanoclay Content (phr) Measured at 50°C

The viscosity of pure epoxy resin at 50°C was 19.500 Pa·s with shear rate of 66.66 1/sec. With the addition of nanoclay, the viscosity increased continuously. With a clay loading of 2 phr, the viscosity increased to 25.125 Pa·s, which is 29% higher than that of pure resin. When clay loading increased to 10 phr, the viscosity of the system increased up to 54.375 Pa·s, which is 179% higher than that of the pure epoxy resin.

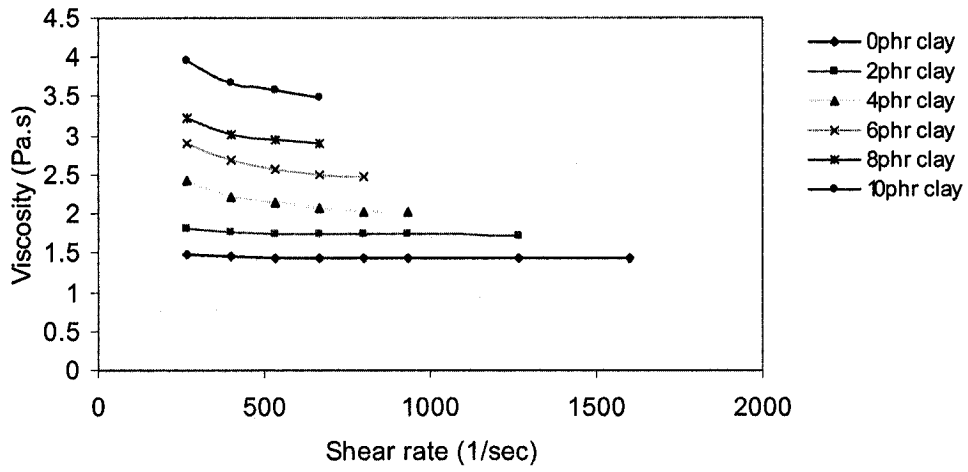

Figure 3. 6 Viscosity with Shear Rate and Nanoclay Content (phr) Measured at 75°C

The viscosity of pure epoxy resin tested at 75°C, at shear rate of 66.66 1/sec, was 1.491 Pa·s. Compared to the number at 50°C, it was only 7.65%. The viscosity drop was quite apparent. This phenomenon indicates that the epoxy resin used is very sensitive to temperature alteration. With a clay loading of 2 phr, the viscosity increased to 1.819 Pa·s, which is 23% more than that of pure resin. Similarly, when clay loading increased to 10 phr, the viscosity increased to 3.947 Pa·s, which is 165% higher than that of pure resin.

Usually, for wet processing of thermosets, typically viscosities of less than 1 Pa·s are preferred [5]. Therefore, the processing temperature of the epoxy used in this project definitely should be higher than 75°C, especially to the systems containing nanoclay.

3.3 Gel Time Test

When a thermosetting resin is curing, the viscosity of the resin changes from low to

very high due to the formation of crosslinks. Eventually, the resin will become a gel-like solid without flowability. The interval of time extending from the introduction of a curing agent into a liquid resin system to its gellation is called "gel time". This data is essential for the composite manufacturing process. In this project, to determine appropriate curing cycles of epoxy and epoxy/nanoclay systems, gel time is an essential characteristic to test.

Gel time test is aimed at determining the time from the initial mixing of the reactants of a thermosetting polymer composition to the time when solidification commences under conditions approximating the conditions of use. Gel time should be obtained in sufficiently precise and reproducible form or application evaluation, quality control, and material characterization of a thermosetting polymer. To obtain most meaningful results, the experimental conditions should approximate as closely as possible the conditions of application of the material.

3.3.1 Sample Preparation and Experiments

The sample preparation before introducing curing agent into the system was very similar to the preparation method of viscosity test. The first step was heating the epoxy/nanoclay mixture to 135°C~140°C accompanied by mechanical stirring. The preheated (at 135°C for 60 minutes) curing agent-DDS was then carefully added to the previous mixture and stirred at a speed of 1000 rpm for 15 minutes. After this, the whole mixture was degassed in vacuum oven for 20 minutes. A measured quantity of the prepared mixture was then poured into a clean test tube for gel time test.

In most cases, the viscosity of thermosetting resin increases slowly at the beginning of the curing reaction. Then, at a certain moment, the viscosity will increase very fast. In practice, there are several testing methods for determining gel time. In this project, Sunshine Gel Meter 22A with Model 2295 Digital Temperature Controller (see Figure 3.7) was selected for this experiment according to ASTM D 3056.

In this test, the gel time of different systems at different temperatures was measured. The principle parts of the Gel Time Meter, constant temperature bath, test tube, rotating spindle, torsion wire, synchronous motor, cooling system, electrical contact pins, time

Figure 3. 7. Sunshine Gel Meter 22A with Model 2295 Digital Temperature Controller at CONCOM

counter and temperature controller are shown in Figure 3.8. To keep a constant high temperature, an oil bath was applied in this experiment.

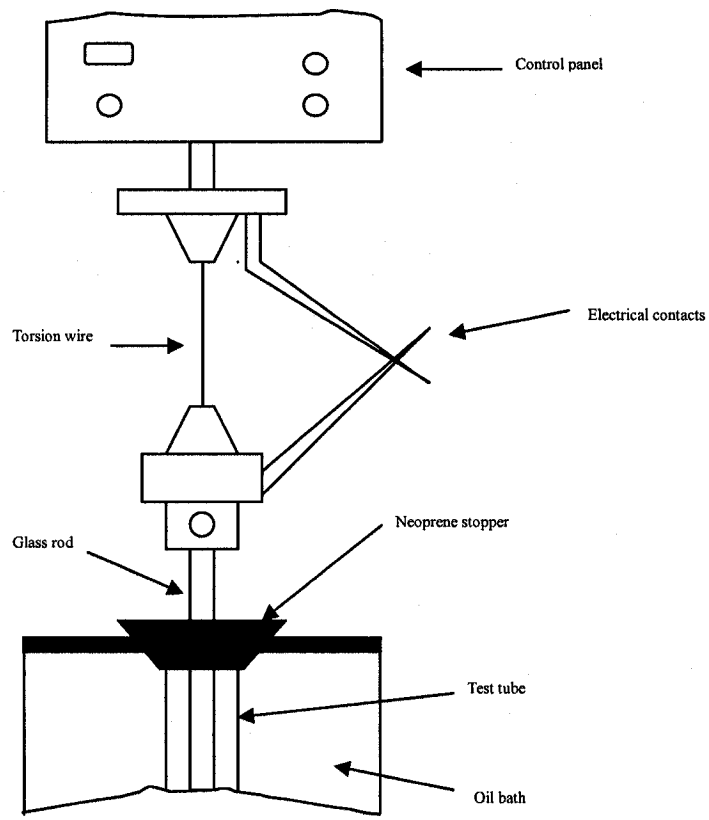

Figure 3. 8. Schematic Diagram of Gel Time Meter

The switch of the test circuit consists of two contacts that are fixed to the opposite ends of the torsional wire spring; the contacts are adjusted to form a 3/32" gap when there is no load. The drive motor rotates counter clockwise, therefore, the upper contact lags behind the lower one. Once the resin gels, the upper contact will touch the lower one. At this moment, the timer stops, and the alarm buzzes. The machine measures the time required for a sudden change in viscosity because of both chemical reaction and filling effect. Due to clay addition can increase viscosity, the gel time measured using this system does not indicate only gel time due to chemical reaction.

Before testing, epoxy, curing agent and nanoclay are mechanically mixed and a certain amount of resin is poured into test tube. In this project, the gel time was tested at 140°C, 160°C and 180°C. The compositions of tested samples are listed in Table 3.4.

Table 3. 4. Compositions of Gel Time Test Samples

Composition	Materials	Ratio (phr)
Resin	Araldite® MY720 (TGDDM)	100
Curing Agent	Aradur™ 976-1 (DDS)	44
Nanoclay	Nanomer® I.30E	0, 2, 4, 6

3.3.2 Results and Discussion

For each experimental condition, three samples were tested to determine the precise gel time. The testing results shown in Figure 3.9 indicate that the gel time decreases when the nanoclay loading increases and when test temperature increases. The gel time of pure resin at 140°C was 120.8 minutes; it became 42.4 minutes at 160°C and 21.3 minutes at 180°C. That means that the gel times decreased by 64.9% and 82.4%. With the addition of nanoclay, the gel time of different systems apparently dropped. In the case at 140°C, gel time is shortened by 9.6%, 22.3%, and 28.2% when clay loading was 2 phr, 4 phr, and 6 phr respectively. From the figure, we can see that the gel time is much more sensitive to the change of temperature. This phenomenon matches the viscosity test results very well. The presence of clay does not affect the cure reaction, but it affects the

viscosity of the tested systems. Higher viscosity will result in earlier stop of the rotating spindle of gel time meter. Thus, gel time can be shortened.

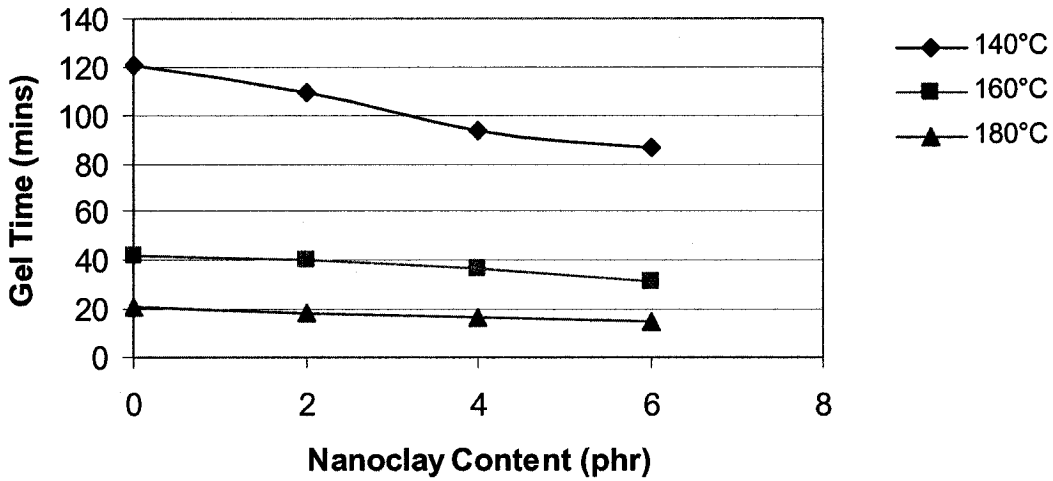

Figure 3. 9. Gel Time vs Nanoclay Content

3.4 Thermal properties

To manufacture nanoclay-containing composites, it is necessary to obtain the information on the fundamental characteristics of curing behavior, curing degree, and some other thermal properties.

A thermal analysis technique, Differential Scanning Calorimetry (DSC) measures the amount of energy (heat) absorbed or released by a sample as it is heated, cooled, or held at a constant temperature. Typical applications include determination of melting point temperature and the heat of melting; measurement of the glass transition temperature; curing and crystallization studies; and identification of phase transformations. It is based

on an enthalpy-change method in which the difference in energy inputs into a substance and that of a reference material is measured as a function of temperature while the substance and the reference material are subjected to a controlled temperature program.

When a sample and an inert reference are heated at a known rate in a controlled environment, the increase in sample and reference temperatures will be the same, unless a heat related change takes place in the sample. If this change takes place, the temperature difference between sample and reference from such a heat change is directly related to the differential heat flow.

The curve obtained from DSC is a record of heat flow. From the DSC profile, it is usually possible, not only to characterize a thermal event as exothermic or endothermic, but also to define the type of transformation involved.

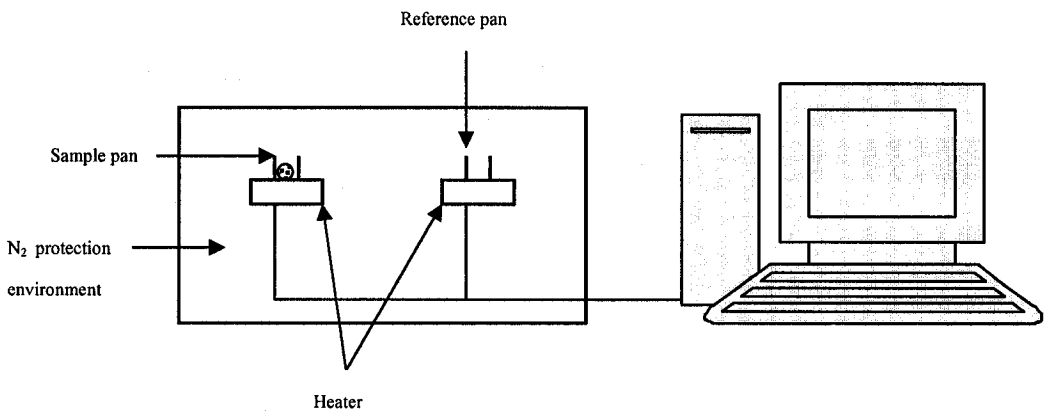

Figure 3. 10. Schematic Diagram of a DSC System

The schematic diagram of DSC system is shown in Figure 3.10. DSC may be applied to study any process involving change in enthalpy; a major general application is to

determine the temperature and enthalpy corresponding to a phase change in the curing process of a thermoset resin.

With appropriate enthalpy and temperature calibration, the area, A (Figure 3.11), enclosed by a DSC peak is directly proportional to the corresponding enthalpy change ΔH, in accordance with the general relationship:

$$A = km\Delta H$$

where

k-calibration constant

m-sample mass.

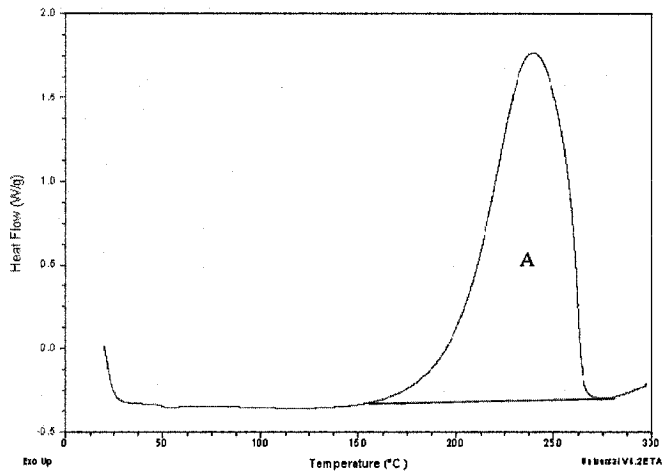

Figure 3. 11. The Area Enclosed by a DSC Peak

3.4.1 Influence of Nanoclay on Cure Process

Nanoclays have effect on the curing of some epoxies, and do not have effect on some

other epoxies. Therefore it is necessary to do DSC tests to verify. The thermal properties of a sample with different compositions were measured by TA Q10 DSC (see Figure 3.12). In order to determine the influence of nanoclay on curing process, TGDDM/nanoclay systems were tested by DSC. Figure 3.13 illustrates the results.

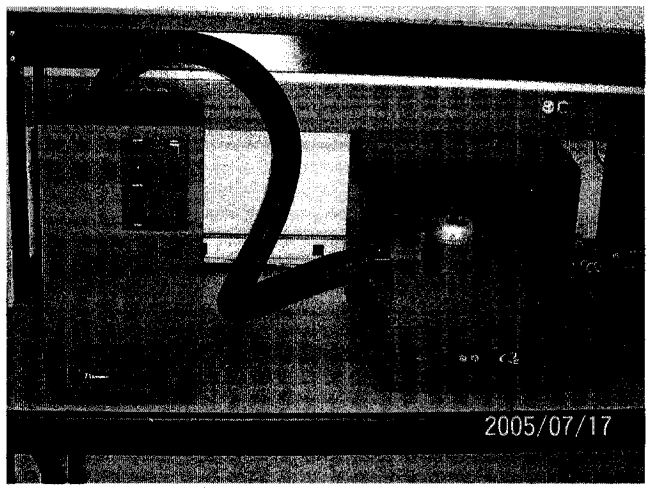

Figure 3. 12. TA-Q10 DSC System at CONCOM

The features of curing process of different systems are shown in Figure 3.13.

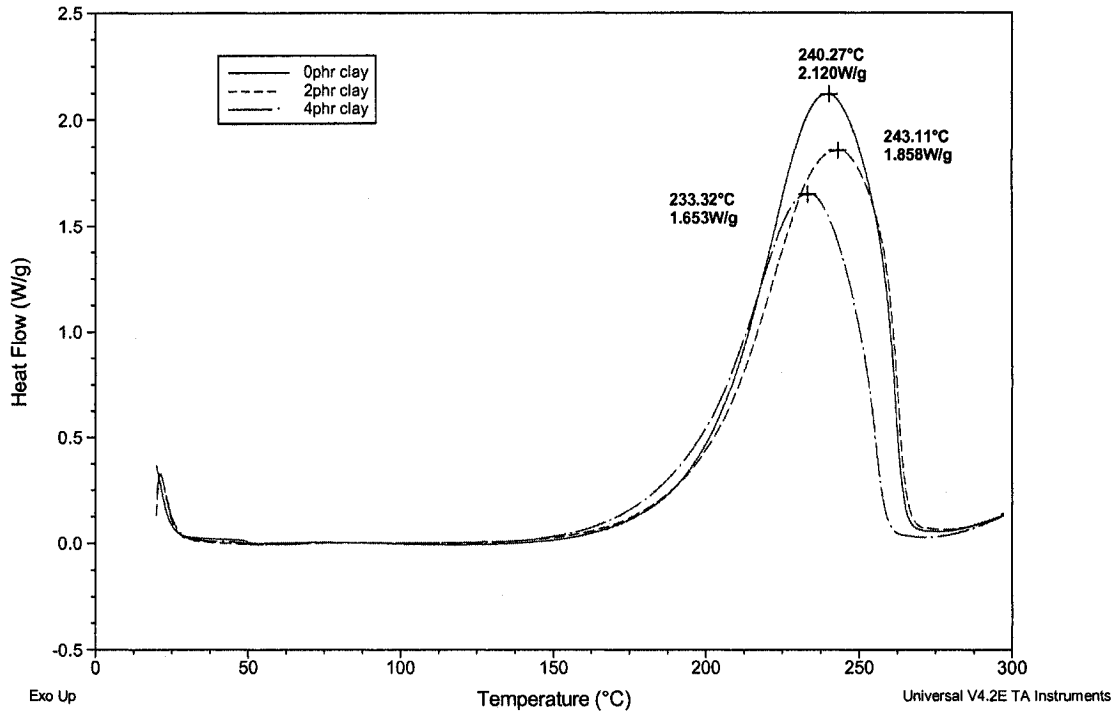

Figure 3. 13. DSC Curves of TGDDM/DDS/Clay Systems

From Figure 3.13, we can see that the peak temperatures of samples with 0 phr, 2 phr, and 4 phr clay are 240.27°C, 243.11°C, and 233.32°C respectively. The corresponding heat flow values are 2.120 w/g, 1.858 w/g, and 1.653 w/g respectively. These numbers indicate that the addition of 2 phr and 4 phr nanoclay slightly influenced the cure process of TGDDM epoxy. However, there is a clear phenomenon that the heat flow decreased with the addition of nanoclay. The heat flow drops by 18.3% when the addition of clay grows to 4 phr.

To investigate the influence of nanoclay on epoxy curing behavior, two samples were

made by adding 4 phr and 8 phr nanoclay. This work aimed at determining if the existence of nanoclay could facilitate or inhibit the cure process of TGDDM epoxy.

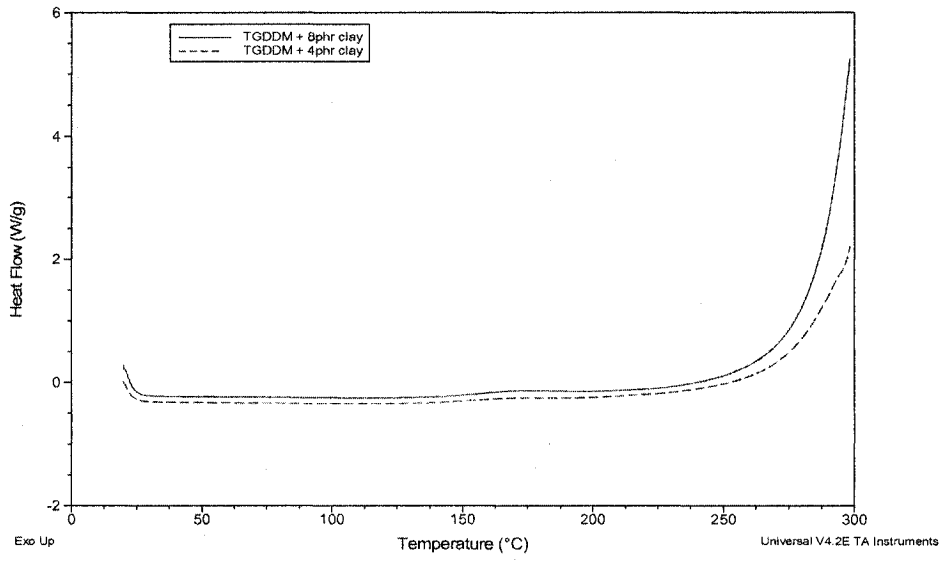

Figure 3. 14. DSC Curves of TGDDM/Clay Systems

Figure 3.14 shows that a TGDDM/nanoclay system's thermal behavior up to 300°C. Below 250°C, there is no any apparent exothermal peak. Considering that our curing temperature will be around 180°C, we can draw a conclusion that the present nanoclay in the systems has no influence on the curing process at our prospective experimental temperature. Thus, there is no need to take into account the nanoclay when curing cycle is determined.

3.4.2 Determination of Degree of Cure

For the composites manufacture process, epoxy degree of cure is indispensable.

The samples (postcure and no postcure) were made by the same method as the samples

used in gel time test. What is needed to do further is following a cure cycle:

135°C (1hour) - 150°C (1.5hours) - 177°C (2Hours).

Some samples were treated by postcure process at 200 °C for 8 hours.

DSC may also be used to determine the degree of cure of a certain system by the following formula.

$$Degree\ \ of\ \ cure\ \ = (1-\frac{\Delta H_p}{\Delta H_t})\times 100\%$$

ΔH_p --- partial exotherm

ΔH_t --- total exotherm

Samples undergoing postcure and non-postcure process were tested by DSC as well. The results are shown in Figures 3.16 and 3.17. Clearly, sample with postcure treatment produced much less heat than those without postcure treatment.

Samples without nanoclay

Figures 3.15 and 3.16 indicate that the degree of cure of the cured sample (no postcure) is:

$$Degree\ \ of\ \ cure\ \ = (1-\frac{\Delta H_p}{\Delta H_t})\times 100\% = (1-\frac{33.22}{581})\times 100\% = 94.28\%$$

In the case with postcure, the heat flow of sample decreased significantly to 9.606J/g; the degree of cure in this case became 98.34%.

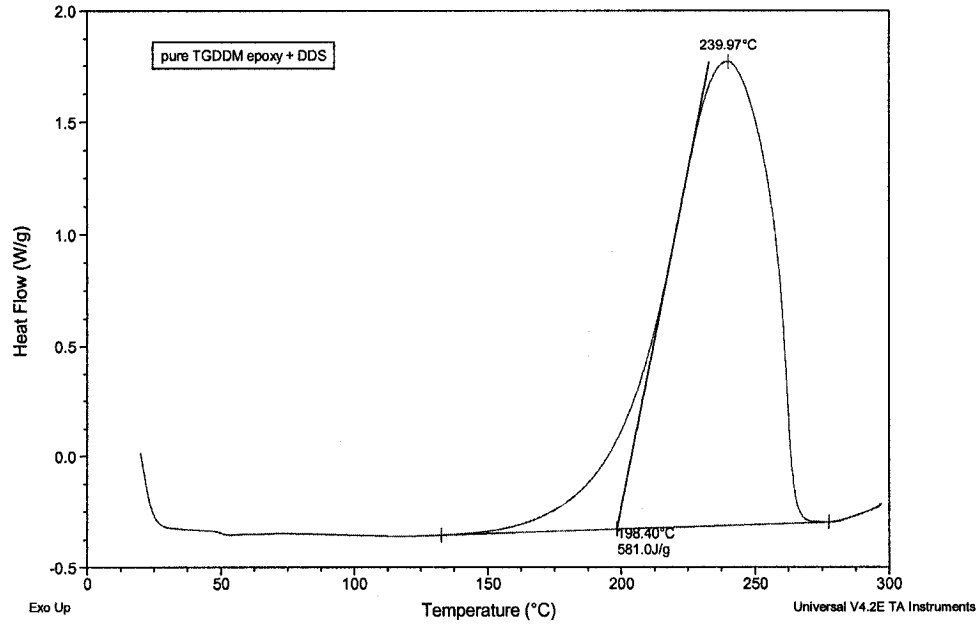

Figure 3. 15. DSC Curve of Pure TGDDM Epoxy/DDS System

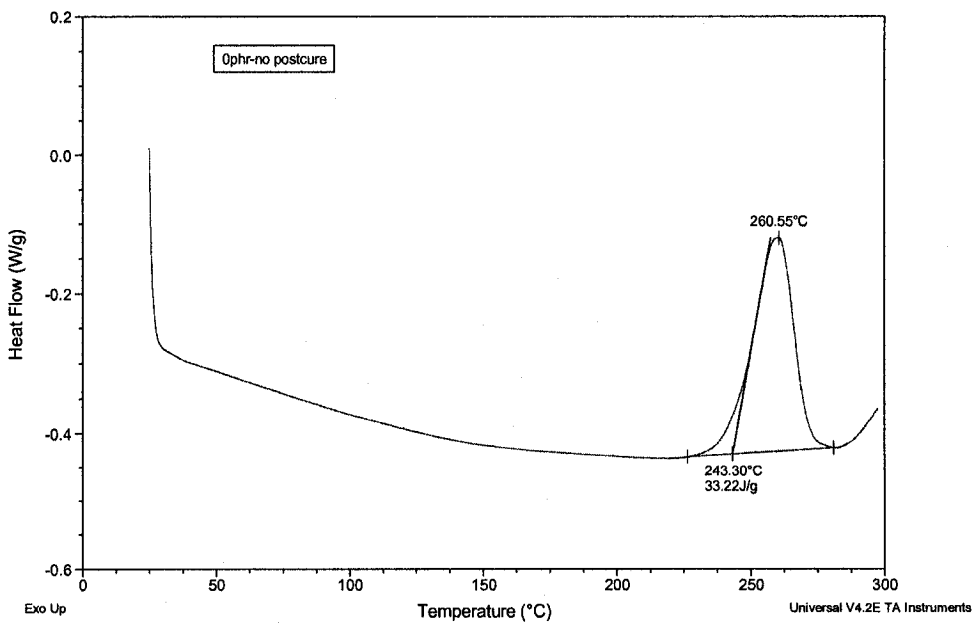

Figure 3. 16. DSC Curve of Cured TGDDM /DDS System (no postcure)

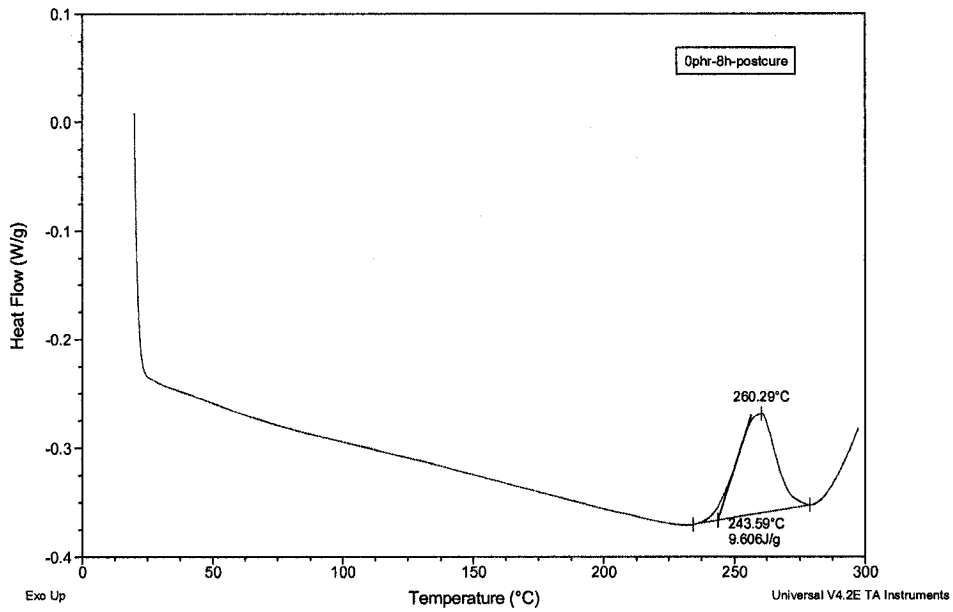

Figure 3. 17. DSC Curve of Cured TGDDM /DDS System (postcure)

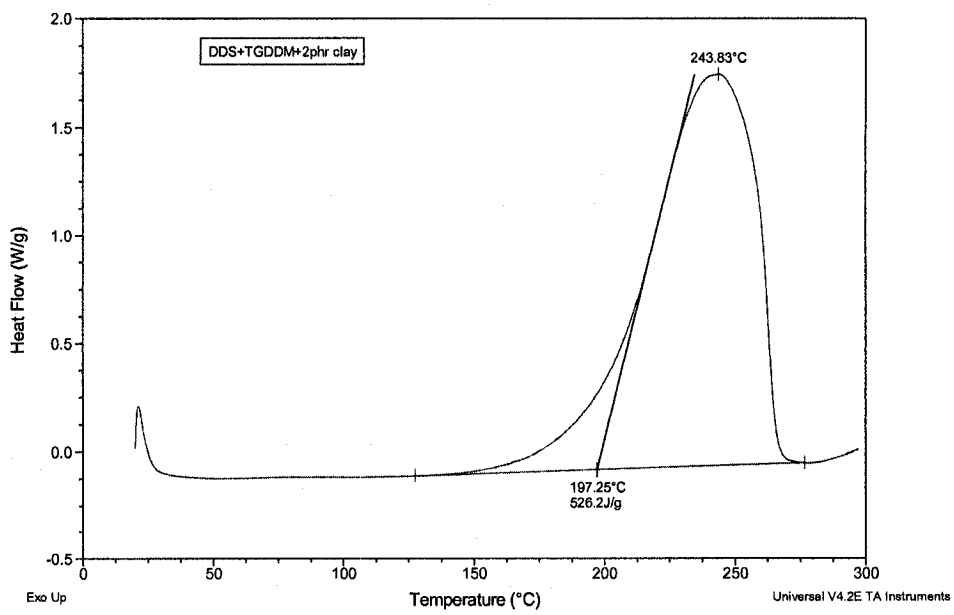

Figure 3. 18. DSC Curve of TGDDM /DDS/2phr-Clay System

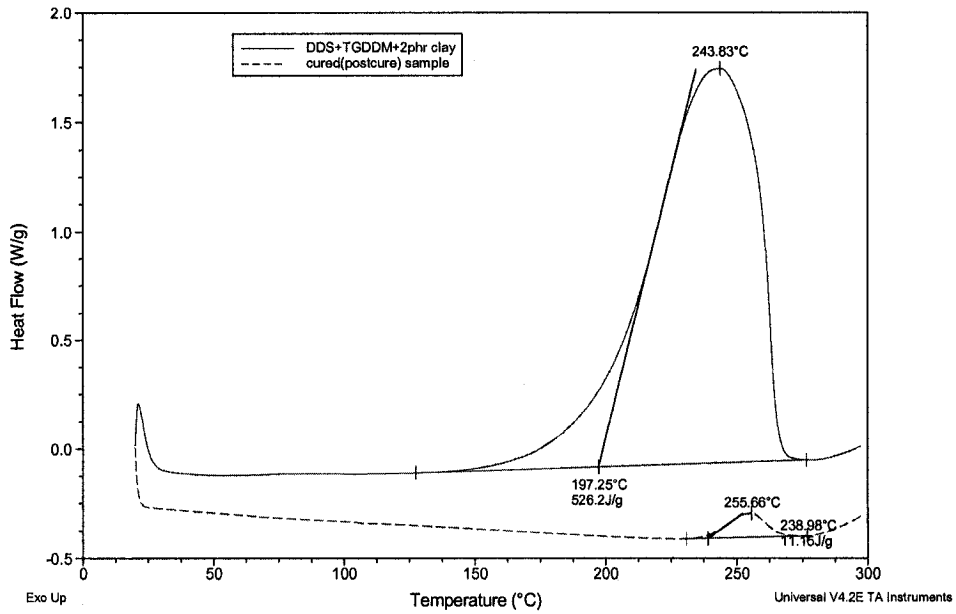

Figure 3. 19. DSC Curve of Cured TGDDM /DDS/2phr-Clay System

From Figure 3.19 above, we can see that the sample containing 2 phr clay produced less heat (526.2J/g) than the epoxy system without nanoclay (581J/g) during DSC test. Furthermore, the degree of cure in this case is 97.88%.

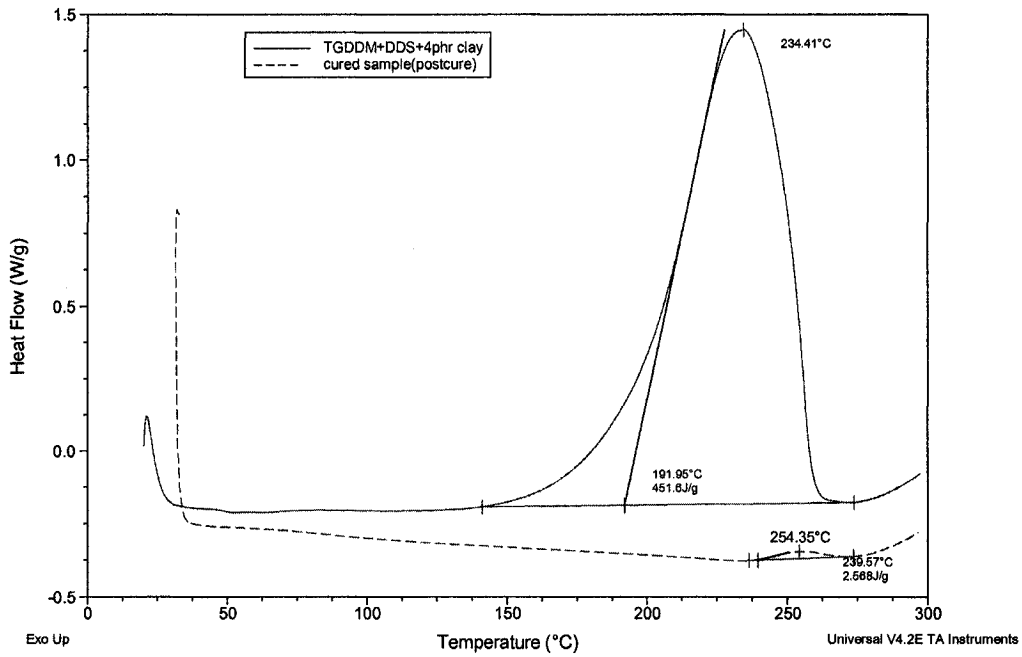

Figure 3. 20. DSC Curve of Cured TGDDM /DDS/4phr-Clay System

The DSC test result of sample containing 4 phr clay is shown in Figure 3.20. In this case, less heat was generated from system (451.61J/g), and the degree of cure is 99.43%. Figure. 3.21 compares the DSC test results of cured TGDDM /DDS systems containing 0, 2, 4phr clay system. All those samples were treated by postcure process. The results show that the heat generated from the samples is all very small. It indicates that the curing schedule used in our project is feasible and reliable.

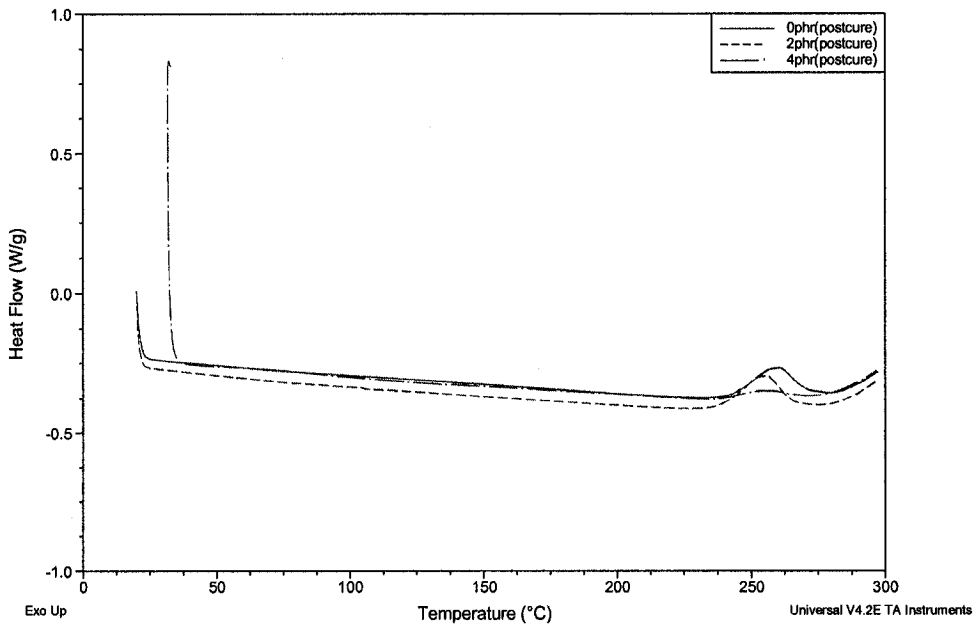

Figure 3. 21. DSC Curve of Cured TGDDM /DDS/0,2,4phr-Clay System (postcure)

3.5 DMA Tests

Dynamic Mechanical Analysis (DMA) is a technique used to investigate and characterize materials. It is mainly used to measure the viscoelastic nature of polymer. It provides information on the ability of materials to store and dissipate mechanical energy upon deformation, which is used to determine which materials can be used in dynamic applications. The basic properties obtained from a DMA test include storage modulus (E' or G'), loss modulus (E" or G") and tan delta (tanδ). Tan delta is particularly important for polymers because it is related to the material's ability to dissipate energy in the form of heat. Glass transition temperature (Tg) can also be determined. The DMA

data allow the development of structure-property-performance relationships for a polymer. The displacement of a sample resulted from an oscillating force can be measured. Correspondingly, modulus of material can be determined.

The samples used in this experiment have a uniform size of 50 × 12.5 × 3 mm. The samples were tested at a fixed frequency of 1 Hz with a heating rate of 3 °C/min by TA DMA 983 system (Figure 3.22).

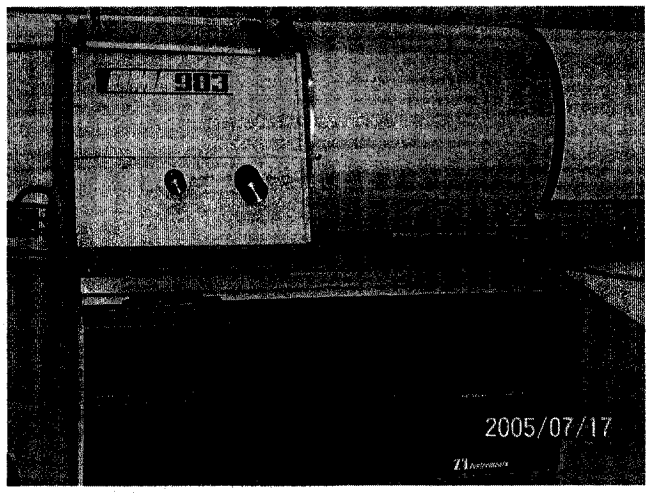

Figure 3. 22. TA DMA 983 System at CONCOM

The DMA tests results indicate that the tan δ peak temperature (Tg) almost remains the same when nanoclay is introduced (Figure 3.23). Meanwhile, the storage modulus value is dependent on the nanoclay content (Figure 3.24). Evidently, the storage modulus values of the samples containing 2 and 4 phr nanoclay are higher than the value

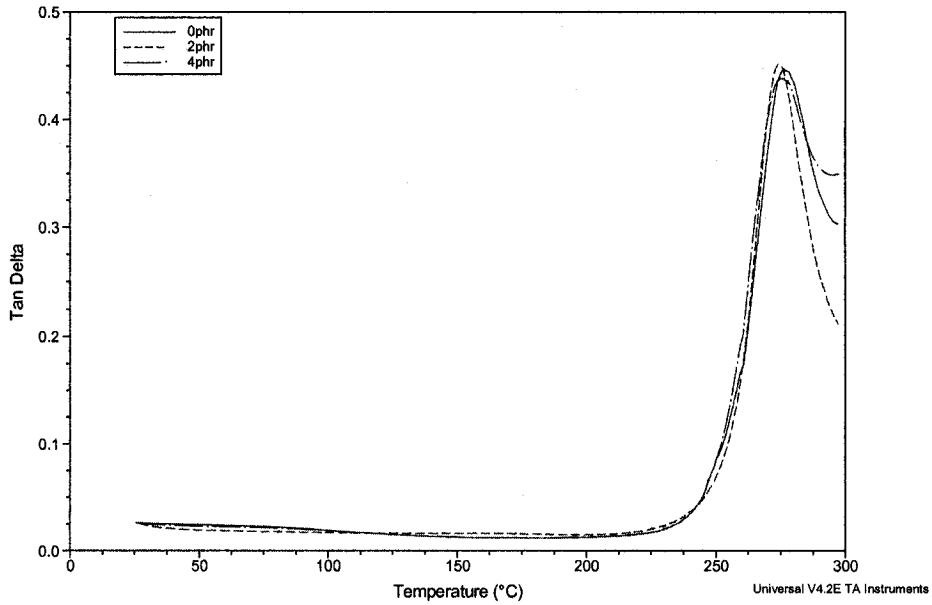

Figure 3. 23. Loss Tangent *versus* Temperature Graph of Different Samples

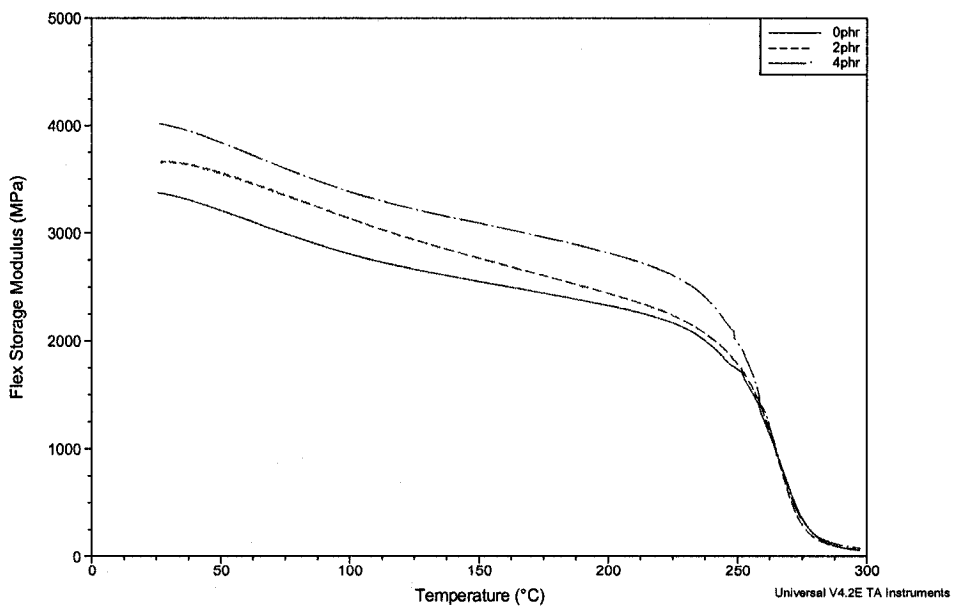

Figure 3. 24. Flex Storage Modulus *versus* Temperature

of non-filled sample. All the results indicate that the composite made in the project can maintain the original glass transition temperature (Tg) and the modulus of nanoclay-filled composite is slightly increased.

3.6 Summary

The degree of cure of samples was determined by scanning the samples in the DSC from 25°C to 300°C at a ramp of 10°C/min. We can see that the heat generated from the original system is 581.00 J/g; the heat from the cured samples is simply 9.6J/g. That means the degree of cure of the cured sample is very high. To sum up, the experimental results indicate that the nanoclay has no influence on the TGDDM/DDS system with respect to the curing process. In addition, high degree of cure can guarantee the strong crosslinks in systems and corresponding mechanical properties. The introduction of nanoclay does not lead to a drop in Tg, and it even makes an slight augmentation of storage modulus.

Chapter 4 Carbon-Fiber-Reinforced Epoxy Nanocomposites Manufacturing

In chapter three, the fundamental characteristics of TGDDM/DDS/nanoclay systems were investigated and analyzed. All the investigation focused on epoxy matrix and the nanoclay factors. In this chapter, the epoxy/nanoclay matrix systems mentioned above will be further reinforced by carbon fiber to manufacture composite laminates.

There are many composite fabrication processes that are used widely both in the high-performance aerospace application and other commercial markets. Some examples are: hand-lay-up, resin transfer molding (RTM), vacuum-assisted resin transfer molding (VARTM), pultrusion, autoclave etc. Most of the processes are amenable to low viscosity resins. In this project, the selected reinforcing material is unidirectional carbon fiber; the epoxy resin used is MY720 (TGDDM). For some of the high viscosity resins, like MY720 (TGDDM), there is a restriction on the processes that can be used.

Although there are many ways to fabricate advanced composites, hand lay-up followed by autoclave cure is by far still the most important process in terms of aerospace production because it is flexible and is capable of making a wide variety of shapes [21]. Nevertheless, hand lay-up processes are labor intensive and part quality is very sensitive to the experimenter's lay-up skill. There are three major lay-up processes: wet lay-up, spray-up, and low temperature curing vacuum bag (LTVB) prepreg lay-up. Considering the high viscosity characteristic of the matrix material, wet lay-up and autoclave

processes were applied to the fabrication of nanocomposites. Furthermore, lay-up process in our experiment was carried out at elevated temperature in order to obtain a preferred low viscosity that is amenable to wet lay-up.

The whole manufacture process includes the following steps: nanoclay paste fabrication, mixing of nanoclay paste and epoxy, mixture degassing, wet lay-up, vacuum bag making, autoclave cure, and postcure treatment.

4.1 Experimental Materials

4.1.1 Matrix, Curing Agent, and Nanoclay

TGDDM (Araldite® MY720), DDS (Aradur™ 976-1), and nanoclay (Nanocor I.30E) were chosen for the manufacture of carbon fiber reinforced nanocomposites. The properties and specification of these materials are shown in Tables 3.1, 3.2, and 3.3 of Chapter 3.

4.1.2 Carbon Fiber

The reinforcing fiber chosen for this project is TORAYCA® T300 carbon fiber (see Figure 4.1) in tow size 12k from Toray Carbon Fibers America, Inc. TORAYCA® T300 has outstanding properties of light weight, strength and rigidity. Because of these characteristics, it finds uses in a wide variety of industry sectors: in aeronautical applications such as the tail plane and floor beams of the state-of-the-art Boeing 777; in sports applications such as golf club shafts and tennis racket frames; and general industrial applications such as compressed natural gas fuel tanks for automobiles and

wind turbine blades [58]. T300 carbon fibers are used in aerospace applications, having over 30-year production history. It is well known for its balanced composite properties, high quality, consistency, reliability and applicability. The major properties of TORAYCA® T300 carbon fiber 12K are listed in Table 4.1.

Table 4. 1 Major properties of TORAYCA® T300 carbon fiber 12K (TORAYCA Data Sheet)

Fiber Type	PAN carbon fiber
Modulus of Elasticity	230 GPa
Density	1.76 g/cm^3
Tensile Strength	3.53 GPa
Elongation at Break	1.5 %
Thermal Expansion	-0.41 $\times 10^{-6}$ /K
Shear Modulus	12.543 GPa
Compression strength	2.169 GPa
Filament Diameter	7 μm

4.2 **Experimental Steps**

4.2.1 Nanoclay-acetone paste

Nanoclay-acetone paste is critical to the whole composites manufacture process; it is the decisive factor in the improvement of dispersion of nanoclay into epoxy matrix.

There were many different nanoclay/resin mixing methods for different systems. In this project, a high pressure mixing method developed at CONCOM was applied to provide good dispersion of nanoclay.

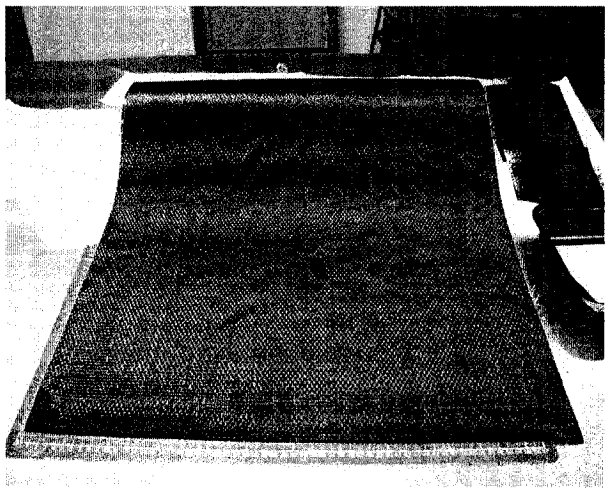

Figure 4. 1. TORAYCA® T300 Carbon Fiber (12K)

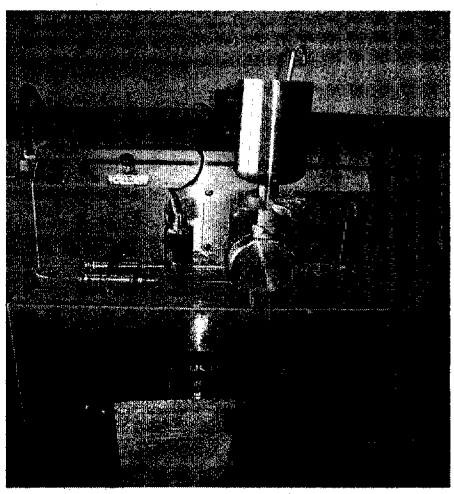

Figure 4. 2. Microfluidizer Processor at CONCOM

Nanoclay (I.30E) was baked in an oven to drive moisture out at 120°C for 2 hours before processing. The dry nanoclay was mixed with acetone solvent by a ratio of 10 wt% to form a nanoclay-acetone suspension. The fully stirred suspension was then poured into a high pressure mixing machine named Microfluidizer (shown in Figure 4.2). The suspension was treated under extremely high pressure ranging from 15000psi ~ 20000psi (103 ~ 138 MPa) to obtain a creamy white nanoclay-acetone paste (see Figure 4.3). The high-pressure treatment was repeated at least twice in order to get a completely mixed paste.

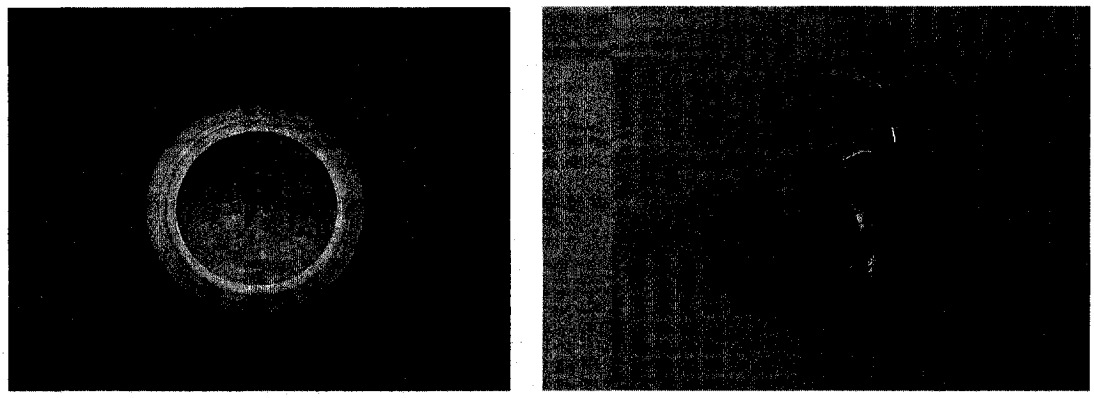

Figure 4. 3. Nanoclay-Acetone Paste and TGDDM Epoxy

4.2.2 Nanoclay-epoxy systems synthesis

A certain amount of TGDDM (MY720) epoxy was scooped out, slightly heated to 40°C, and manually mixed with a small amount of acetone in a glass beaker at room temperature. The mixing lasted until the whole system became uniform. The desired amount of nanoclay-acetone paste was then added into the above system followed by

manual stirring until a uniform system is obtained again (see Figure 4.3).

Under a special fume hood, the mixture made above was mechanically stirred at a speed of 1000 rpm at room temperature for 30 minutes (see Figure 4.4). An aluminum foil was used to cover on the top of the beaker to prevent acetone from evaporating too fast. After 30 minutes, an adjustable heater was turned on; the mixture in the beaker was continuously heated from room temperature to 120°C, and was held at 120°C for 60 minutes.

Figure 4. 4. Mixing Mechanism

Before the next step, the curing agent (DDS) was baked in an oven at 140°C for 120 minutes. The epoxy-clay system was further heated to 135°C~140°C; the baked DDS was carefully added into the beaker, accompanied by mechanical stirring for 15 minutes. Finally, the whole Nanoclay-TGDDM-DDS system was degassed by Thinky vacuum mixer (see Figure 4.5) for 1.5 to 2 minutes.

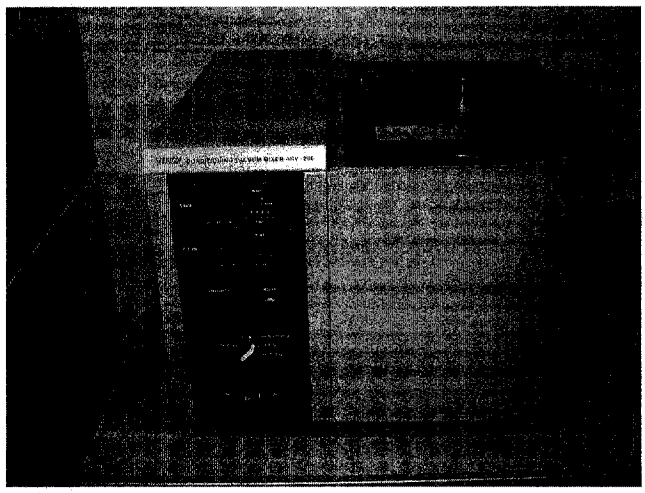

Figure 4. 5. Thinky Conditioning Vacuum Mixer ARV-200 at CONCOM

The TGDDM epoxy used in this project is a tetrafunctional epoxy, which is extremely reactive chemically, careful temperature control during mixing and degassing is critical to prevent the occurrence of an exothermal reaction that could result in a fire.

4.2.3 Carbon fiber reinforced composites laminates manufacture

Carbon fiber tape was cut into smaller pieces of size 150mm×150mm; 10 pieces of carbon fiber tapes were prepared for each laminate $[0^{o}]_{10}$ (see Figure 4.6).

Usually, carbon fiber is impregnated by epoxy to form a commercial prepreg. Prepreg is the most prevalent product form used in advanced composites manufacture. Prepreg can be fabricated by hot-melt impregnation, solvent impregnation, and resin filming. Although solvent impregnation is usued exclusively for high-temperature resins, which are not amenable to hot-melt methods, its disadvantage is that the residual solvent may

remain in the system and cause volatile and void problems during cure. Therefore, hot-melt method was used.

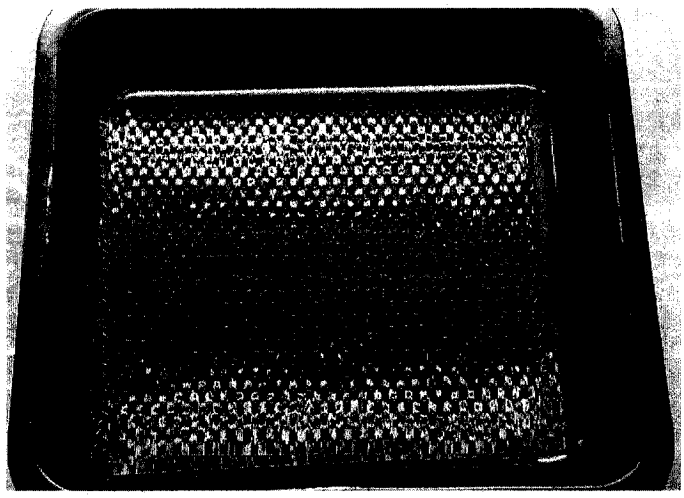

Figure 4. 6. Carbon Fiber Tapes

Figure 4. 7. Resin Film Containing Nanoclay

Considering the extraordinary high viscosity of TGDDM/DDS/Nanoclay system, all treatments must be accomplished at elevated temperature. Resin filming process is not suitable to our case because the film becomes very brittle after cooling down from mixing and degassing temperature (see Figure 4.7). The brittle film is difficult to drape over fiber tape to make laminates

Solution Method

Although there were some disadvantages of the solution method, we still attempted to use it for manufacturing carbon/epoxy composites owing to high viscosity of this resin. The purpose of this attempt was to compare the experimental result between solution method and hot melt method.

When the solution method was carried out, TGDDM epoxy was firstly warmed to 40°C and stirred in acetone solvent at a 1:1 ratio until around 30% solid weight solution was obtained. Then, the curing agent DDS was added and dissolved. The whole system was continuously stirred until the solution became homogeneous. The mixture was then brushed on the carbon fiber stitched cloth, assisted by Teflon roller whenever it was necessary. The impregnated carbon fiber tapes were stacked up and cured by autoclave process. The curing cycle and other experimental conditions were the same as the following hot-melt method.

Most of the samples obtained from solution method include large voids like the one shown in Figure 4.9; that is to say, the experiments results have proven that solution method is not feasible to manufacture carbon fiber/TGDDM epoxy nanocomposites. By

solution method, the good quality of composites will be hardly controlled and guaranteed.

Figure 4. 8. Void in Sample Made by Solution Method

Hot Melt Method

As mentioned above, both solvent method and resin film method are not appropriate process for this project. Therefore, hot-melt method was eventually applied. However, the hot-melt method was not exactly the same as some commercial processes. In the commercial hot-melt process, the fibers were fed from a creel, and impregnated with the melted resin and then immediately cooled prior to spooling on the roll. In this project, brush and roller were used to help the impregnation of fiber. Because of the high viscosity, the epoxy resin was preheated to an appropriate temperature in the oven before it was brushed on the surface of the fiber.

The epoxy-brushed fiber tape was stacked up and aligned carefully (Figure 4.10). A 50kg weight was placed on the top of the stack whenever a new piece was put on, to keep the whole stack compact to prevent voids during cure.

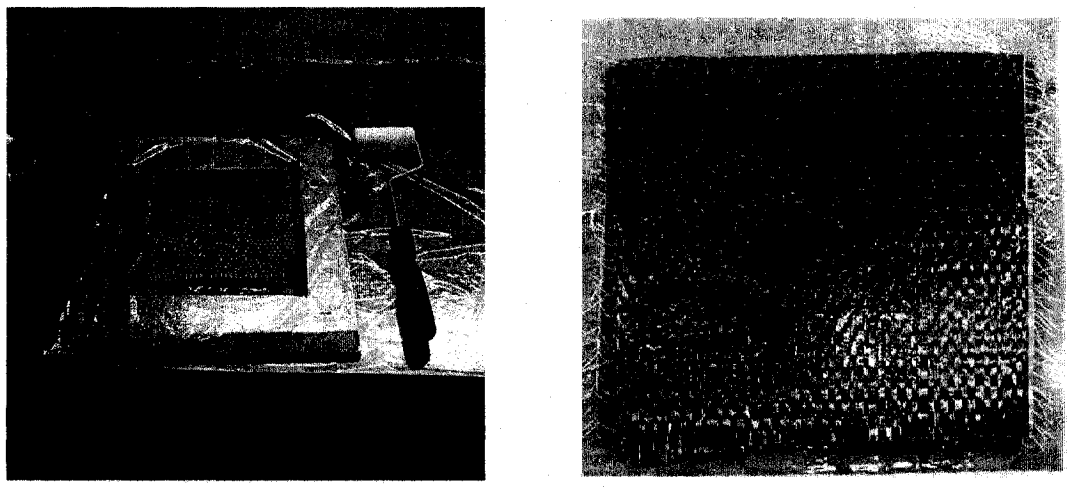

Figure 4. 9. Stack of Fiber Tape

The whole schematic wet lay-up process is shown in Figure 4.10.

A slight amount of release agent was coated on the surface of tool and held for 30 minutes, in order to improve stripping after autoclave treatment (shown in Figures 4.11 and 4.12). The next step is vacuum bagging. In this step, fiber laminate, peel ply, release film, bleeder, and breather were stacked up on the top of tool in sequence. Then, the assembly is placed inside a vacuum bag and vacuum is applied.

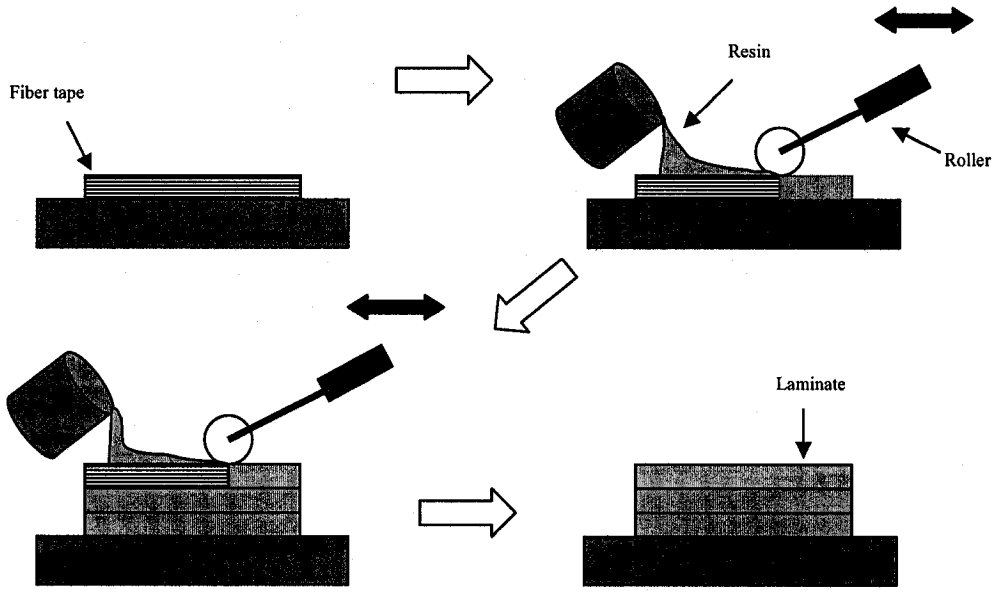

Figure 4. 10. Schematic Wet Lay-up Process

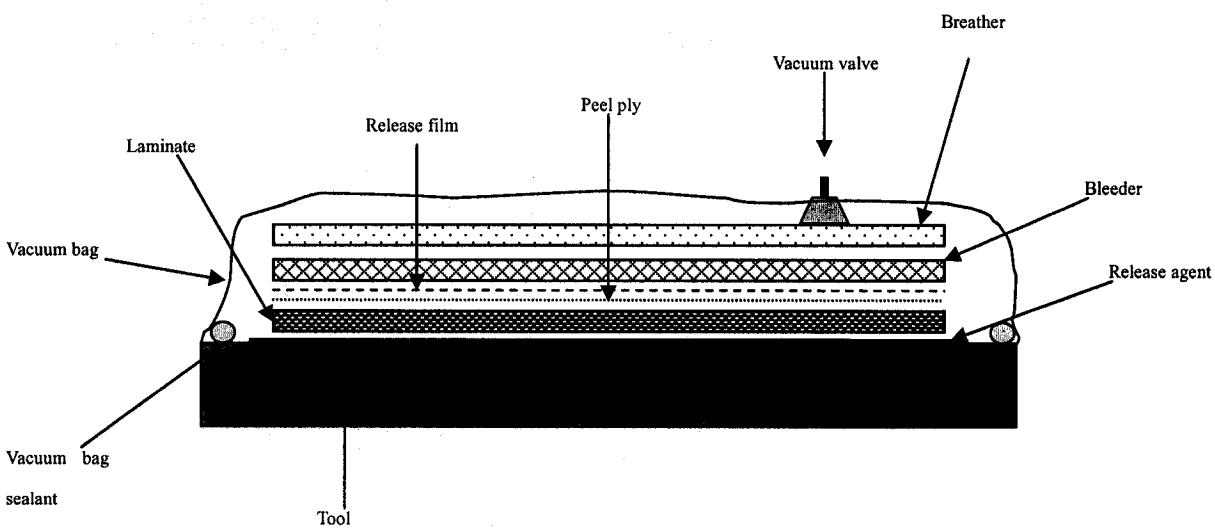

Figure 4. 11. Schematic Vacuum Bagging Configuration

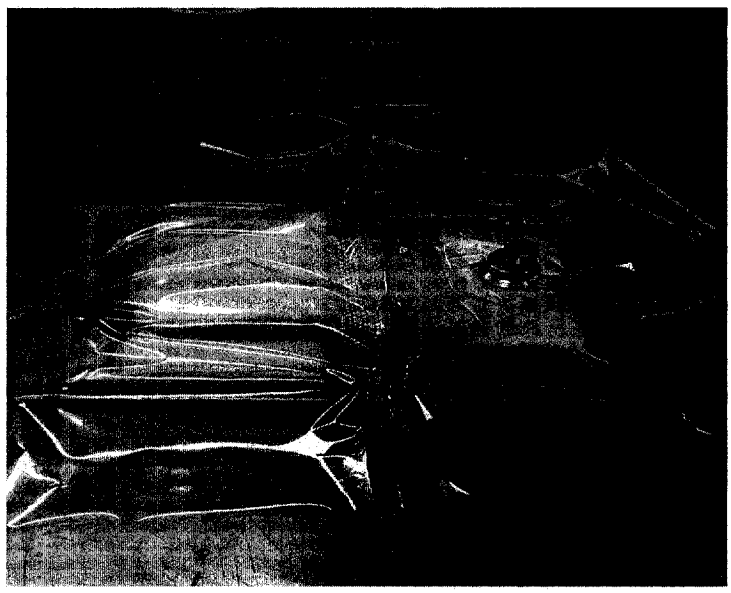

Figure 4. 12. Vacuum Bag for Autoclave Process

4.2.4 Autoclave Curing Process

Autoclave is a large pressure vessel with an integral heating facility. Autoclave curing is the most widely used method of producing high-quality laminate in laboratory and industry. Almost any shape can be cured in autoclave. A typical autoclave system, as illustrated in Figures 4.13 and 4.14, consists of a pressure vessel, a control system, an electrical system, a gas generation system, and a vacuum system. Most parts made by hand- lay-up must be cured by a combination of heat, pressure, and vacuum atmosphere. To achieve proper cure, the part is placed into a vacuum bag inside an autoclave. A vacuum is applied to the bag to remove air and volatile products. Heat and pressure are

applied for curing. In certain cases, an inert atmosphere is provided inside the autoclave through the introduction of nitrogen or carbon dioxide. Air can be used for autoclave, but it might increase the danger of a fire during the cure cycle. In this project, the size of laminate was not very large, compared to the commercial parts; therefore, air was used to provide high pressure.

One of the most critical items of laminate autoclave process is the determination of cure cycle, which includes a schedule of time, temperature, and pressure. The typical carbon/epoxy cure cycle is illustrated in Figure 4.15.

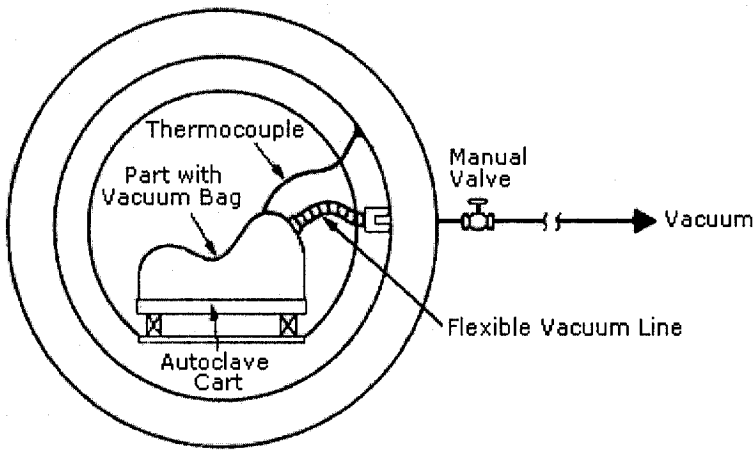

Figure 4. 13. Schematic Autoclave System [59]

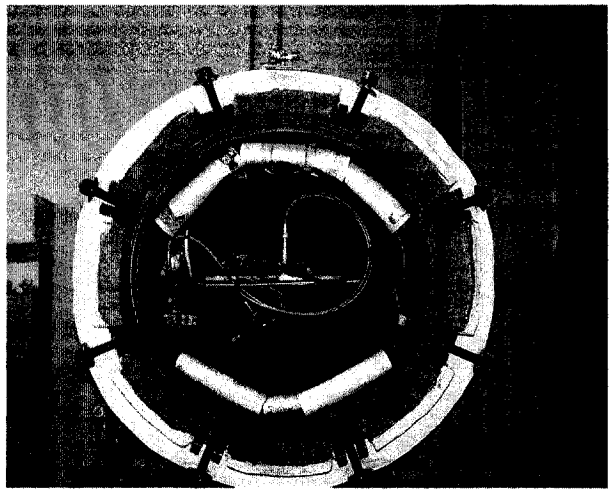

Figure 4. 14 Autoclave System at CONCOM

The cure cycle contains two ramps and two isothermal holds. The first ramp and isothermal hold, usually in the range of 240-280 °F (116 °C-138 °C), is used to allow the resin to bleed and volatiles to escape. In our experiment, 280 °F (138 °C) was chosen for the first hold because of the high-viscosity of TGDDM resin. During this period, the semi-solid epoxy resin melts on heating and undergoes a dramatic drop in viscosity (Figure 4.16). The second ramp and hold is the polymerization portion of the cure cycle. Classic temperature for second hold is 350 °F (177 °C). During this portion, the resin viscosity initially drops slightly due to the application of additional heat and then rises dramatically as the cross-linking process has started. The resin gels into a solid and the cross-linking process continues during the second isothermal hold.

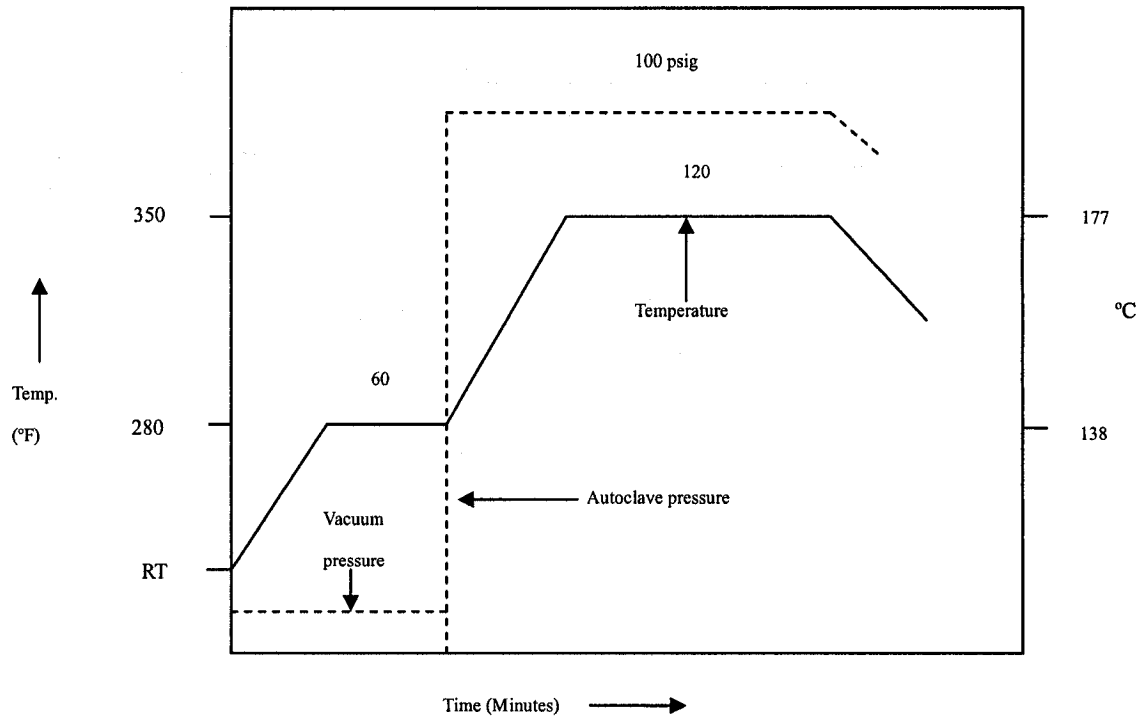

Figure 4. 15. Classical Carbon/Epoxy Cure Cycle [5]

Pressure application is another important factor in autoclave process. High pressure is commonly used to provide ply compaction and suppress void formation. Autoclave pressure is transferred to the laminate duo to the pressure difference between the autoclave environment and the vacuum bag interior. The classical pressure cycle is also illustrated in Figure 4.15. During the ramp-up to the first hold, only vacuum is applied and maintained until the end of the first isothermal hold. At the beginning of the second ramp-up, autoclave pressure is applied. Normally 85~100psig (0.59~0.69 MPa) for epoxy and the vacuum pressure is removed by venting to the atmosphere. The vacuum applied can help to remove volatiles from the melting resin while the higher autoclave pressure tends to trap

them in the laminate. At the end of the first isothermal hold, full autoclave pressure is applied to insure that the laminate is well compacted before the resin viscosity rises to gel. The high-pressure is critical to avoid numerous voids and porosity.

In this experiment, the first and second hold temperatures were slightly modified to 140°C and 180 °C as there was a small temperature difference between the laminate and the autoclave chamber when curing was in process.

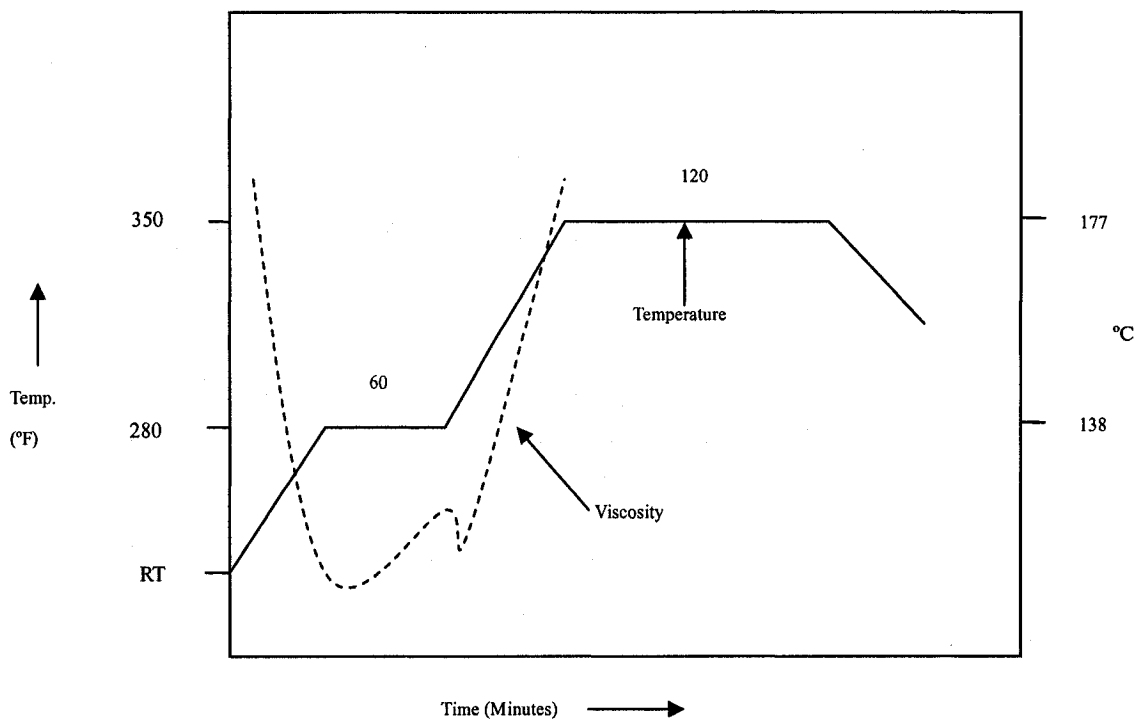

Figure 4. 16. Classical Carbon/Epoxy Cure Cycle (Viscosity) [5]

All composite samples made by autoclave process were postcured at 200°C in vacuum oven for 4 hours to obtain higher cure degree.

4.2.5 Composites Quality Analysis

In chapter three, the cure degree has been tested and analyzed. Under the experimental conditions in this project, high curing degree can be guaranteed. Therefore, porosity and voids could be the major problems in composite laminate.

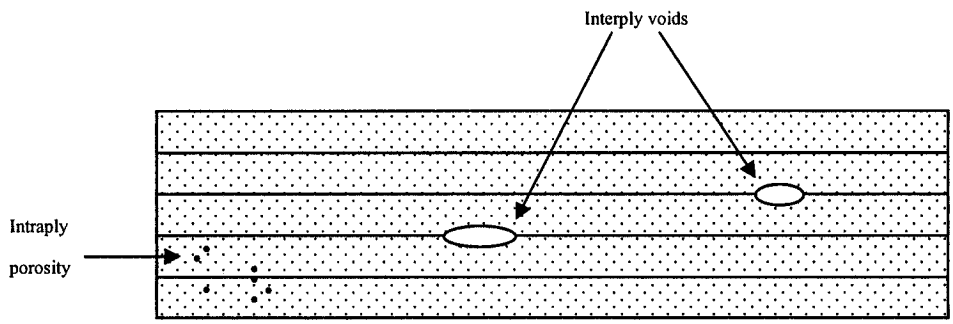

Figure 4. 17. Interply and Intraply Voids and Porosity

As shown in Figure 4.17, voids and porosity can occur at either the ply interfaces (interlaminar) or within the individual plies (intralaminar). Usually, the term "void" implies a large pore, whereas "porosity" implies a small pore.

To analyze the microstructure of the composites samples, appropriate samples must be made following a certain sample-making procedure, which consists of sample cutting, alignment and cure in epoxy-filled holder, and sample polish. To obtain clear and sharp image, sample polish must be done following a strict polishing procedure. The

composites laminate and the fully polished samples are shown in Figures 4.18 and 4.19 respectively.

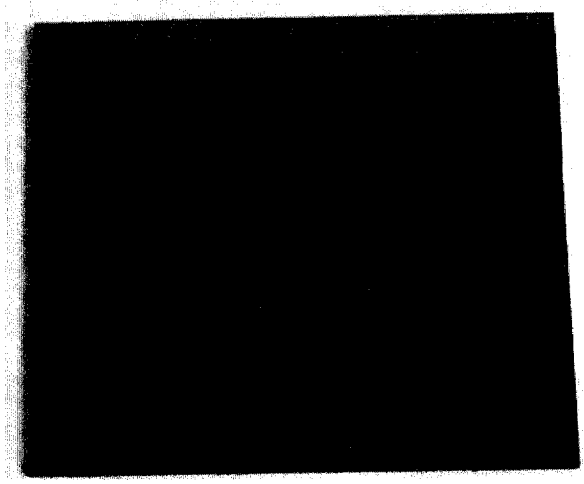

Figure 4. 18. Composite Laminate

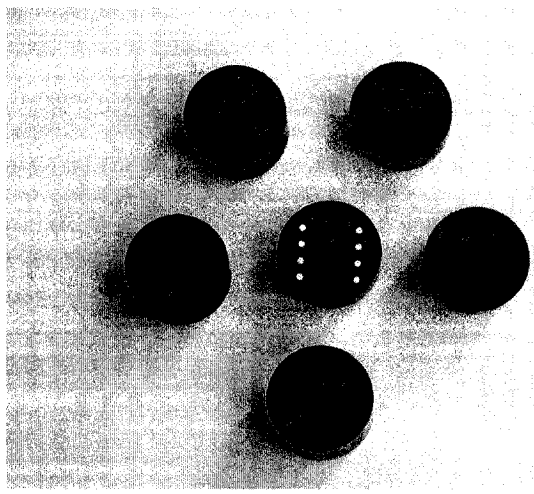

Figure 4. 19. Photos of Polished Samples

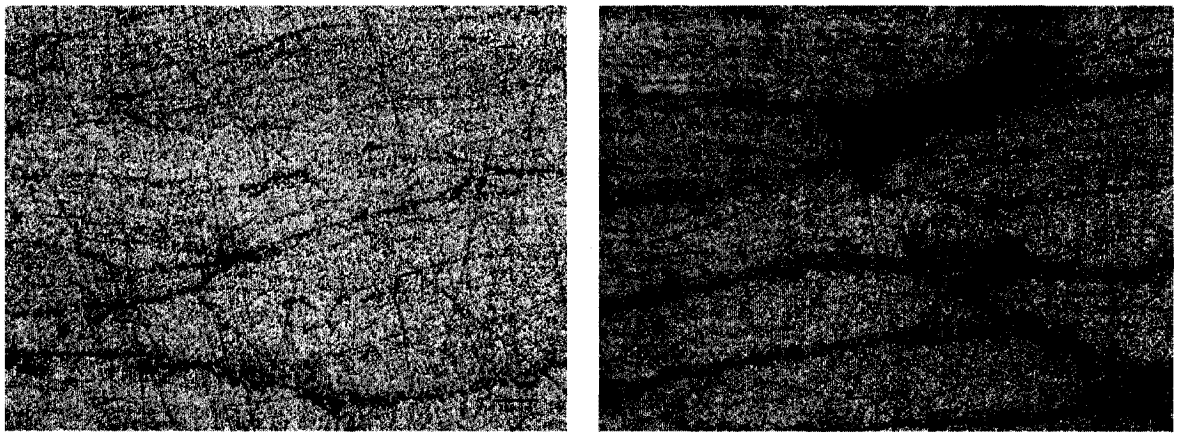

(a) (b)

(c)

Figure 4. 20. Images of Samples Cured at 100psi (0.69 MPa) (×50). (a) 0phr clay (b) 2phr clay (c) 4phr clay

The samples related to Figures 4.20, 4.21, and 4.22 were manufactured following the schedule in Figure 4.15. The only variation is that the hold temperatures slightly changed to 140°C and 180°C. By means of the microscopy, some phenomena were found. Firstly, the sample without nanoclay (0 phr) had less resin rich areas than those containing nanoclay (see Figures 4.20 and 4.21). The resin rich area mostly occurs between laminate plies. The more nanoclay content, the larger is the resin rich area. Secondly, from Figure

4.21, some voids were observed in the samples containing nanoclay. On the contrary, there was no apparent big void found in samples without nanoclay. Thirdly, from Figure 4.22, more dry spots (fiber-fiber contact) were observed in sample without nanoclay than

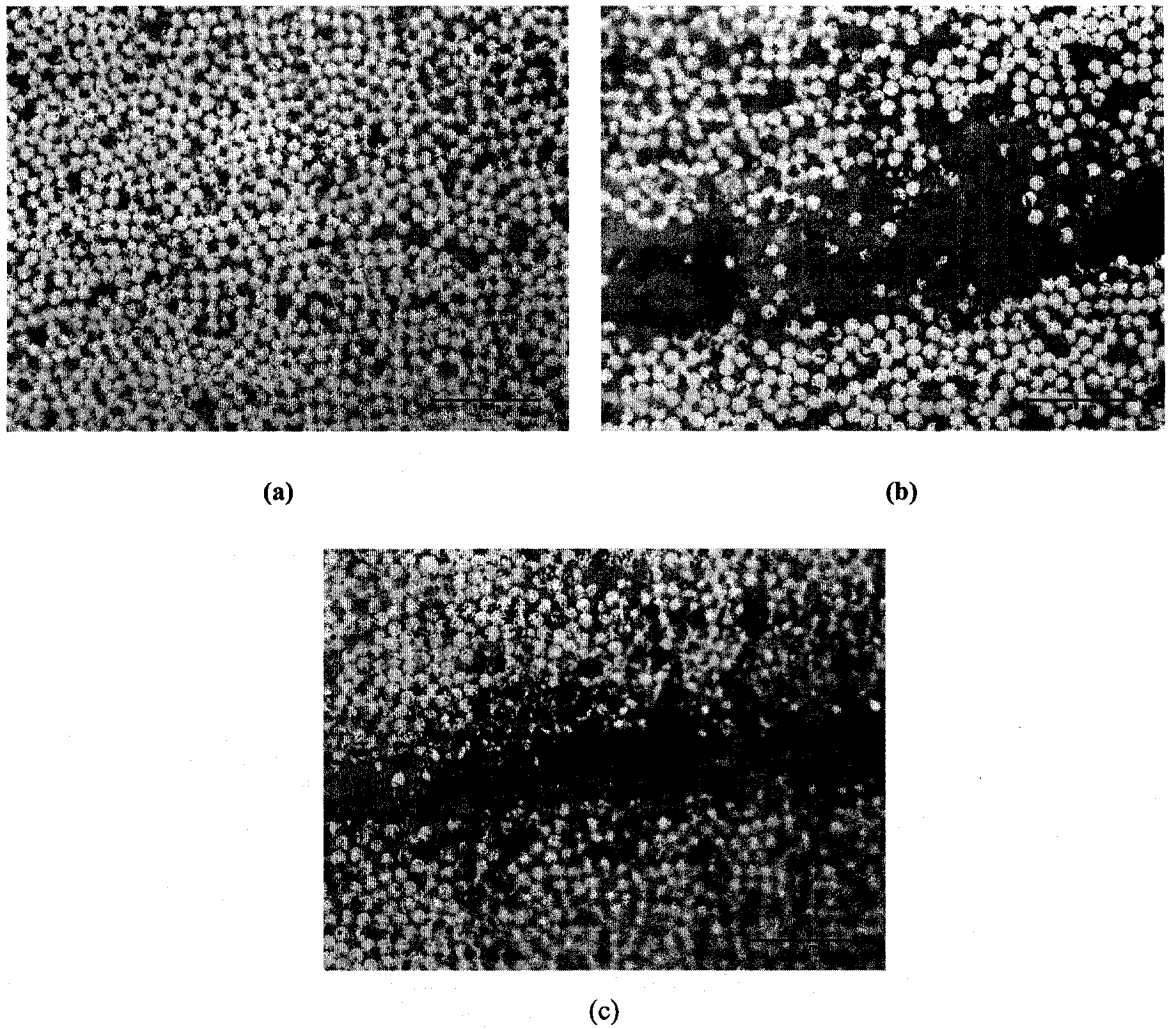

Figure 4. 21. Images of Samples Cured at 100psi (0.69 MPa) (×500) (a) 0phr clay (b) 2phr clay (c) 4phr clay

those containing nanoclay. The fiber-fiber contact could make the fiber bundle potentially load-bearing when compressed in the transverse direction. By image analysis,

the fiber volume fractions were 73.8%, 66.5%, and 64.2% for 0 phr, 2 phr, and 4 phr nanoclay samples respectively. That means there was an apparent difference between the fiber volume fractions.

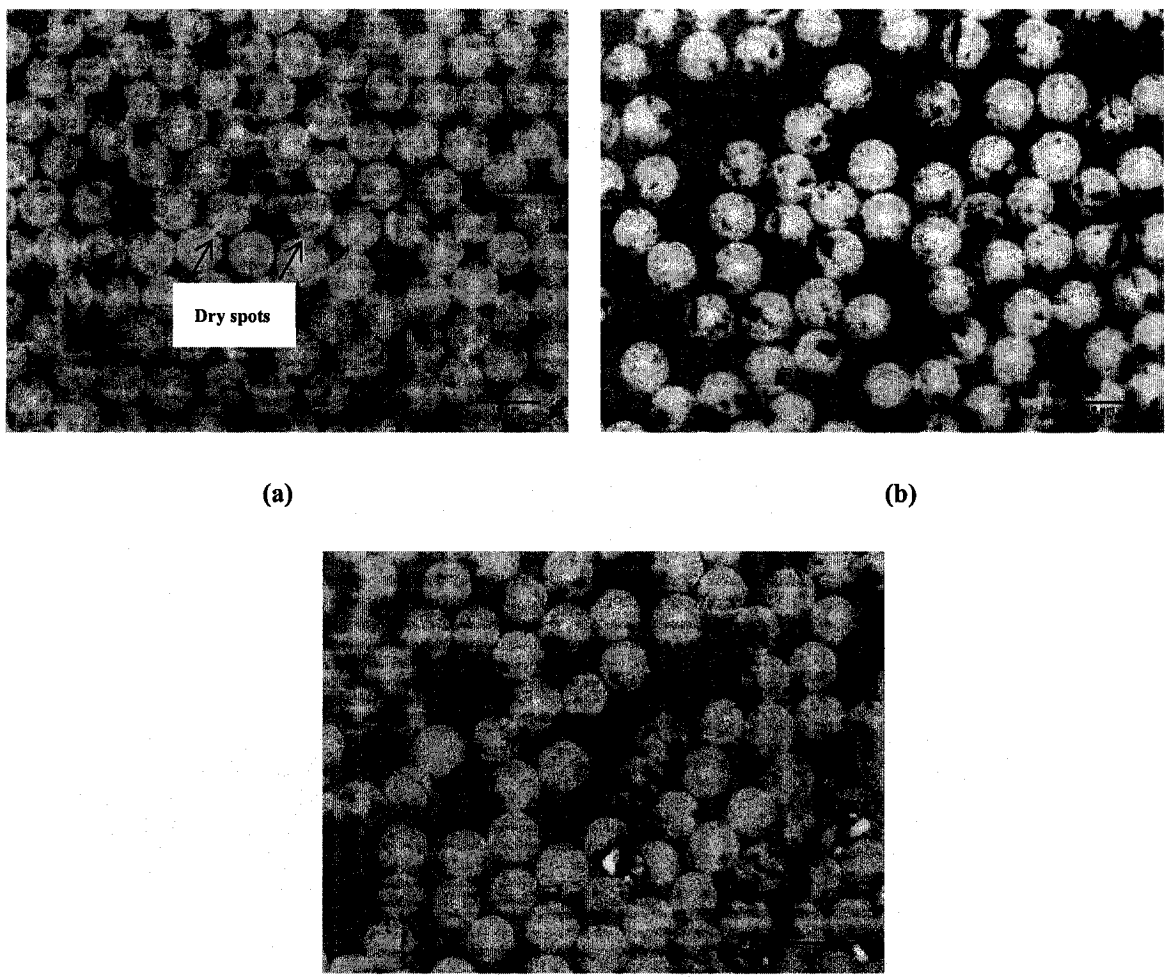

Figure 4. 22. Images of Samples Cured at 100psi (0.69 MPa) (×1600) (a) 0phr clay (b) 2phr clay (c) 4phr clay

Technically, the large resin rich areas existing in samples containing nanoclay were caused by the higher viscosity of the matrices. Under same experimental conditions,

especially under the same pressure, the laminate with lower viscosity matrix was compacted to a thinner laminate. In other words, low-viscosity matrix was easier to be driven by pressure to impregnate and wet the fibers. The voids and volume differences in samples also resulted from by high viscosity matrices. Therefore, to improve the quality of carbon/epoxy nanocomposites, the factors of pressure, temperature, and mixing process should be seriously taken into account.

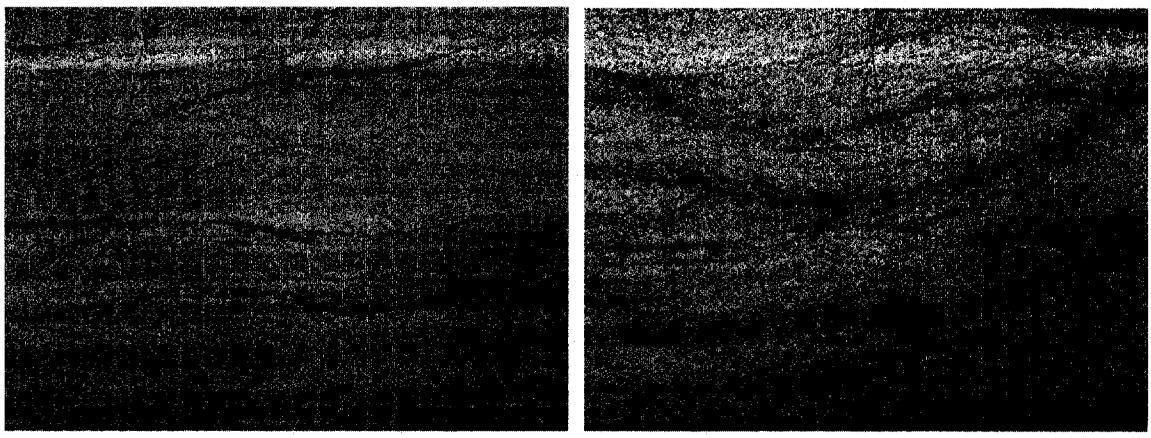

(a) (b)

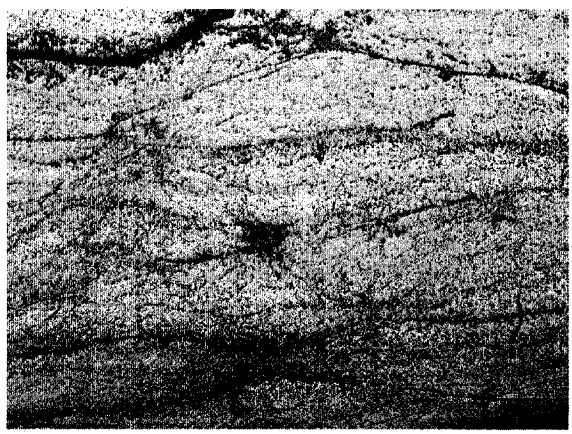

(c)

Figure 4. 23. Images of Samples Cured at 80psi (0.55 MPa), Modified Process (×50) (a) 0phr clay (b) 2phr clay (c) 4phr clay

For the samples containing nanoclay, the degassing time and vacuum degree must be raised in order to completely eliminate the potential voids. In addition, the autoclave pressure should be altered in order to get more compact material and approximate fiber volume fraction. For the samples without nanoclay, the autoclave pressure should be

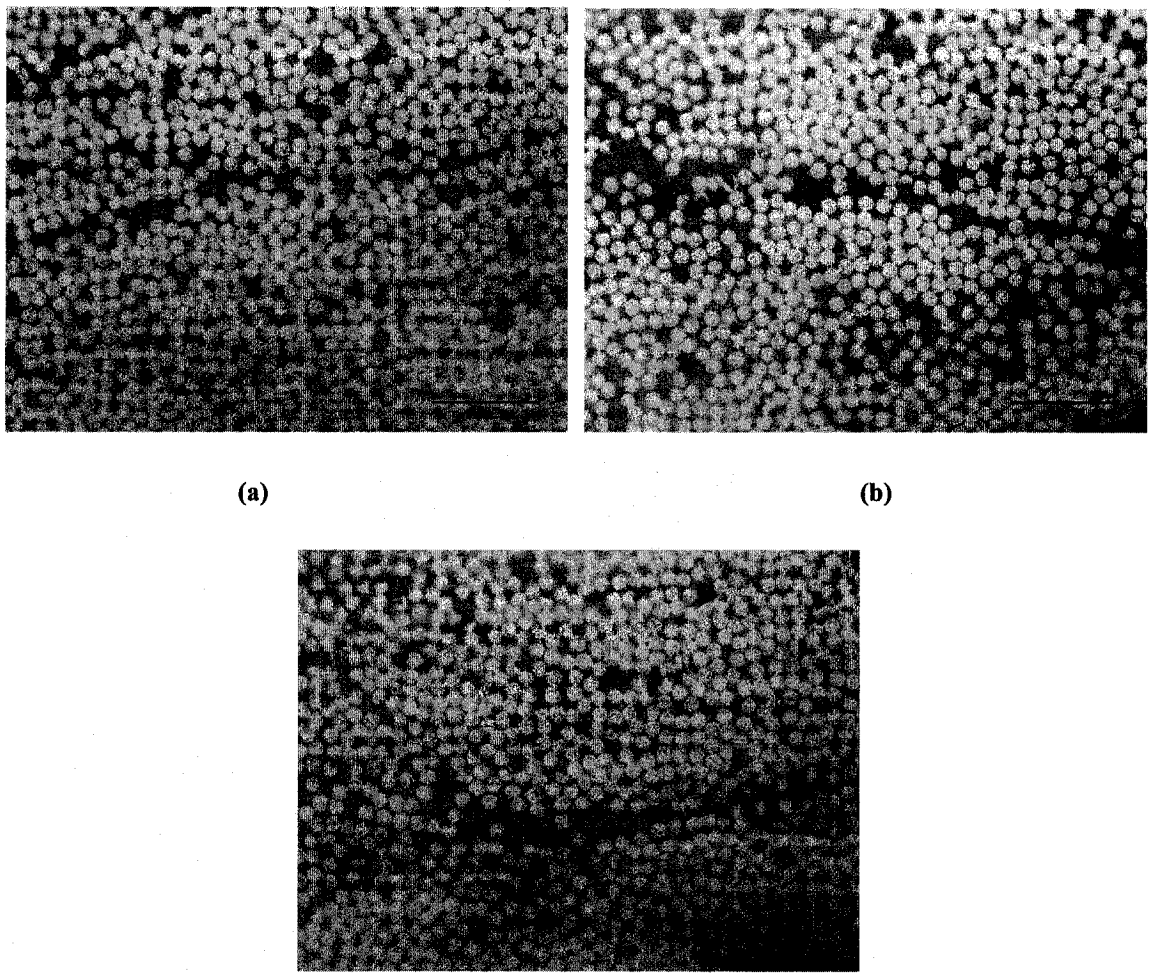

(a) **(b)**

(c)

Figure 4. 24. Images of Samples Cured at 80psi (0.55 MPa), Modified Process (×500) (a) 0phr clay (b) 2phr clay (c) 4phr clay

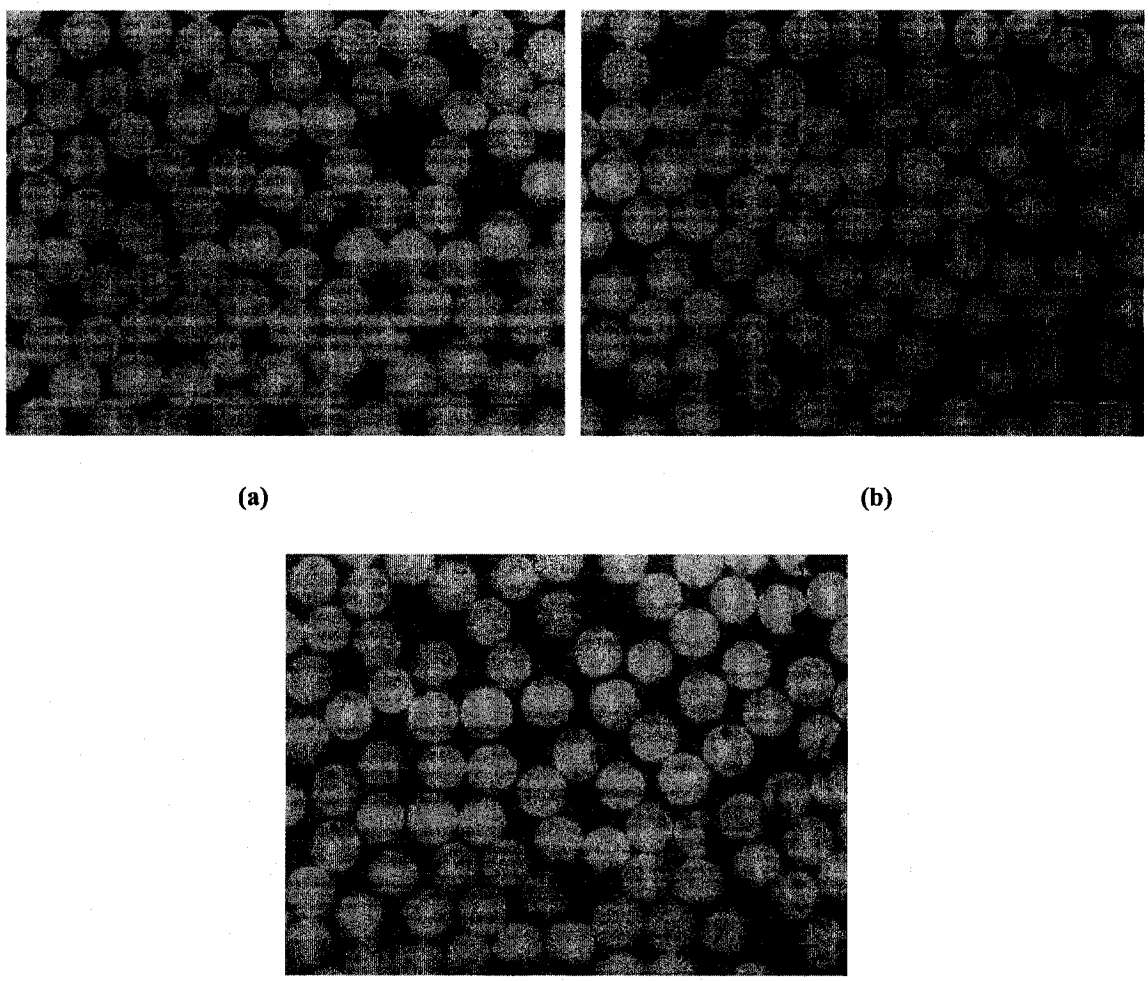

Figure 4. 25. Images of Samples Cured at 80psi (0.55 MPa), Modified Process (×1600)

(a) 0phr clay (b) 2phr clay (c) 4phr clay

properly decreased to avoid too many dry spots. In general, the target was to fabricate nanocomposites having similar fiber volume fraction, low voids, and less resin rich area.

According to the above analyses, the composite manufacture process was correspondingly modified and optimized. The mixing method did not alter. However, the degassing time for samples containing nanoclay was prolonged to 3 minutes in order to remove the bubbles more completely. Due to the interplay voids were mostly caused by

the gap between layers, the stack of fiber tape was pressed by vacuum bag to ensure a more compact laminate. As for autoclave process, autoclave pressure was adjusted to 80 psi (0.55 MPa) for samples without nanoclay. Meanwhile, a pressure of 100 psi (0.69 MPa) was kept for the samples containing nanoclay.

From Figures 4.23 to 4.25, the images of samples fabricated by the modified process are illustrated. Much less resin rich areas are observed; much less big voids are found; the distribution of fiber becomes more uniform. By means of image analysis, the fiber volume fractions were obtained as 65.1%, 61.9%, and 60% for 0 phr, 2 phr, and 4phr nanoclay content samples respectively. Thus, this result indicates that the modified composite manufacture process was acceptable for fabricating samples for mechanical and thermal properties investigation.

4.3 Summary

Against our anticipation, the resin film and solution methods are completely not feasible to manufacture carbon/TGDDM/nanoclay composites of good quality. The hot melt method was chosen to impregnate fiber tape; the lay-up and autoclave processes were applied to fabricate the composite laminate. The quality of composite laminate was apparently improved after the process parameters were appropriately modified. The laminate included less resin rich areas, less voids, and more uniform laminates were obtained.

Chapter 5 Mechanical Properties of Nanocomposites

Fracture is one of the most important properties of composites, especially for the structural materials. Epoxies are generally brittle; therefore, to meet various application needs, toughened epoxies should be developed. Epoxy can be toughened by rubber or thermoplastics. Through the reliable processes, the nanoclay-toughened composites of good quality were manufactured in this project. The following work will focus on the mechanical properties testing defined by ASTM D 5045-99, D5528-01, and D 790. The testing work consists of the following tasks:

- Plain-Strain Fracture Toughness and Strain Energy Release Rate of Composites (SENB, Single-Edge-Notch Bending)
- Mode I Interlaminar Fracture Toughness of Unidirectional Fiber-Reinforced Epoxy Matrix Composites
- Flexural properties

5.1 Plain-Strain Fracture Toughness and Strain Energy Release Rate of Composites

For the testing of Plain-Strain Fracture Toughness and Strain Energy Release Rate of Composites, the experimental specimens were made from pristine epoxy and nanoclay-filled epoxy. All the experiments aim at the matrix-dominating characteristics testing, in which the matrix plays the most critical role.

This test is designed to characterize the toughness of composites in terms of the critical-stress-intensity factor, K_{Ic}, and the energy per unit area of crack surface or critical strain energy release rate, G_{Ic}, at fracture initiation. The property K_{Ic} (G_{Ic}) characterizes the resistance of a material to fracture in the presence of a sharp crack under severe tensile constraint, such that the state of stress near the crack front approaches plane strain, and the crack-tip plastic region is small compared with the crack size and specimen dimensions in the constraint direction. A K_{Ic} (G_{Ic}) value is believed to represent a lower limiting value of fracture toughness. This value may be used to estimate the relation between failure stress and defect size for a material in service wherein the conditions described above would be expected [60].

5.1.1 Experimental Work

The epoxy, curing agent, and nanoclay used for this test are exactly the same as those used for former experiments. Besides, the mixing and degassing work follow the same procedures used in the last two chapters.

The fully mixed and degassed liquid resin system was poured into silicone rubber mold,

which was made from Aircast 3700 having low shrinkage and high strength, and being suitable for casting and moldmaking. The rubber mold was made by the male mold shown in Appendix. Before casting, the rubber mold was preheated at 80 °C for 2 hours.

The curing schedule was:

0.5hr/80 °C + 0.5hr/100 °C + 1.5hr/120 °C + 2hr/177 °C + 4 or 8hr-postcure/200 °C.

The specimens with different nanoclay contents are shown in Figure 5.1.

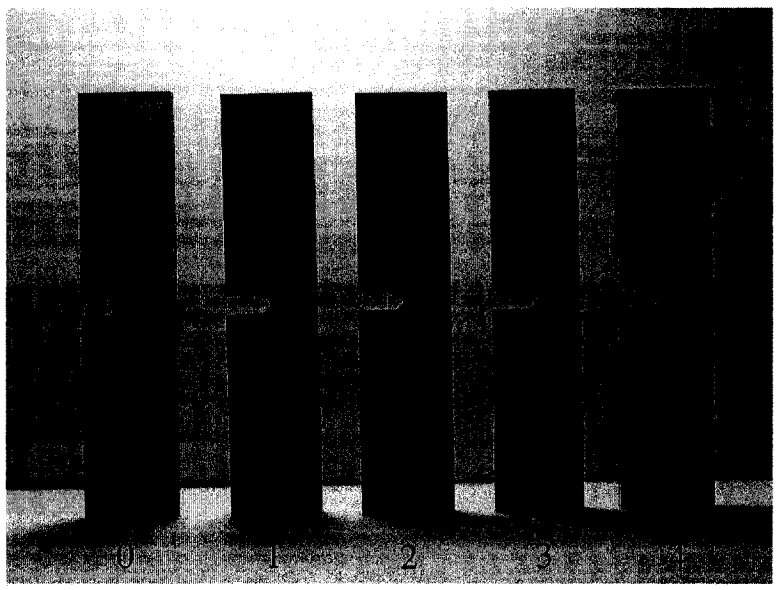

Figure 5. 1. Specimens for SENB Test, Nanoclay Content: 0-0 phr, 1-1 phr, 2-2phr, 3-3 phr, 4-4 phr

SENB specimen dimensions and testing configuration are shown in Figure 5.2. The relation between sample width, W, and sample thickness, B, is $2 < W/B < 4$. The crack length, a, should be $0.45 < a/W < 0.55$. The specimen size is $100 \times 22 \times 7.3$ mm.

For this experiment, the crack must be sufficiently sharp to ensure that a minimum value of toughness is obtained. A sharp crack was obtained by inserting a fresh razor

blade and tapping. The depth of the crack must be at least two times longer than the width of the sawed-in slot (see Figure 5.3). The basic test condition includes room temperature (23 °C) and a loading rate of 5mm/min. For each experimental condition, three to five replicated tests were made.

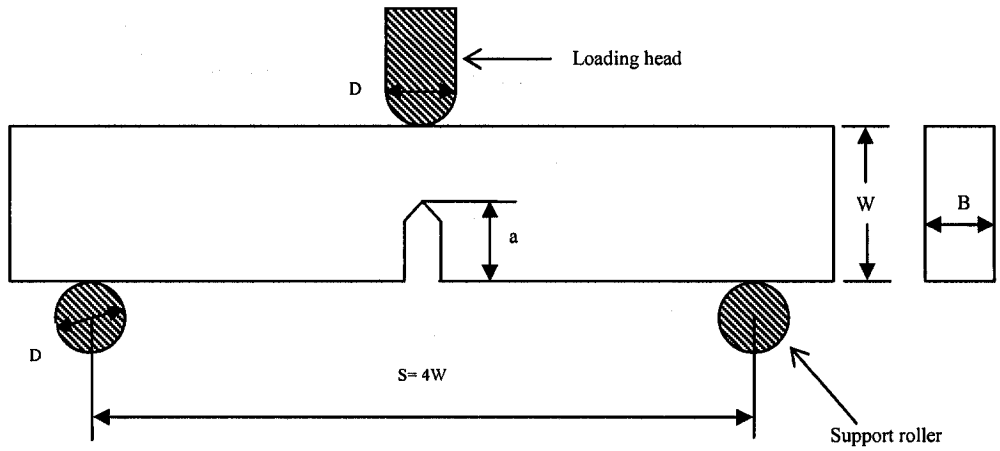

Figure 5. 2. SENB Specimen Testing Configuration

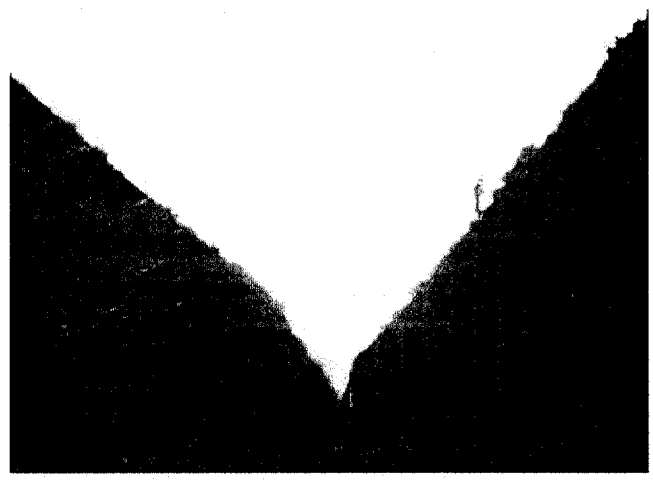

× 50

Figure 5. 3. Crack Tip for SENB Sample

5.1.2 Calculation and Analysis of Results

The critical-stress-intensity factor, K_{Ic}, was calculated by the following formula.

$$K_{Ic} = \left(\frac{P_{max}}{BW^{1/2}}\right) f(x) \quad , \text{MPa·m}^{1/2}$$

$$f(x) = 6x^{1/2} \frac{\left[1.99 - x(1-x)(2.15 - 3.93x + 2.7x^2)\right]}{(1+2x)(1-x)^{3/2}}$$

$$x = a/W \quad (0 < x < 1)$$

P_{max} – maximum load, kN,

B – specimen thickness, cm,

W – specimen width, cm,

a – crack length, cm.

Tabulated values of $f(x)$ are available in ASTM D-5045.

The critical strain energy release rate, G_{Ic}, was calculated by the formula below.

$$G_{Ic} = \frac{U}{(BW\Phi)}, \quad \text{kJ/m}^2$$

$$\Phi = \frac{A + 18.64}{dA/dx}$$

$$U = (1/2)P_{\max}(u_{\max} - u_i)$$

$$A = [16x^2(1-x)^2]\left(8.9 - 33.717x + 79.616x^2 - 112.952x^3 + 84.815x^4 - 25.672x^5\right)$$

$u_{\max}$ – maximum displacement, mm

u_i – indentation displacement, mm (obtained by testing an uncracked calibration specimen, see Fig. 5.4)

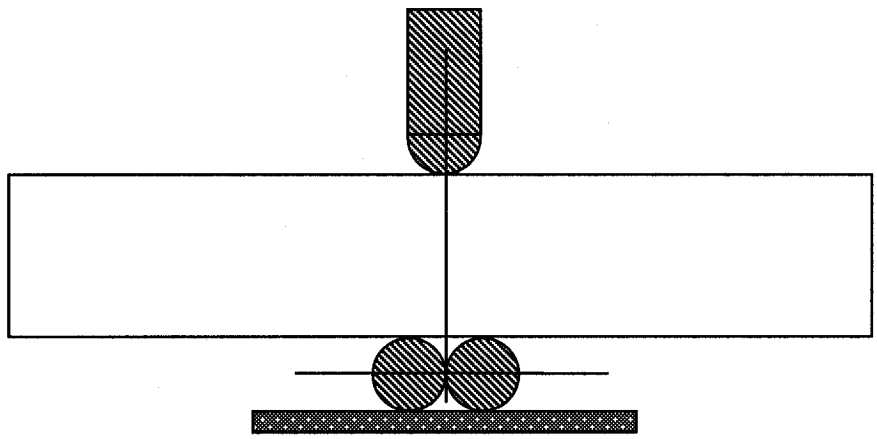

Figure 5. 4. Arrangement for Finding Indentation Displacement

Tabulated values of the energy calibration factor, Φ, are also available in ASTM D-5045.

The experimental results of SENB testing, including both 8-hour postcure and 4-hour postcure at 200 °C, are shown in Figures 5.5 and 5.6. The K_{Ic} values in Figure 5.5 indicate that the facture toughness obviously increased with the addition of nanoclay.

With the addition of 1 phr, K_{Ic} increased by 92.3%; then it increased relatively slower, to 109.2%

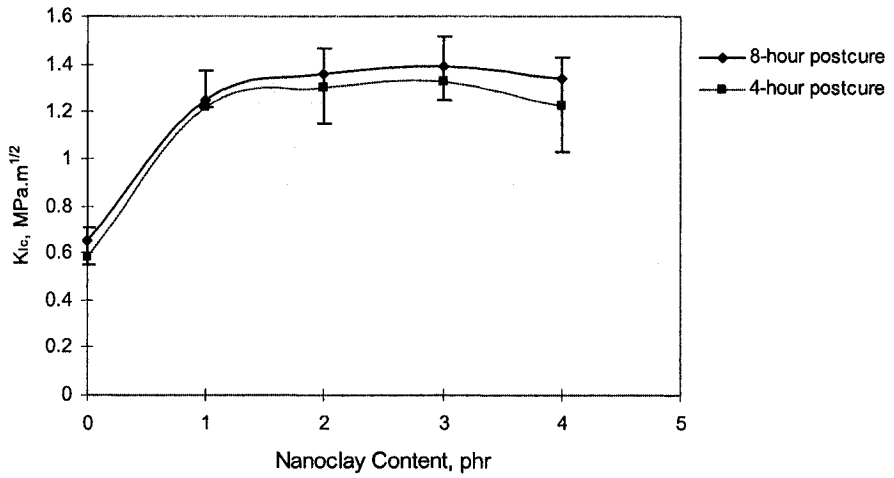

Figure 5. 5. Relationship between K_{Ic} and Nanoclay Content

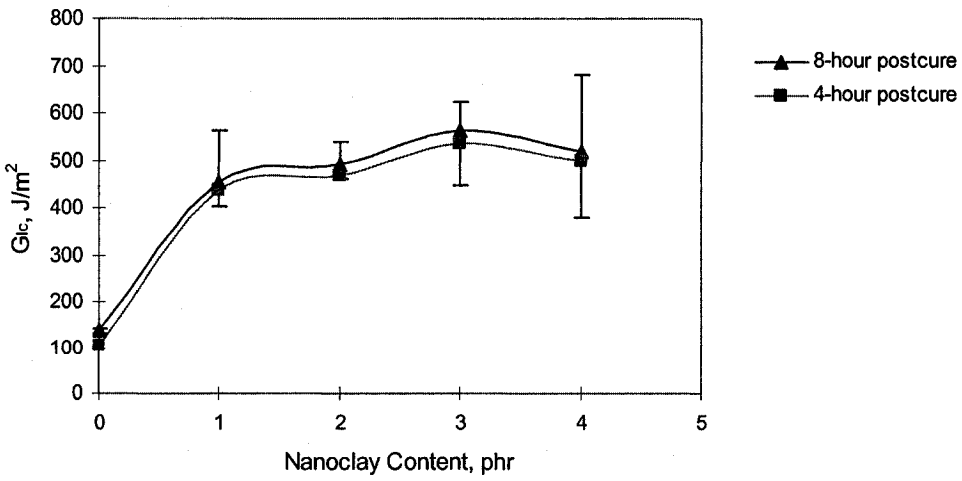

Figure 5. 6. Relationship between G_{Ic} and Nanoclay Content

and 113.8% for 2 and 3 phr nanoclay content respectively. When the nanoclay content increased to 4 phr, the K_{Ic} value slightly dropped, but still increased by 106.2%, compared to the number at 0 phr.

A similar phenomenon was found for G_{Ic} values. The increase rate of G_{Ic} for 1, 2, 3 phr nanoclay are 229.7%, 257.4%, 308.7% respectively. Once nanoclay content increases to 4 phr, the G_{Ic} values also slightly dropped. Similarly, G_{Ic} still increases by 277.2%, compared to the value at 0 phr.

The above results are also very similar to the work that has been done previously at CONCOM for SENB testing [9, 20]. The difference of K_{Ic} and G_{Ic} augmentation might be caused by the difference of raw epoxy resin. Although the epoxy used in this project has the same chemical name (Araldite® MY720) as the one used in previous work, the viscosity of the epoxy used in this project is higher (20Pa·s) than the viscosity in previous work (16 Pa·s). Dispersion of nanoclay becomes more difficult and challenging. Besides, more voids might exist in composites. Consequently, it leads to a drop of fracture toughness. However, the augmentation of fracture toughness is still quite evident and significant.

To explain the causes of the augmentation of fracture toughness, different theories have been put forward [7,61–63].

The augmentation of critical-stress-intensity factor, $K_{Ic,}$ and critical strain energy release rate, G_{Ic}, was resulted from the addition of nanoclay and the corresponding "Crack Pinning Mechanism" (Figure 5.7). The propagation of cracks can be impeded by

rigid, impenetrable and well-bonded particles. Once a propagating crack reaches the nanoclay particles, it gets pinned, and then bows out between the particles. Thus, secondary cracks are formed; the crack propagation needs more absorption of energy due to the formation of new facture surfaces and non-linear crack front.

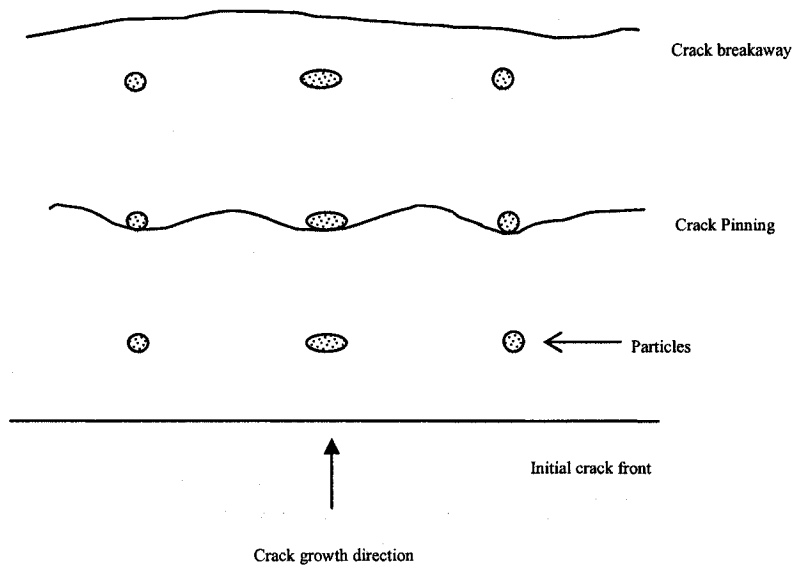

Figure 5. 7. Crack Pinning Mechanism [7]

In the course of a crack's propagation, crack may be blunted due to localized shear yielding or damage zone, such as debonding of the particle/matrix interface and fracture of particles. Rigid particles act as stress concentrators since they have different elastic properties compared to pristine epoxy. When the local stress exceeds the yield stress of the matrix or the adhesive strength of the particle/matrix interface, shear yielding or debonding phenomena will occur. Thus, the composite may absorb more energy.

With respect with the causes of toughening, some other theories or models also

contribute to the interpretation, such as crack-path deflection mechanism and crack bridging mechanism of toughening. However, only one theory cannot explain all the experimental phenomena and results because different researchers might use different materials and manufacturing methods. Moreover, fracture behavior of material is a quite complicated mechanical phenomenon; toughening mechanism may be a combination of several mechanisms [4].

5.1.3 Microscopy Analysis of SENB Samples

In the last section, the calculation results indicate that both of plain-strain fracture toughness (K_{Ic}) and critical strain energy release rate (G_{Ic}) have been dramatically enhanced by means of the addition of nanoclay. The augmentation of fracture toughness can be interpreted according to some toughening mechanisms. In this section, the

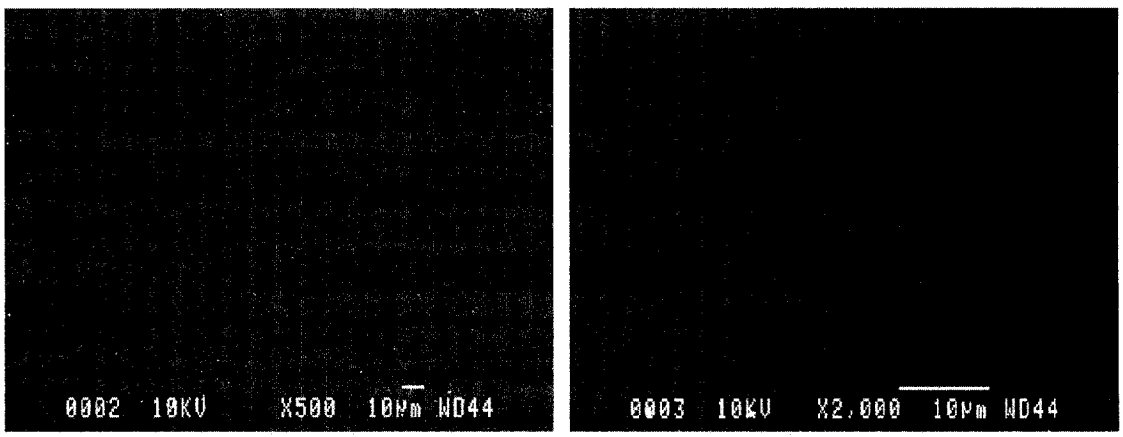

(a) (b)

Figure 5. 8. Fracture Surface of SENB Specimen without Nanoclay (a) ×500,(b) ×2000

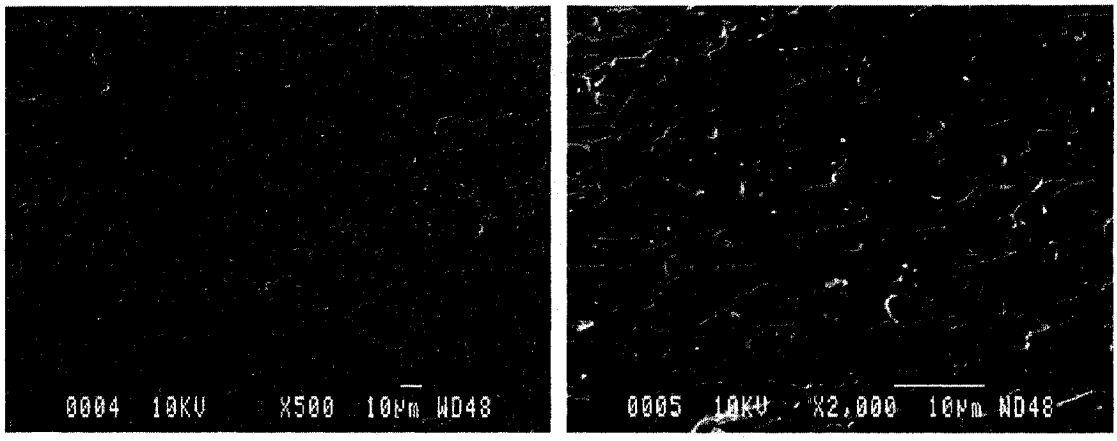

(a) (b)

Figure 5. 9. Fracture Surface of SENB Specimen Containing 2 phr Nanoclay (a) ×500, (b) ×2000

microstructure of the sample's fracture surface was investigated by means of scanning electron microscope (SEM).

The SEM graphs of the specimen without nanoclay are shown in Figure 5.8. These pictures illustrate that the fracture surface of the neat epoxy matrix is characterized by large smooth areas, having no evident protuberances, hackles, and crack branches. In other words, the fracture surface is very smooth and sharp. This phenomenon indicates that the fracture of neat epoxy matrix is a brittle behavior due to a weak resistance to crack propagation.

Figure 5.9 illustrates the SEM graphs of the specimen containing 2 phr nanoclay. Obviously, the fracture surface of this specimen is much rougher than the one of neat epoxy specimen. The whole fracture surface is full of hackles and humps, which look like fish scales. In addition, there are a few small holes, which may be caused by the pull-out of nanoclay agglomerates. The micrographs of the specimen containing 4 phr

nanoclay also illustrate the similar microstructure of the fracture surface. It was noticed

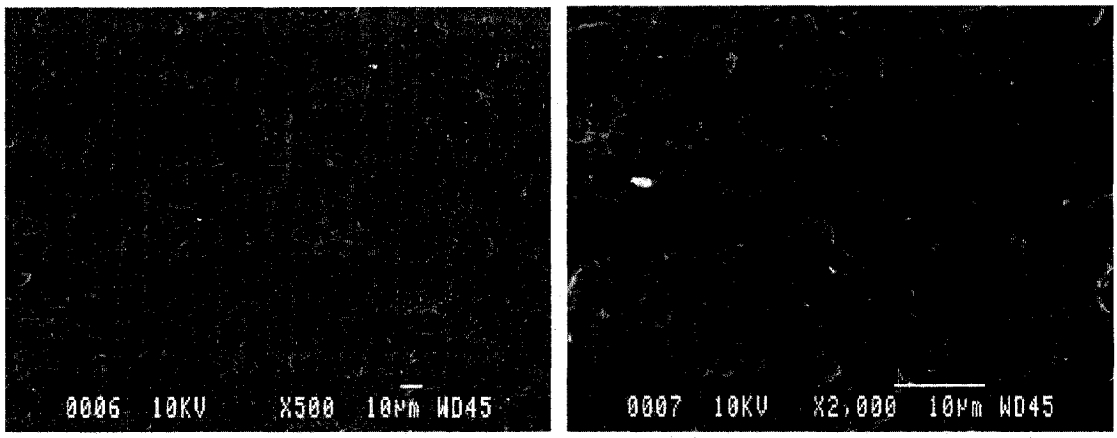

(a) (b)

Figure 5. 10. Fracture Surface of SENB Specimen Containing 4 phr Nanoclay (a) ×500,(b) ×2000

that the 4 phr nanoclay samples had more voids, which were resulted from its high viscosity and the difficulty of full degassing (Fig 5.10). Generally, the augmentation of fracture toughness may be caused by the energy-consuming mechanisms, such as crack front pinning, secondary cracks, and particle debonding etc.

5.2 Mode I Interlaminar Fracture Toughness of Unidirectional Carbon Fiber-Reinforced Composite

Susceptibility to delamination is one of the major weaknesses of many advanced laminated composite structures. Over the past two decades, it has become common practice to characterize the resistance to delamination using fracture mechanics [46].

Knowledge of a laminated composite material's resistance to interlaminar fracture is useful for product development and material selection.

Interlaminar cracking or delamination can occur under three basic modes, opening or peel mode (Mode I), forward sliding shear mode (Mode II), scissoring shear mode (Mode III), or under combinations thereof (see Figure 5.11). The resistance to delamination growth is expressed in terms of the interlaminar fracture toughness, which has three forms corresponding to the three basic delamination modes. The interlaminar fracture

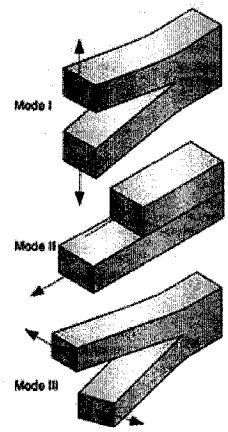

Figure 5. 11. Basic Delamination Modes in Composite Material [64]

toughness is measured by the strain energy release rate (G_I, G_{II}, or G_{III}), which is the energy dissipated per unit area of delamination growth [64].

In this project, ASTM D5528-01 [65] was used to determine the opening Mode I interlaminar fracture toughness, G_{Ic}, of unidirectional carbon fiber-reinforced epoxy composite by means of the double cantilever beam (DCB) specimen (Figure 5.12). A

measurement of the Mode I interlaminar fracture toughness, independent of specimen geometry or method of load introduction, is useful for establishing design used in damage tolerance analyses of composite structures made from these materials.

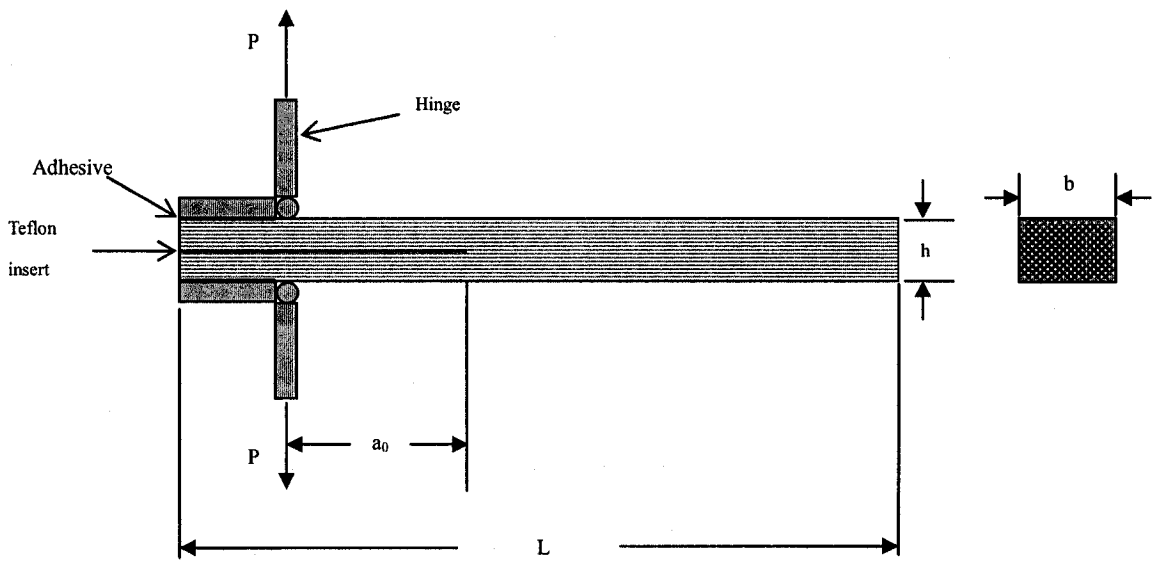

Figure 5. 12. Double Cantilever Beam Specimen

5.2.1 Experimental Work

The epoxy, curing agent, nanoclay, and carbon fiber used in this experiment are the same as the one used in chapter 4. Extraordinarily, Teflon film was used in the specimens to create an initiation site for the delamination of laminate. The Teflon film has thickness of 13μm, which was courteously provided by DuPont.

The test laminates contain 12 plies of unidirectional carbon fiber, with delamination

growth occurring in the 0° direction. A non-adhesive insert (Teflon film) is implanted at the midplane of the laminate during lay-up to form an initiation site for the delamination, which is very meaningful for interlaminate fracture toughness test. According to reference [65], teflon film was used in this experiment because it could avoid problems of folding or crimping at the end of the insert. Besides, Teflon film can definitely resist the curing temperature (180 °C) in this experiment.

The composite panels were manufactured following the manufacturing processes introduced in Chapter 4. All the specimens were cut from the panels, having a size of 125 mm (L) × 25 mm (b) × 3 mm (h). The insert length is approximately 63 mm. This distance corresponds to an initial delamination length of approximately 50 mm plus the extra length required for bonding the hinges. The bonding surfaces of the loading hinges were scrubbed with sandpaper, then properly cleaned with acetone to remove any contamination. The specimen prepared for the test is shown in Figure 5.13. Before testing, a thin layer of water-based typewriter correction fluid is coated on both edges of the specimen just ahead of the insert, to aid in visual detection of delamiantion onset. The specimens were marked with thin vertical lines every 1 mm for the first 5 mm section, and every 5 mm for the remaining section. The delamination length is the sum of the distance from the loading line to the end of the insert plus the increment of growth determined from the tick marks.

The specimen prepared was mounted in the grips of the loading machine (MTS), aligned and centered (Figure 5.14). The load is applied to the specimen at a constant

crosshead rate of 1 mm/min. The load, the displacement and the delamination values are

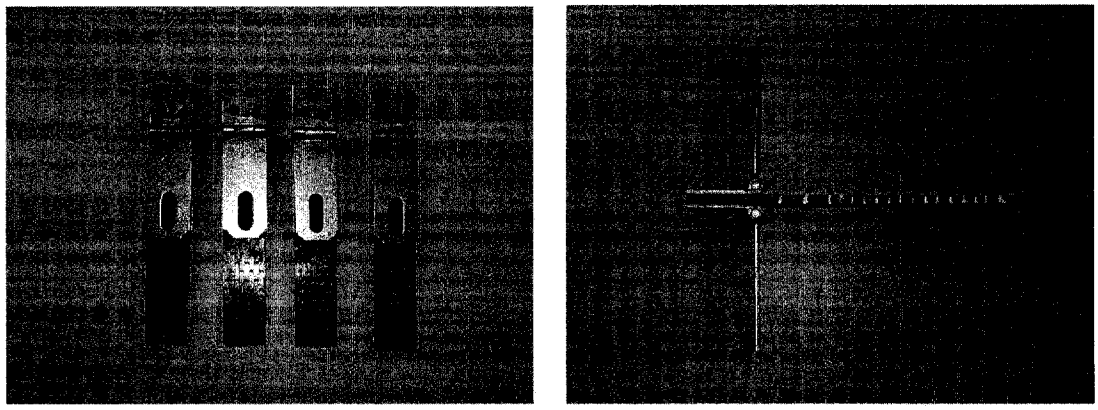

Figure 5. 13. Specimen for Mode I Interlaminar Fracture Toughness Testing

continuously recorded. To aid in the observation of the delamination front as it extends along one edge during the test, a traveling optical microscope with a magnification 70 ×, was positioned on one side of the specimen.

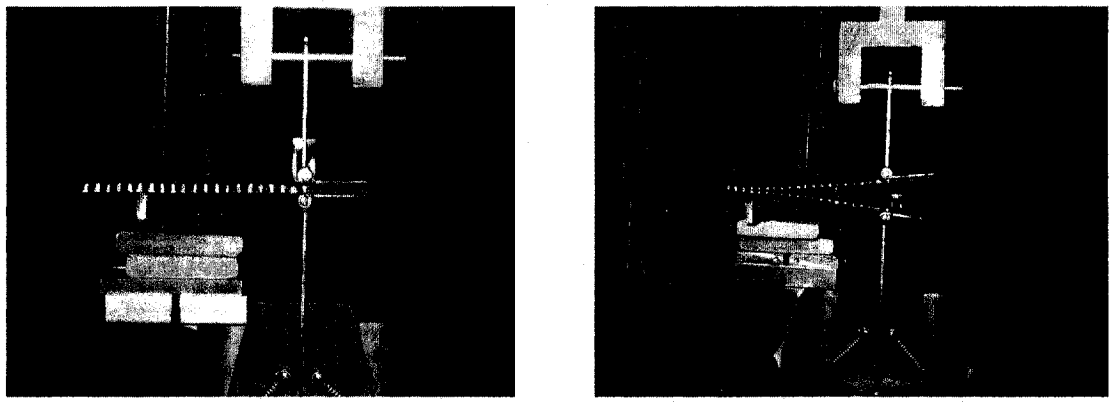

Figure 5. 14. Mode I Interlaminar Fracture Toughness Testing Setup

5.2.2 Calculation and Results Analysis

Three methods for calculating G_{Ic} values have been proposed [65]. These consisted of a modified beam theory (MBT), a compliance calibration (CC) and a modified compliance calibration method (MCC). None of the three was clearly superior to the others. However, the MBT method yielded the most conservative values of G_{Ic} for most cases [44]. Therefore, MBT was used to calculate G_{Ic}.

The modified beam theory expression for the strain energy release rate of a double cantilever beam is as follows:

$$G_I = \frac{3P\delta}{2ba}$$

Where:

P — load,

δ — load point displacement,

b — specimen width,

a — delamination length.

In practice, this expression will overestimate G_I because the beam is not perfectly built-in. One way of correcting is to treat the DCB as if it contained a slightly longer delamination, $a+|\Delta|$, where Δ may be determined experimentally by generating a leasts squares plot of the cube root of compliance, $C^{1/3}$. Here, C is the ratio of the displacement to the applied load, $\frac{\delta}{P}$ (Figure 5.15). Thus, the Mode I interlaminar fracture toughness can be calculated as follows:

$$G_I = \frac{3P\delta}{2b(a+|\Delta|)}$$

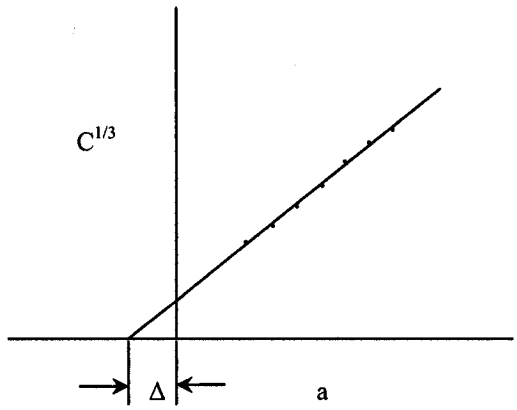

Figure 5. 15 Modified Beam Theory

In the DCB test, as the delamination grows from the insert, a resistance-type fracture behavior typically develops where the calculated G_{Ic} first increases, and then stabilizes with further delamination growth. A resistance curve (R curve, Figure 5.16) depicting G_{Ic} as a function of delamination length was generated to characterize the initiation and propagation of a delamination in the unidirectional specimen.

Three definitions for an initiation value of G_{Ic} have been evaluated in reference [44]. These include G_{Ic} values determined using the load and deflection measured (1) at the point of deviation from linearity in the load-displacement curve (NL), (2) at the point at which delamination is visually observed on the edge (VIS) measured by the microscope, and (3) at the point at which the compliance has increased by 5% or the load has reached the maximum value (5%/max). The NL G_{Ic} value, which is typically the lowest of the

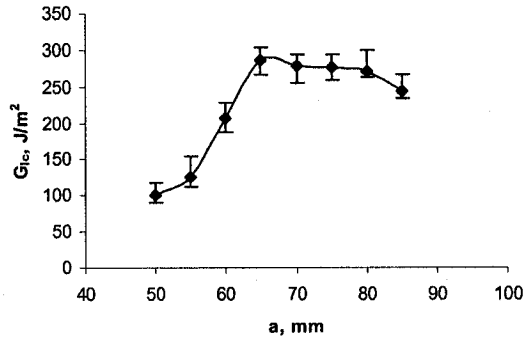

(a)

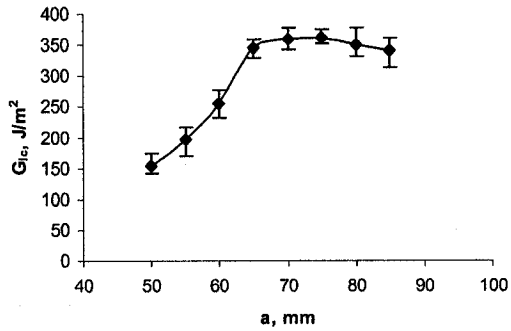

(b)

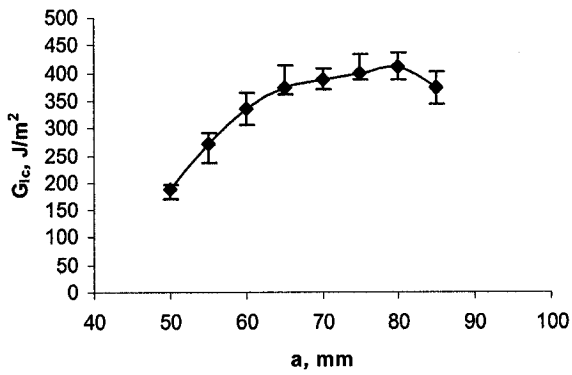

(c)

Figure 5. 16. Delamination Resistance Curves (R Curves) (a) 0 phr, (b) 2 phr, (c) 4 phr

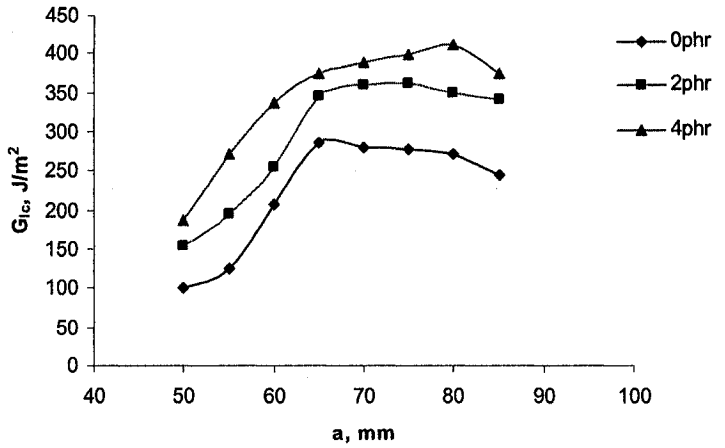

Figure 5. 17. A Combination of Delamination Resistance Curves (R Curves)

three G_{Ic} initiation values, is recommended for generating delamination failure criteria in durability and damage tolerance analyses of laminated composite structure. For brittle matrix composites, such as TGDDM composites, the difference between NL and VIS G_{Ic} values is negligible [65].

Figure 5.16 indicates that the specimens containing nanoclay possess higher G_{Ic} compared to the specimens without nanoclay. In all cases, G_{Ic} increases relatively faster at the first 15~20 mm delamination, and then it becomes relatively stable. In this project, the initiation G_{Ic} values are considered as interlaminar fracture toughness. Obviously, the initiation G_{Ic} values are 101.1 J/m^2, 154.3 J/m^2, and 187 J/m^2 for 0, 2, 4 phr nanoclay content respectively. That is to say, with the addition of nanoclay, the interlaminar fracture toughness increased by 52.6% and 85%.

As mentioned above, NL G_{Ic} value is recommended as interlaminar fracture toughness. However, a complete R curve was illustrated to depict G_{Ic} as a function of delamination

length. The principle reason for the observed resistance to delamination is the development of fiber bridging resulting from growing the delamination between 0° unidirectional plies. Due to the nesting inherent in unidirectional laminates, fibers above and below the midplane tend to bridge the delamination as it grows from the implanted insert (Figure 5.18). The result of this bridging mechanism is an evident increase in toughness with delamination growth reflected through R curve. In fact, fiber bridging is an artifact of unidirectional DCB specimen and does not occur in structural composites laminates where delamiantion typically form between plies of dissimilar orientation. Therefore, the G_{Ic} values calculated beyond the end of the implanted Teflon insert is not entirely reliable [44, 46]. An initiation value of G_{Ic} measured from the end of the insert is more reasonable and trustable.

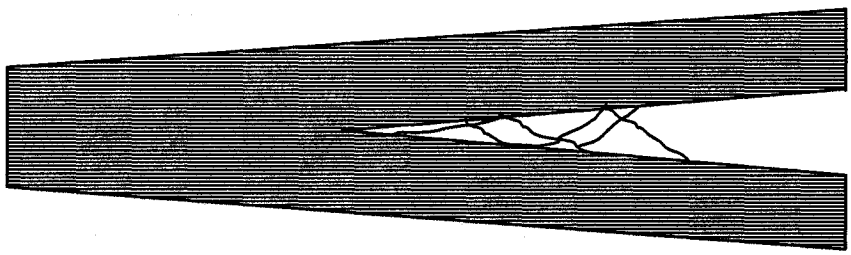

Figure 5. 18. Fiber Bridging in DCB Test Specimen

There is another question here: "Now that the initiation value of G_{Ic} is preferred, why an entire R curve is still drawn?" The reason is that the R curve resulting from the continuous measurement of delamination growth beyond the Teflon insert can provide

useful insight into the validity of the onset value from the insert. Furthermore, the entire R curve is also useful to compare the difference of facture behavior of specimens with different nanoclay content.

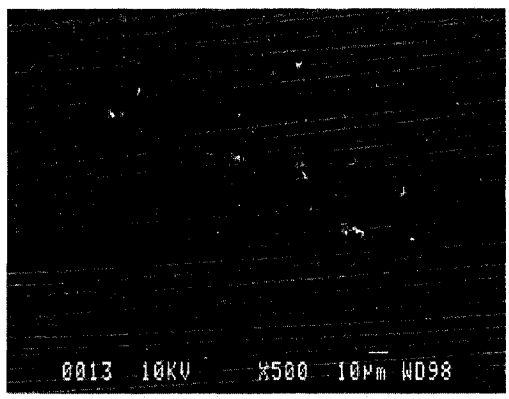

(a-1)

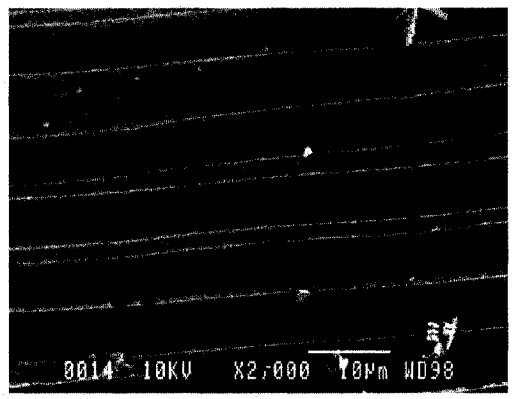

(a-2)

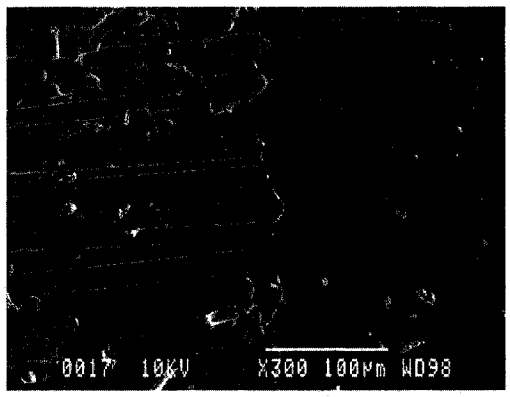

(b)

Figure 5. 19. Fracture Surface of DCB Specimen without Nanoclay. (a-1) and (a-2) fracture surface, (b) crack initiation area

In Figures 5.19, 5.20, and 5.21, the SEM micrographs of fracture surfaces are illustrated. The fracture surface of the specimen without nanoclay is very clean and regular; there are no evident hackles, fiber and matrix debonding, fiber pull-out, fiber

bridging, and fiber fracture. On the contrary, the fracture surfaces of the specimens containing nanoclay are obviously much rougher. The hackles, fiber-matrix interface debonding, fiber pull-out, fiber bridging, and fiber fracture phenomena are observed. From the micrographs, on the fracture surfaces, post-debonding friction and stress

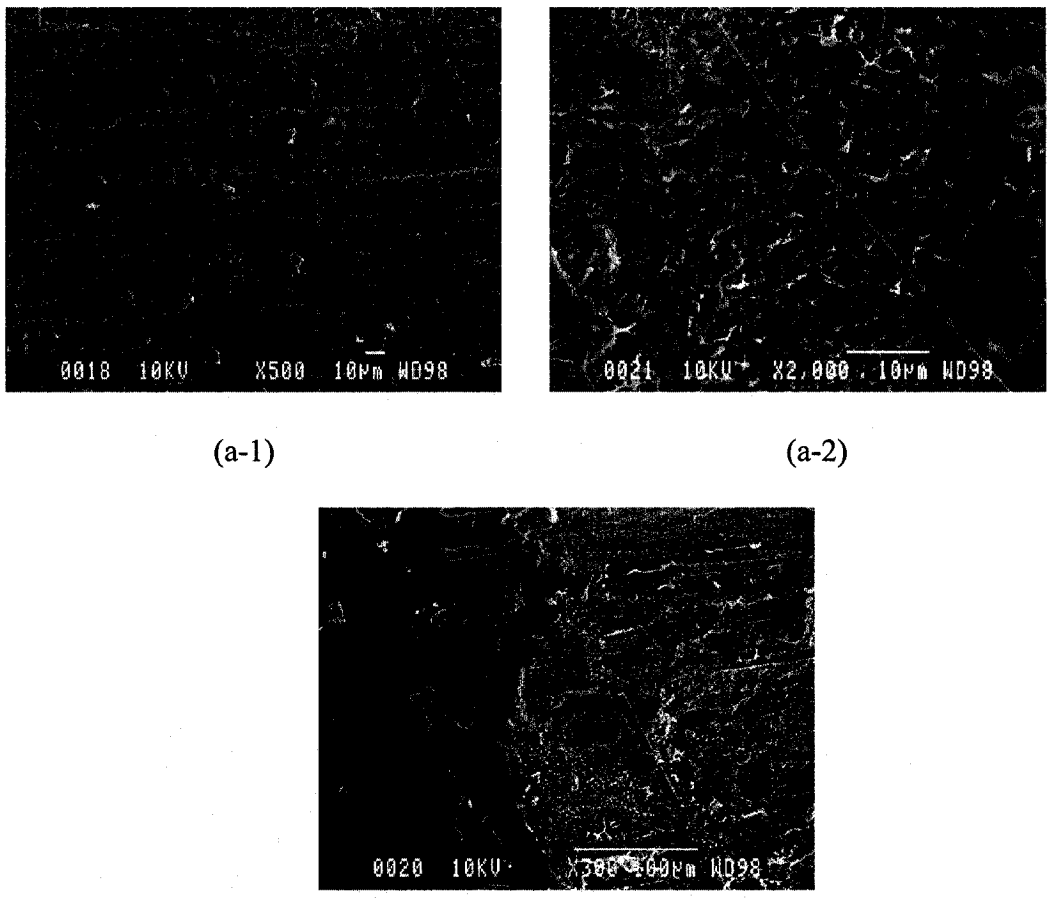

(a-1) (a-2)

(b)

Figure 5. 20. Fracture Surface of DCB Specimen containing 2 phr Nanoclay. (a-1) and (a-2) fracture surface, (b) crack initiation area

redistribution might also occur in the course of delamination. All of these phenomena consume energy and contribute to the toughness of the composites. More importantly,

addition of nanoclay made a big change to the epoxy matrix; the matrix definitely was toughened by nanoclay, as discussed in Chapter 4. The addition of nanoclay plus other fracture mechanisms result in the augmentation of interlaminar fracture toughness of composites.

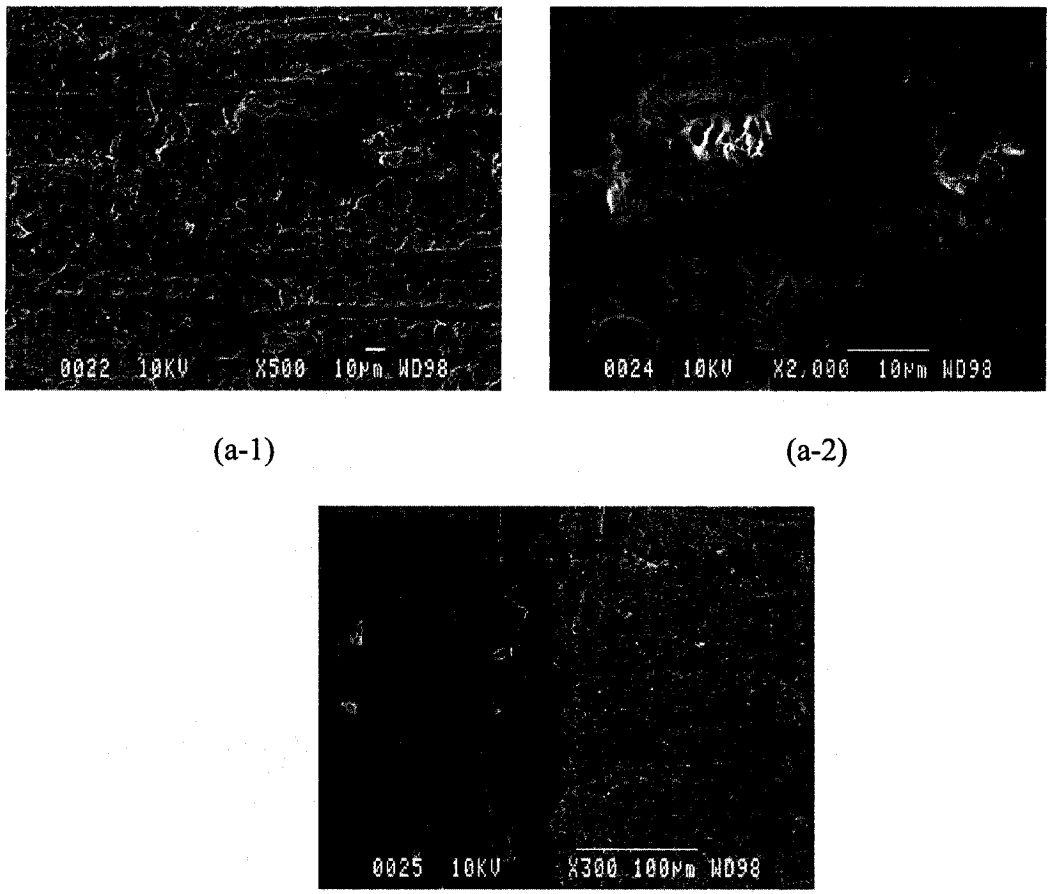

Figure 5. 21. Fracture Surface of DCB Specimen containing 4 phr Nanoclay. (a-1) and (a-2) fracture surface, (b) crack initiation area

5.3 Flexural Properties of Carbon Fiber-Reinforced Nanocomposites

The determination of flexural properties is meaningful for quality control and specification purposes. Flexural strength and modulus were determined by 3-point bend test (Figure 5.22) in this project.

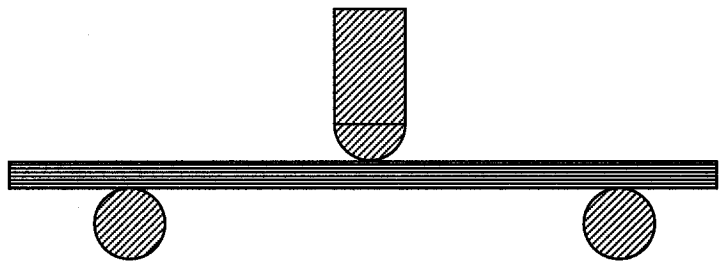

Figure 5. 22. Three-Point Bend Test Configuration.

The test follows ASTM D 790. The specimens were cut into a size of 130 × 12.7 × 3.2 mm from composite plates. The span-depth-ratio is 16:1. The nanoclay contents for samples are 0 phr, 2 phr, and 4 phr respectively. Flexural strength is calculated by the following equation:

$$\sigma_f = 3PL / 2bd^2$$

σ = stress in the outer fibers at midpoint, MPa,

P= load at a given point on the load-deflection curve, N,

L= support span, mm,

b= width of beam tested, mm,

d= depth of beam tested, mm.

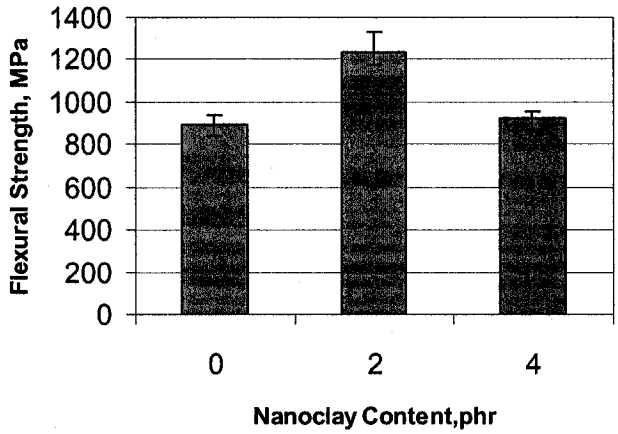

Figure 5. 23. Flexural Strength vs Nanoclay Contents

The testing results indicate that the flexural strength increased by 38.25% when 2 phr nanoclay was added into the epoxy matrix (Figure 5.23). However, 4 phr clay addition led to an apparent drop of flexural strength. This phenomenon might be resulted from the comparatively poorer dispersion of nanoclay and more possibility of the existence of voids in composites.

The tangent modulus of elasticity, often called the "modulus of elasticity," is the ratio, within the elastic limit, of stress to corresponding strain. It is calculated by drawing a tangent to the steepest initial straight-line portion of the load-deflection curve and using the following equation:

$$E_B = L^3 m / 4bd^3$$

where:

E_B = modulus of elasticity in bending, MPa,

L = support span, mm,

b = width of beam tested, mm,

d = depth of beam tested, mm,

m = slope of the tangent to the initial straight-line portion of the load-deflection curve, N/mm.

The testing result of the modulus of elasticity is shown in Figure 5.24.

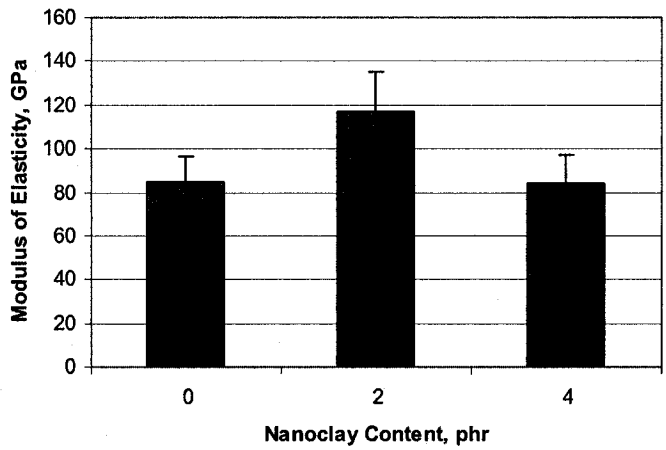

Figure 5. 24. Modulus of Elasticity vs Nanoclay Content

The results indicate that the modulus of elasticity increased by 37.38% with an addition of 2 phr nanoclay. There was no evident variation in modulus when 4 phr nanoclay was filled. Referring to the results of flexural strength, and fracture toughness, it seems that an amount of 2 phr nanoclay can evidently enhance the mechanical properties, however, an introduction of more nanoclay does not enhance mechanical properties, even could have adverse effect on the mechanical properties.

5.4 Summary

Through SENB tests, plain-strain fracture toughness nanoclay-filled TGDDM epoxy is augmented by 92.3%, 109.2%, 113.8%, and 106.2% for nanoclay content of 1 phr, 2 phr, 3 phr, and 4 phr respectively. In the meantime, strain energy release rate is augmented by 229.7%, 257.4%, 308.7%, and 308.7% respectively. In mode I interlaminar fracture toughness of unidirectional carbon fiber-reinforced composite test, interlaminar fracture toughness was also increased by 52.6% and 85% owing to the existence of 2 and 4 phr nanoclay. The SEM images, in both cases, illustrated that the fracture surface of nanoclay-filled specimen was much rougher than the fracture surface of neat epoxy specimen. This indicates that nanoclay absolutely contributed to the toughening mechanisms and the augmentation of fracture toughness. Referring to the result of Chapter 3, more importantly, we have attained the goal of increasing the fracture toughness without losing the Tg and moduli of the composites. A small amount of nanoclay (2 phr) evidently contributes to the augmentation of flexural strength and modulus. However, more nanoclay does not enhance the flexural strength and modulus.

Chapter 6 Flammability and Thermal Properties

Flammability and thermal properties are very important factors that must be taken into account in the application of composites. These factors involve the structural stability and safety of composites when they are used in elevated temperature environment or even in fire. This chapter aims at the flammability and thermal properties of nanocomposites investigation, attempting to find the influence of nanoclay on the flammability of composites.

Flammability is the ease with which a substance will ignite, causing fire or combustion. Combustion is a complex physico-chemical process between a fuel and an oxidizing agent accompanied by heat evolution and light phenomena [66]. Flammability testing of polymer was commenced in the mid-fifties. Some test methods have been standardized by the specialized organizations. Meanwhile, a number of testing procedures still exists individually according to the different requirements in different industries. In this project, the "ASTM Standard Test Method for measuring the Minimum Oxygen Concentration to support Candle-Like Combustion of Plastics (Oxygen Index), D 2863-97 and Thermogravimetric Analysis (TGA) were chosen to evaluate the flammability of composites.

6.1 Minimum Oxygen Concentration Measurement

Minimum oxygen concentration (Limiting Oxygen Index, LOI) was measured according to the ASTM standard D 2863-97. The principle of this test is measuring the minimum concentration of oxygen that will support flaming combustion in a flowing mixture of oxygen and nitrogen. This test can be used to measure and describe the properties of materials in response to heat and flame under controlled laboratory conditions. The results of this test may be used as elements of a fire risk assessment which takes into account all of the factors which are pertinent to an assessment of the fire hazard of a particular end use.

6.1.1 Experimental Work

Clay containing epoxy specimen was selected for investigation. Composites were cut into the size of 80 × 7 × 3 mm. A reference mark was drawn 10 mm below the top of the specimen. Another mark was drawn 50 mm below the reference line above (Figure 6.1).

The experimental equipment layout is shown in Figure 6.2, consisting of limiting oxygen index chamber (Qualitest), gas supplier, flame igniter, and other subsidiary devices. According to the criterion of Oxygen Index Measurements, the period of burning after ignition is 180 seconds; the extent of burning is 50 mm below the upper reference mark.

Before ignition, the gas mixing and flow controls are set so that an oxygen/nitrogen mixture at 23 ± 2 °C, containing the desired concentration of oxygen, is flowing

through the chimney at a rate 40 ± 2 mm/s. The gas flow is allowed to purge the chimney for at least 30 seconds. To propagate ignition, the igniter is lowered sufficiently to apply the visible flame to the end of the specimen. Once any part of the visibly burning portion reaches the level of the upper reference mark, the specimen is considered to be ignited (Figure 6.3). If neither the period nor extent of burning exceeds the relevant limit (180 seconds, 50mm), an "O" response is recorded, meaning the oxygen index is not less than the specified value. Alternatively, if either the period or extent of burning exceeds the relevant limit, an "X" response is recorded, meaning the oxygen index is less than the specified value.

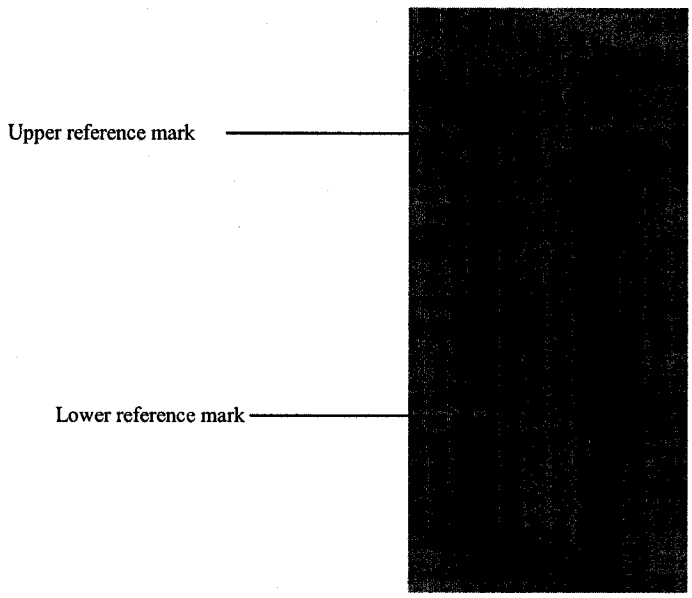

Figure 6. 1. Specimen for Oxygen Index Test

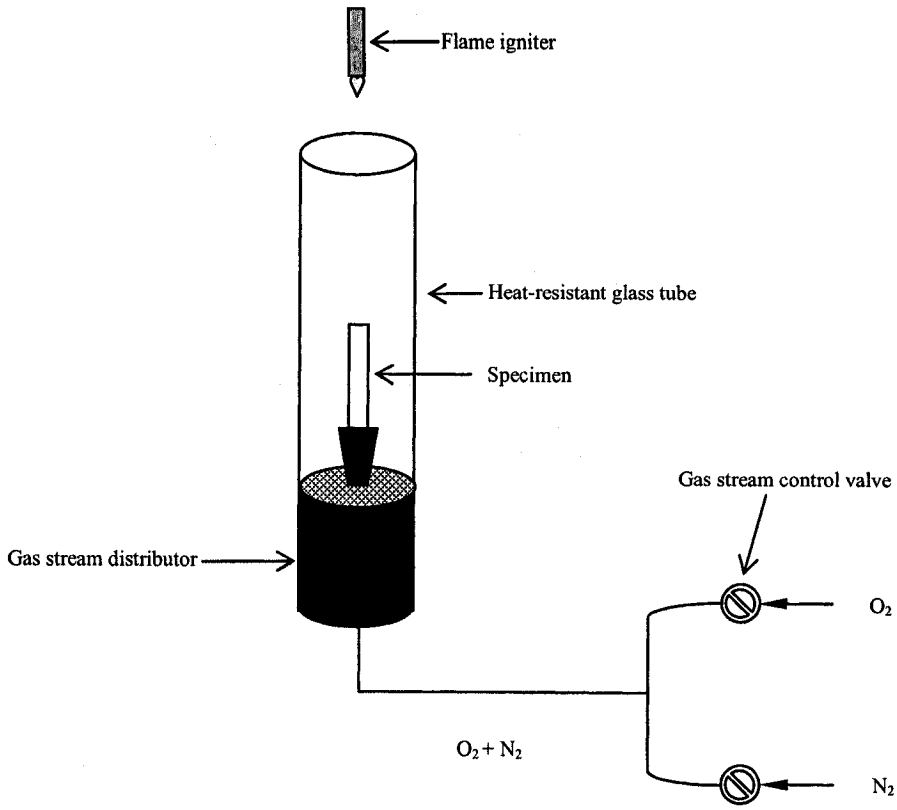

Figure 6. 2. Schematic Oxygen Index Equipment Layout

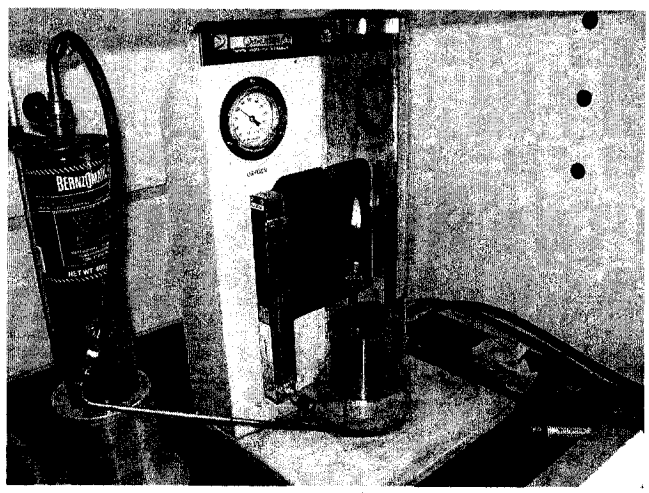

Figure 6. 3. Oxygen Index Measurement Equipment at CONCOM

6.1.2 Results and Analysis

The Limiting Oxygen Index is calculated by the following equation:

$$LOI = \frac{O_2}{O_2 + N_2}$$

where O_2 is the volume flow of oxygen and N_2 is the volume flow of nitrogen.

Three to five specimens were tested to asses the burning behavior. The calculated LOI of the specimens containing nanoclay of different contents is summarized in Table 6.1.

Table 6. 1. Limiting Oxygen Index Test Results

Nanoclay Content	LOI (%)
0 phr	31 ~ 32
2 phr	33 ~ 34
4 phr	35 ~ 36

Compared to the LOI values of other epoxy systems, the LOI value (0 phr) obtained in this investigation is evidently higher. In reference [66] and [67], the LOI values vary from 19 to 27.5, depending on the different epoxy systems. Thus, it indicates that the TGDDM/DDS system is more stable towards thermal oxidation.

Furthermore, the LOI increases with the introduction of nanoclay. The higher LOI values mean that more oxygen is required for sustained burning; therefore, the flammability has decreased. The pictures of the residue of burning are illustrated in

Figure 6.4. Obviously, the dimension of the residue (soot) is quite different for different specimens. The lengths of the residues are roughly 6mm, 25mm, and 40mm respectively. With the introduction of nanoclay, the residue becomes larger and also stronger, indicating that less material has been burnt away; hence, the flammability of the composites containing nanoclay decreases. The composites containing nanoclay are more stable under combustion conditions. The residue produced from the specimens containing nanoclay during combustion is a char reinforced by nanoclay. This kind of char plays the role of a barrier to fuel release, therefore, extends the combustion time of the composites.

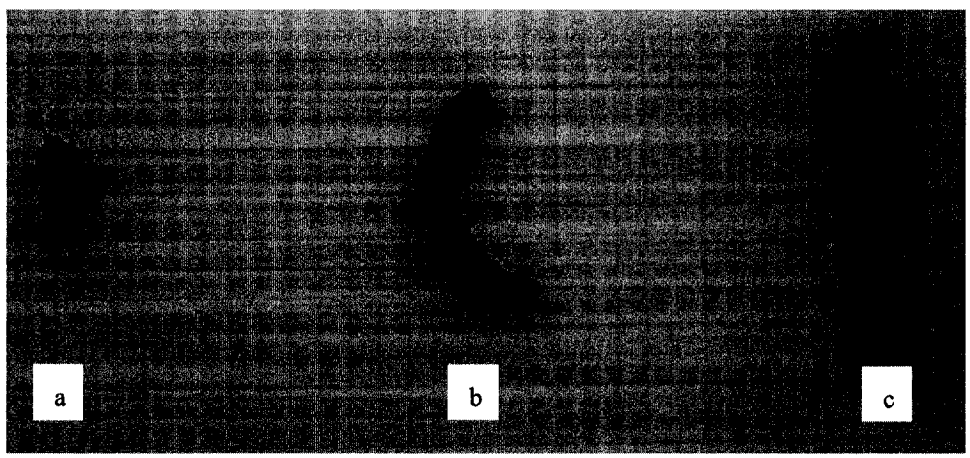

Figure 6. 4. Residue of Composites after LOI Tests (a) 0 phr, (b) 2 phr, (c) 4 phr

6.2 Investigation of Thermal Decomposition through TGA

Thermogravimetric Analysis (TGA) measures changes in mass of a sample with

increasing temperature. Mass loss can be measured in the course of the thermal decomposition by means of a thermobalance. A very tiny sample is placed on a sensitive balance extending into an oven that can be heated at different rates. A record actuated by the thermobalance depicts the mass change as a function of temperature.

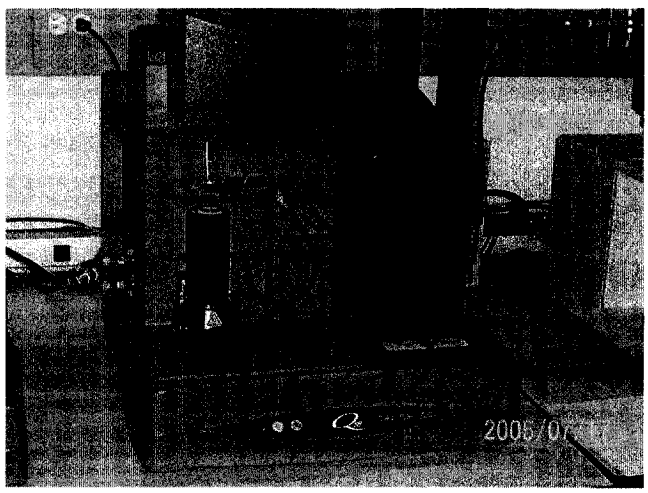

Figure 6. 5. TA-Q50 TGA System at CONCOM

The mass loss of the samples with different nanoclay content was investigated by TA-Q50 TGA System (Figure 6.5). All the tests were carried out in a N_2 atmosphere. Figure 6.6 illustrates that all the samples start decomposing from nearly 350 °C. After about 430 °C, the decomposing rate of the sample without nanoclay becomes faster than the one of nanoclay-filled samples. At 600 °C, the residues of the samples are 23.47%, 36.95%, and 37.05% of the initial weight for samples having nanoclay content of 0 phr, 2 phr, and 4 phr respectively. Obviously, the residue values of 2 phr and 4 phr samples at 600 °C are quite close, but they are almost 60% larger than the value of

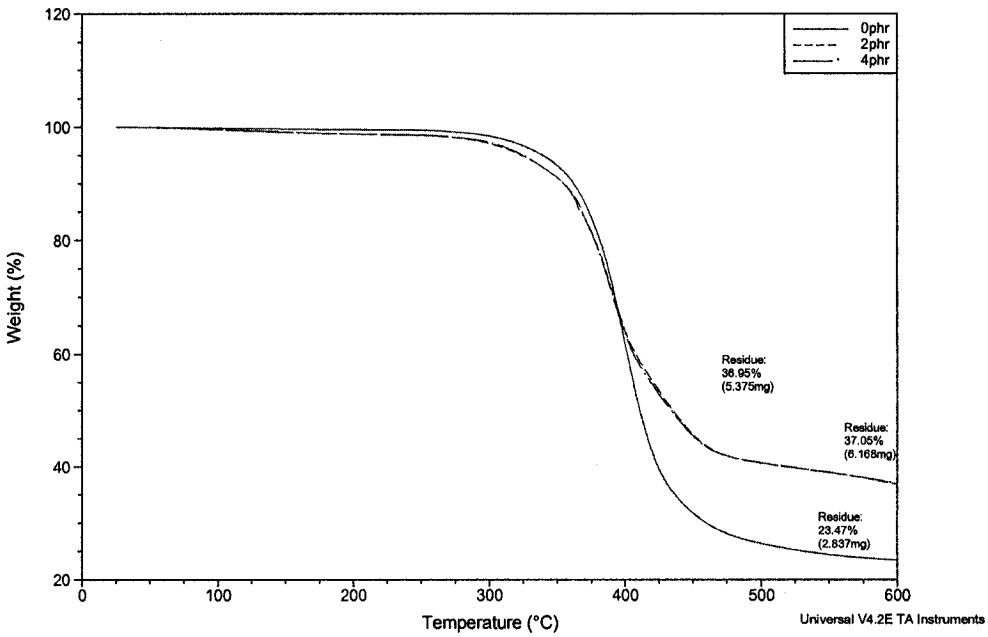

Figure 6. 6. Residue Weight of 0,2,4 phr Samples

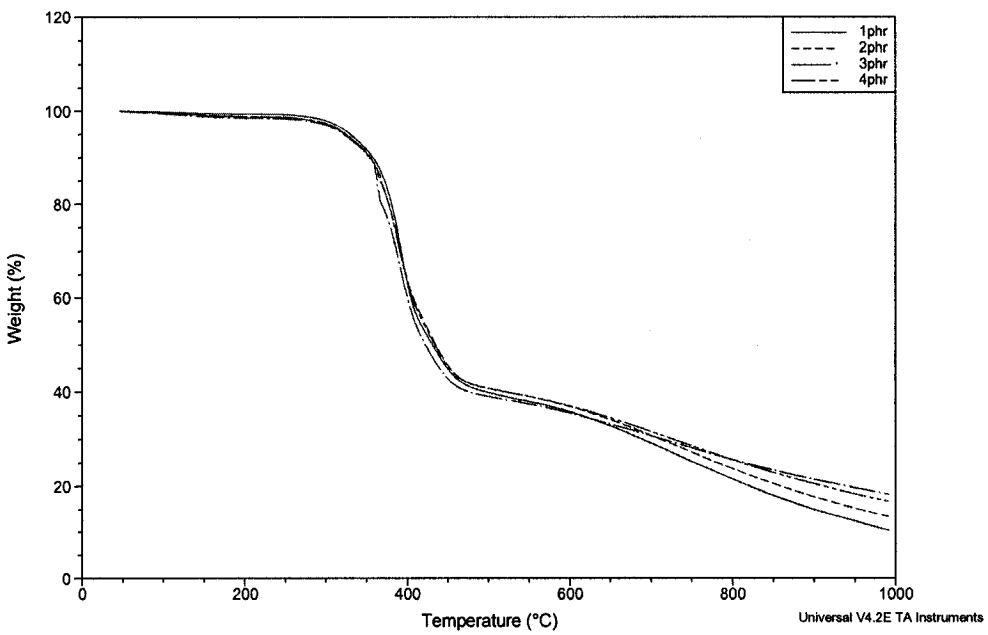

Figure 6. 7. TGA Curve of Nanoclay-Filled Samples

non-nanoclay-filled sample. Therefore, this experimental result also indicates that the flammability of the pristine epoxy composite has been reduced through the introduction of certain amount of nanoclay.

In Figure 6.7, the TGA curves of different samples (0 ~ 4 phr nanoclay) implies that the thermal or combustion behavior is quite similar, especially before 600 °C. At 1000 °C point, the residues are 10.32%, 13.38%, 16.78%, and 18.33% for 1, 2, 3, 4 phr samples, respectively. The original sample weight is 16.053 mg, 20.278 mg, 18.470 mg, and 16.650 mg. In fact, the ratios of clay in different samples are 0.99%, 1.96%, 2.91%, and 3.92% respectively. If we assume that nanoclay does not decompose during the test and deducted these numbers from the numbers above, the "real residues" will be 9.33%, 11.42%, 13.87%, and 14.41%. It seems that introduction of more nanoclay does not significantly increase the fire-resistance. Thus, we can say that a desired improvement of fire-resistance of epoxy composite can be obtained by means of adding of 1 or 2 phr I.30E nanoclay.

With respect to flammability, there are some characteristic temperatures of the decomposition. Among these points, the initial temperature (onset point) of the decomposition step plays an important role in the heat resistance of the composite. From Figures 6.8, 6.9, and 6.10, the initial temperatures of 0, 1, and 2 phr samples are 366.89 °C, 361.39 °C, and 354.72 °C, respectively.

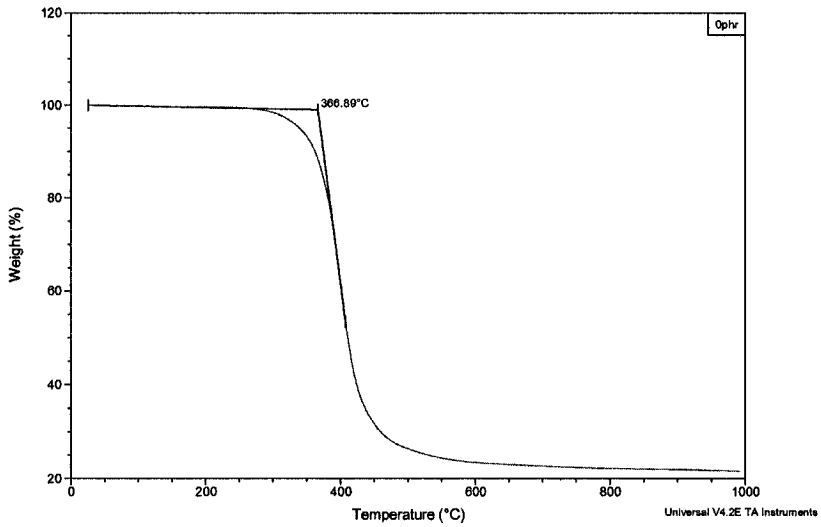

Figure 6. 8. Initial Decomposition Temperature of Pristine Epoxy Sample

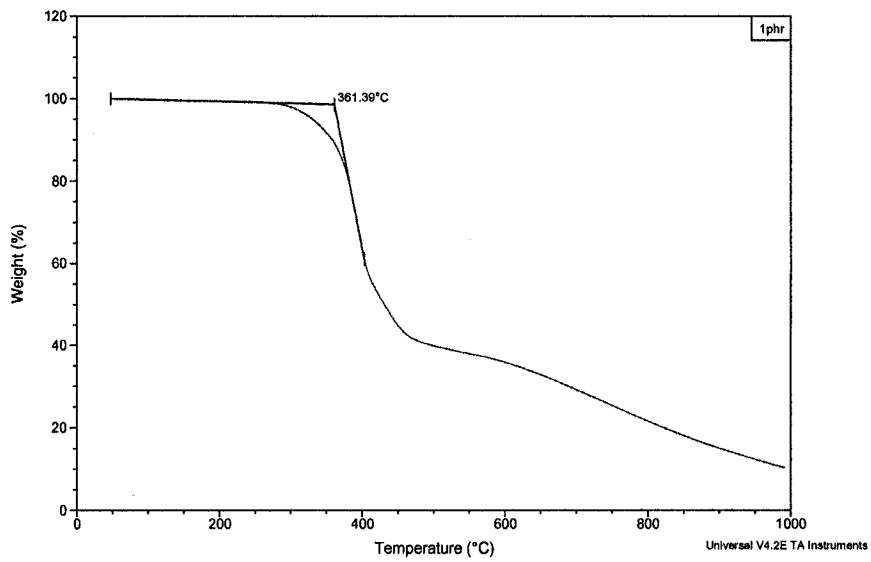

Figure 6. 9. Initial Decomposition Temperature of 1 phr Nanoclay Sample

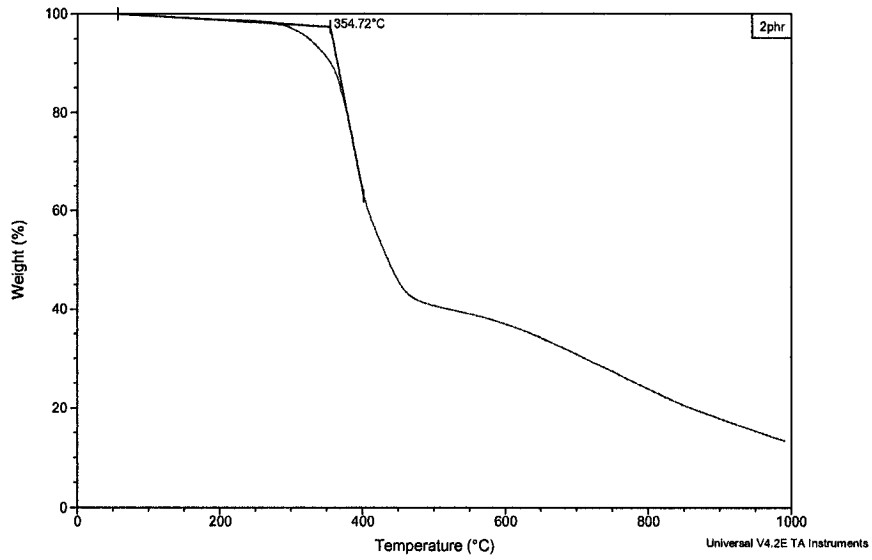

Figure 6. 10. Initial Decomposition Temperature of 2 phr Nanoclay Sample

Seemingly, the initial decomposition temperature slightly decreases with the introduction of nanoclay. This phenomenon might be caused by the improvement of the dynamic situation of the sample's combustion. The samples containing nanoclay may have more tiny voids, therefore provides more channels or surfaces for heat transmission, thus, the decomposition of the sample is initiated lightly earlier. Another possibility is that there might be more residual amines in the samples containing clay because those samples contain intercalants which contains amines. The existence of amine may facilitate the decomposition. However, the whole TGA curve still indicates that the heat resistance of nanoclay-filled samples has been improved because of the addition of nanoclay.

6.3 Thermal Shock Resistance Test

In practical applications, thermal shock resistance is an important property, especially in an environment where temperature changes dramatically. Usually, the brittle materials are particularly vulnerable to thermal shock due to their low toughness or low thermal conductivity.

Thermal shock occurs when a thermal gradient causes different parts of a material to expand by different amounts. This differential expansion can be equivalently understood in terms of stress or strain. At some point, this stress overcomes the strength of the material, causing a crack or microcrack. If nothing stops this crack or microcrack from propagating through the material, it will result in failure of the material.

The epoxy used in this project is brittle material, and it is often used in high temperature environment. Therefore, the investigation of its thermal shock resistance is a meaningful topic.

Thermal shock can be prevented by reducing the thermal gradient, reducing the material's coefficient of thermal expansion (CTE), or increasing its toughness etc. With respect to toughness, the plane-strain fracture toughness and interlaminar fracture toughness have been investigated in Chapter 5, concluding that fracture toughness of the composite is augmented with the introduction of nanoclay. Roughly, the nature of thermal shock phenomenon is fracture, thus a research clue can be obtained.

The non-nanoclay-filled and nanoclay-filled epoxy samples were preheated to a desired

temperature, then they were soaked in a liquid nitrogen bath (- 195.8 °C) for 1 minute. Next, the samples were reheated to the former elevated temperature (120 °C), following by soaking in liquid nitrogen again. Each sample was exposed to 3, 5, or 10 cycles until visible cracks appeared.

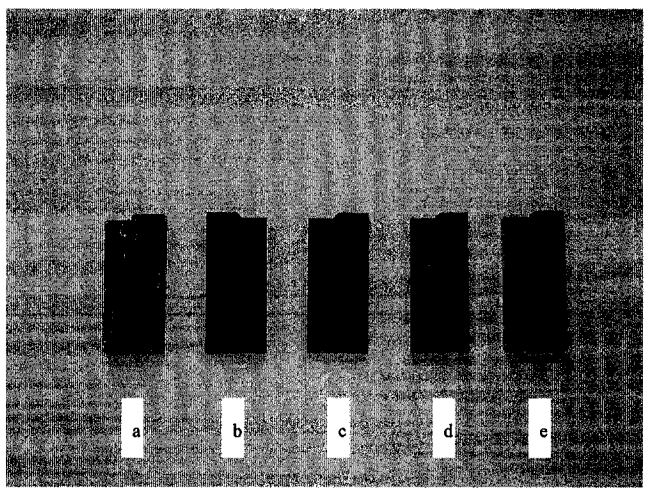

Figure 6. 11. Images of Samples Exposed to 3 Cycles of Thermal Shock Test. a-0phr, b-1phr, c-2phr, d-3phr, e-4phr.

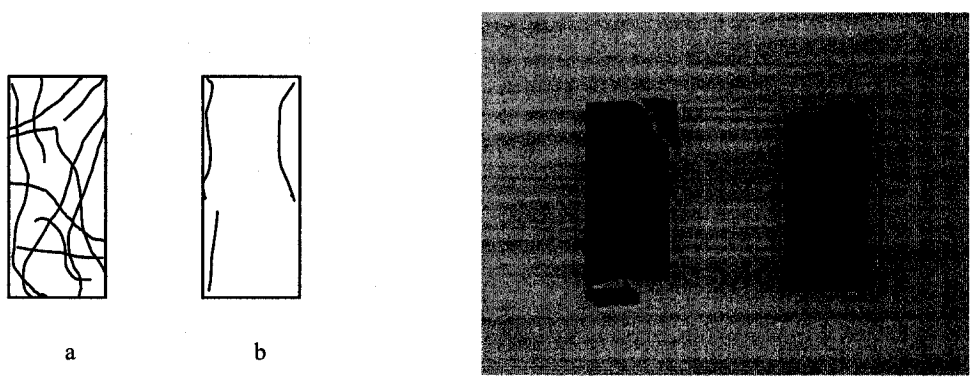

Figure 6. 12. Schematic Crack Density. (a) sample without nanoclay, (b) sample with nanoclay

The cracks were examined by a digital camera and optical microscope at × 50 and ×

500 magnifications. After three cycles of thermal tests, many cracks appeared in the samples without nanoclay. For the samples containing nanoclay, much less cracks were observed (Figures 6.11 and 6.12).

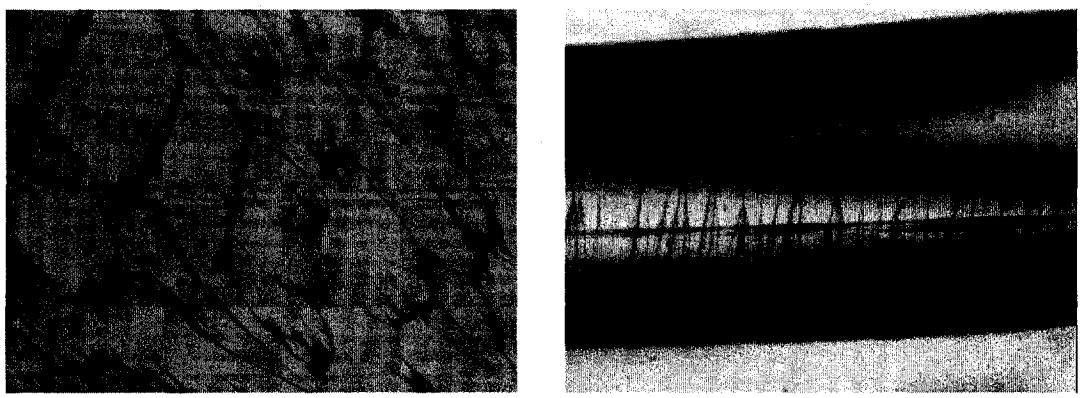

×50

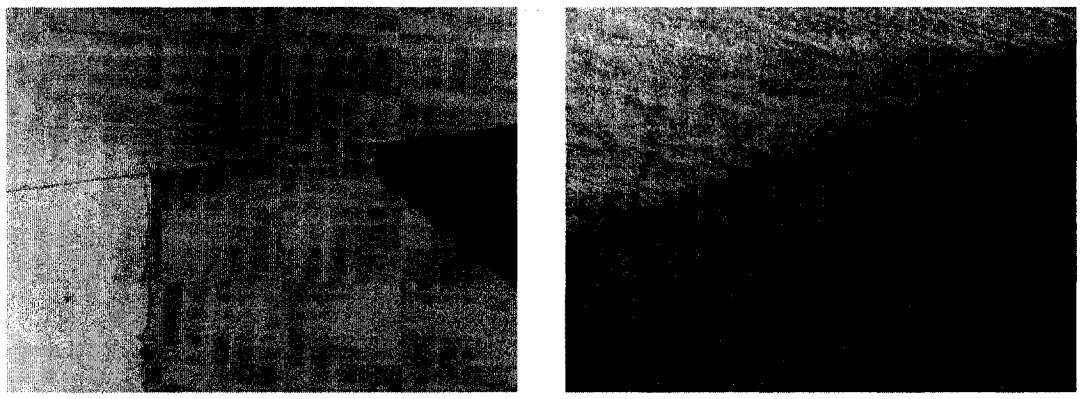

×500

Figure 6. 13. Optical Micrographs of Thermal Shock Sample without Nanoclay

By optical microscope, different types of cracks were observed in the sample without nanoclay (Figure 6.13). It appears that cracks propagate in any direction at random, having fish-scale shape or needle shape. On the contrary, there are fewer cracks observed

in samples containing nanoclay (Figure 6.14). The cracks in those samples are more

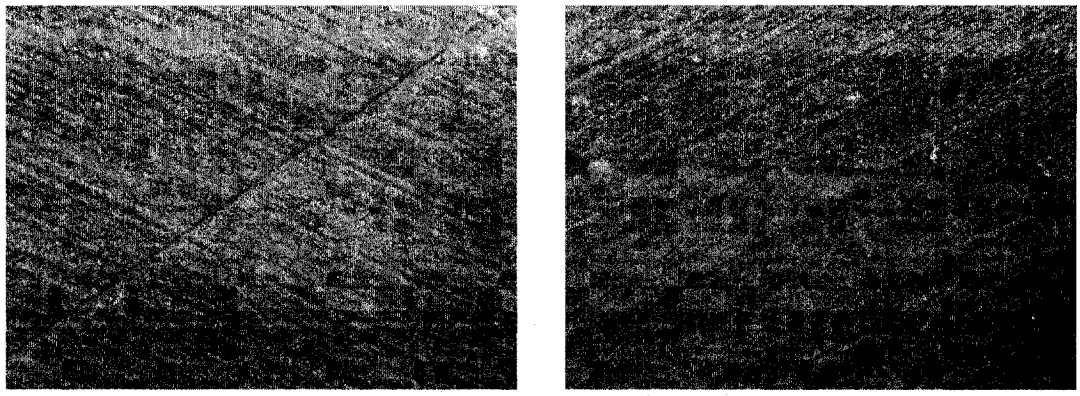

(a) ×500

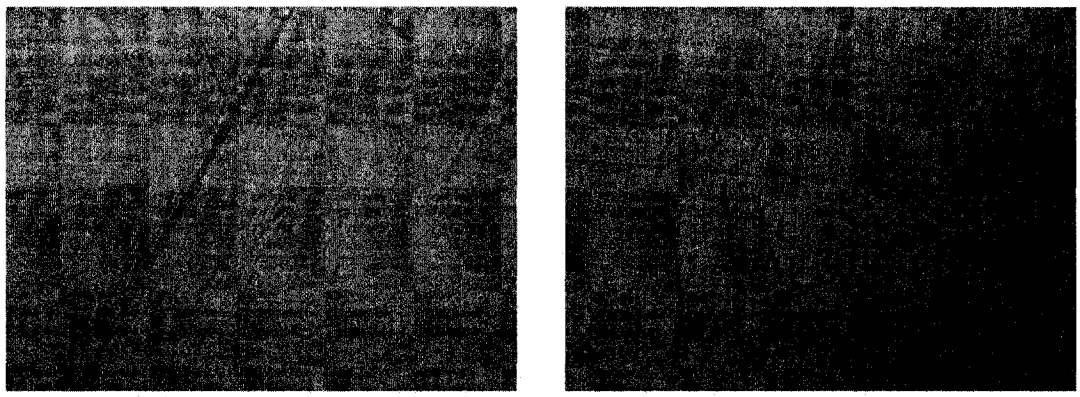

(b) ×500

Figure 6. 14. Optical Micrographs of Thermal Shock Sample Containing Nanoclay. (a) 2 phr clay, (b) 4 phr clay.

regular and have no evident large cracks. The thermal shock resistance was approximately evaluated by an index called crack density (Figures 6.12 and 6.15), which was counted over a certain area from the failed sample. Although the number may not cover all the cracks or microcracks, the variation with the naoclay contents is statistically significant.

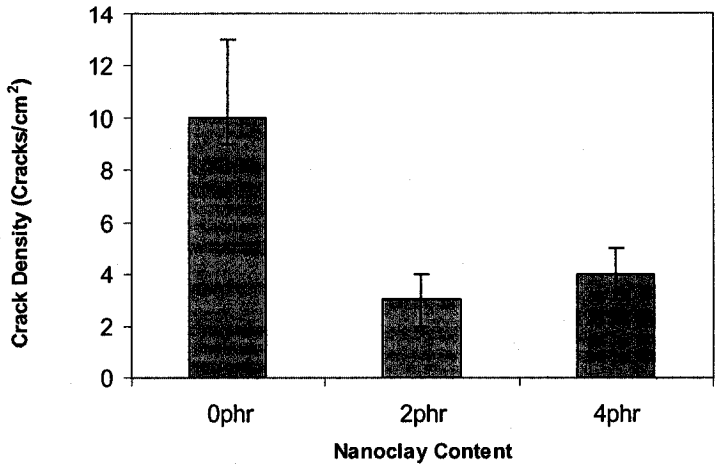

Figure 6. 15. Crack Density Variation with Nanoclay Content

With the introduction of nanoclay, the crack density decreased significantly. For samples containing 2 and 4 phr nanoclay, the variation is not significant. The increase of crack density, when 4 phr nanoclay was filled, might be caused by the relatively poorer dispersion of nanoclay or existing voids. Generally, the CTE of nanoclay-filled sample could be reduced, so the dimensional stability can be increased. Correspondingly, the thermal stress can be reduced.

The carbon fiber-reinforced samples also underwent thermal shock resistance tests. The following pictures (Figure 6.16) illustrate a few high magnification images of different samples. The fiber-reinforced samples underwent 10 cycles of thermal shock tests because there were no evident variation of crack when smaller number of cycles were carried out. Figure 6.16 (a) shows the cracks (or voids) resulted from thermal shock. For 2 and 4 phr samples, there were not large cracks observed, and there was no significant difference between those two nanoclay contents samples.

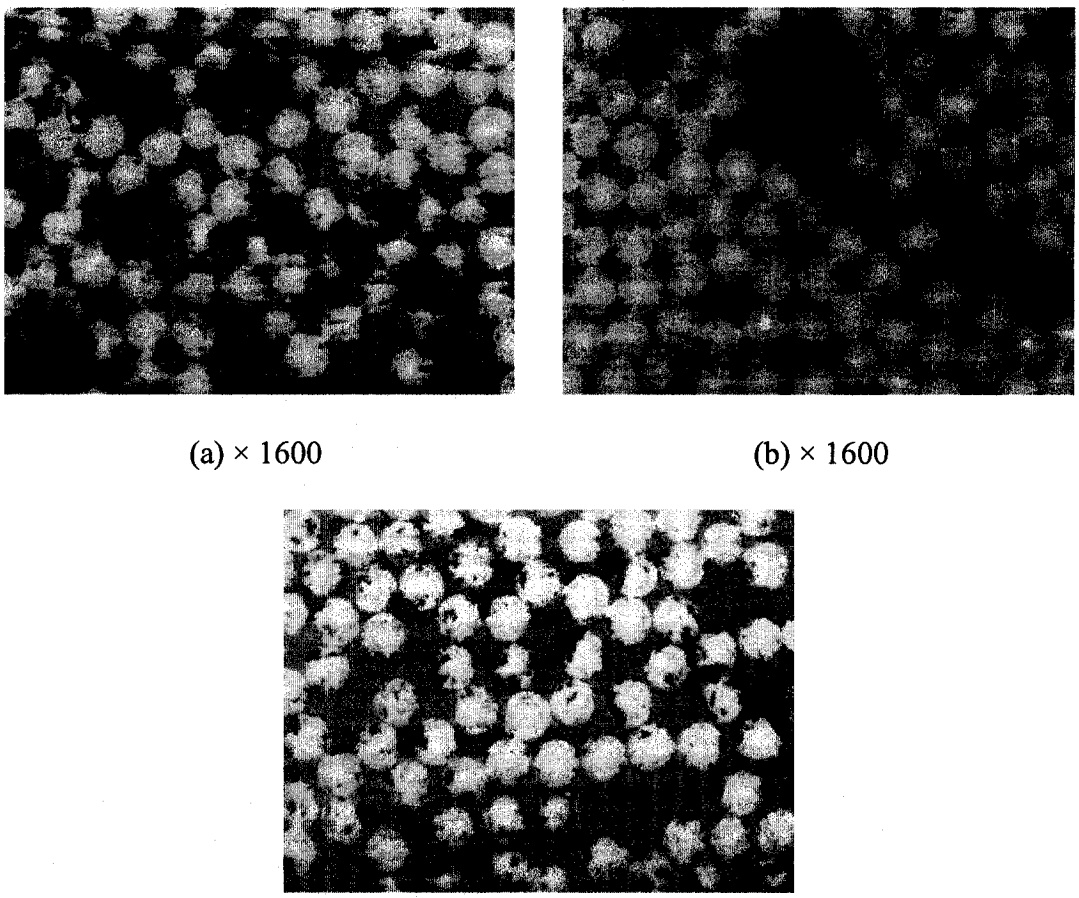

Figure 6. 16. Optical Micrograph of Carbon Fiber-Reinforced Samples after Thermal Shock Tests. (a) 0phr, (b) 2phr (c) 4phr.

The thermal shock test results of carbon fiber-reinforced samples are not as evident as the results of samples without fiber. The reasons may be: (1) there is less resin in fiber-reinforced samples, (2) carbon fiber has extremely low CTE.

6.4 Summary

Limiting Oxygen Index (LOI) of nanoclay-filled samples is higher as compared to the

control samples. TGA investigation shows that combustion residue of nanoclay-filled sample is evidently greater than non-filled sample. Thus, the heat or fire resistance of epoxy composite has been enhanced by means of adding certain amount of nanoclay. The introduction of nanoclay also evidently improved the thermal shock resistance of epoxy matrix nanocomposite.

Chapter 7 Conclusions, Contributions and Recommendations for Future Work

7.1 Conclusions

By means of a Microfluidizer, a high pressure mixing method was applied to the research of nanocomposites. The patented high pressure (up to 20000 psi, 138 MPa) mixing method [10] proved to be an effective way to mix Nanomer® I.30E nanoclay with acetone to obtain a nanoclay/acetone paste. This paste facilitated the dispersion of nanoclay into TGDDM epoxy system.

Viscosity of the TGDDM epoxy was obviously increased due to the addition of Nanomer® I.30E nanoclay. The increment was up to 179% and 165% with a nanoclay addition of 10 phr, when viscosity testing was performed at 50 °C and 75 °C respectively. To make clay-containing nanocomposites, a higher temperature was needed. Gel time becomes shorter owing to the introduction of nanoclay.

The DSC testing results indicate that nanoclay has no evident influence on the curing process of TGDDM/DDS system. Under the curing conditions used in this experiment, a high degree of cure (>94%) was obtained based on the tests results through DSC. DMA analysis indicated that the introduction of nanoclay did not lead to a drop in Tg, and it even makes an slight augmentation of storage modulus.

Resin film infusion (RFI) and solution methods were not feasible to manufacture carbon/TGDDM/nanoclay composites of good quality. The hot melt method was chosen

to impregnate fiber tapes. Lay-up and autoclave process were applied to fabricate the composite laminate. The quality of composite laminate was apparently improved after the process temperatures and pressure were appropriately modified. The laminate included fewer resin rich areas, fewer voids; more uniform laminate was obtained.

Through SENB tests, plain-strain fracture toughness nanoclay-filled TGDDM epoxy is augmented by 92.3%, 109.2%, 113.8%, and 106.2% for nanoclay content of 1 phr, 2 phr, 3 phr, and 4 phr respectively. In the meantime, strain energy release rate is augmented by 229.7%, 257.4%, 308.7%, and 308.7% respectively. Mode I interlaminar fracture toughness of unidirectional carbon fiber-reinforced composite was also increased by 52.6% and 85% with 2 and 4 phr nanoclay. The SEM image analysis illustrated that the fracture surface of nanoclay-filled specimen was much rougher than the fracture surface of neat epoxy specimen. This indicated that nanoclay absolutely contributed to the toughening mechanisms and the augmentation of fracture toughness. A small amount of nanoclay (2 phr) evidently contributes to the augmentation of flexural strength and modulus. However, more nanoclay does not change the experimental results any more.

Compared to the control samples, higher Limiting Oxygen Index (LOI) was obtained for the nanoclay-filled samples. TGA investigation showed that combustion residue of nanoclay-filled sample was larger and stronger than the residue of non-filled sample. The heat or fire resistance of epoxy composite was enhanced by adding certain amount of nanoclay. The introduction of nanoclay also evidently improved the thermal shock resistance of epoxy matrix nanocomposite.

7.2 Contributions

- ❖ The variation of the viscosity of TGDDM/Nanoclay system and the gel time of TGDDM/DDS/Nanoclay with the nanoclay content was found.
- ❖ The influence of nanoclay on the curing process, Tg, and modulus of TGDDM/DDS system was determined by DSC and DMA thermal analysis.
- ❖ Reliable parameters of the manufacturing of carbon-fiber-reinforced/epoxy/ nanoclay-filled composites were determined and can guarantee good quality of the nanocomposites.
- ❖ The effect of nanoclay to the Plain-Strain Fracture Toughness and Strain Energy Release Rate of Composites was further proved to be quite evident. The addition of nanoclay will enhance the mechanical properties. The relationship between the Mode I Interlaminar Fracture Toughness of Unidirectional Carbon Fiber-Reinforced Composite and the addition amount of nanoclay was obtained by mechanical testing and microscopy. The relationship between flexural properties and nanoclay loading was determined.
- ❖ Through LOI tests and TGA analysis, the thermal and combustion phenomena of clay-filled naocomposites were observed and analyzed.

7.3 **Recommendations for Future Work**

Based on the research results in this project, suggestions relating the future work in this field are depicted as follows:

a) Investigate the viscosity of TGDDM/Nanoclay system at higher temperature (>75 °C),

b) Investigate the variation of viscosity during curing process,

c) Use a mixture of TGDDM epoxy with other epoxy or other thermosetting materials to improve the flowability and practicability of resin system,

d) Find a feasible method to make nanoclay-containing epoxy prepreg to obtain nanocomposite of better quality,

e) Use crack gauge to determine crack propagation for more precise result,

f) Investigate fire resistance and combustion phenomenon by optical methods,

g) Make more attempts to Resin Film Infusion (RFI) method,

h) Investigate impact properties of nanocomposites.

References

1. M. M. Schwartz. Composite Materials Handbook, McGraw-Hill (1992).
2. Carbon Fiber Race Car Technology Hits the Streets, High-Performance Composites, 52, July (2005.)
3. L.A.Utracki. Clay-Containing Polymeric Nanocomposites. Volume1. Rapra Technology (2004)
4. W.P. Liu. Epoxy-Clay Nanocomposites for Structural Applications, PhD Thesis, Concordia University (2005).
5. F.C. Campbell. Manufacturing Processes for Advanced Composites, Elsevier (2004).
6. K. Jang, W.J. Cho, C.S. Ha. "Influence of processing method on the fracture toughness of thermoplastic-modified, carbon-fiber-reinforced epoxy composites", *Composites Science and Ttechnology*, 59, 995-1001 (1999).
7. B. Ellis. Chemistry and Technology of Epoxy Resins, Blackie Academic & Professional (1993).
8. W.P. Liu, S.V. Hoa, M. Pugh. "Fracture toughness and water uptake of high-performance epoxy/nanoclay nanocomposites", *Composites Science and Technology,* 65, 2364-2373 (2005).
9. W.P. Liu, S.V. Hoa, M. Pugh. "Organoclay-modified high performance epoxy nanocomposites", *Composites Science and Technology,* 65, 307-316 (2005).
10. Hoa S.V, Liu W.P, Pugh M and Ton-That M-T. "Method and system for making high

performance epoxies and high performance epoxies obtained herein", Patent: PCT/CA 2004/002184.

11. M. Alexandre, P. Dubois. "Polymer-layered silicate nanocomposites: preparation, properties and uses of a new class of materials," *Materials Science and Engineering*, 28 (2000) 1-63.
12. J.H. Koo and L. A. Pilato. "Polymer Nanostructured Materials for High Temperature Applications", *SAMPE Journal*, Vol.41, No.2, 7-19(2005).
13. T.P. Mohan, M.R. Kumar and R. Velmurugan. "Rheology and curing characteristics of epoxy-clay nanocomposites," *Polymer International,* 54 (2005) 1653-1659.
14. C. Chen and D. Curliss. "Processing and morphological development of montmorillonite epoxy nanocomposites", *Nanotechnology*, 14, 643-648 (2003).
15. N. A.St. John, G.A. George, P.A. Cole-Clarket, M.E. Mackay and P.J. Halley. "The effect of impurities on gel times for TGDDM epoxy resins cured with DDS", *High Performance Polymer*, 5, 21-36 (1993).
16. G.Z. Liang, D. Wang. "High-Performance Bismaleimide Resin for Resin Film Infusion", *Polym-Plast. Technol. Eng*, 41(2), 285-295 (2002).
17. G. Zhou, L.J. Lee. "Nano-Clay And Long Fiber Reinforced Composites Based on Epoxy and Phenolic Resins", *ANTEC*, 2094-2098 (2003).
18. H.F. Xie, B.H. Liu, Z. Yuan, J.Y. Shen, R.S. Cheng. "Cure Kinetics of Carbon Nanotube/Tetrafunctional Epoxy Nanocomposites by Isothermal Differential Scanning Calorimetry", *Journal of Polymer Science: Part B*, Vol.42, 3701-3712

(2004).

19. K. Wang, L. Wang, J.S Wu, L. Chen, C.B He. "Preparation of Highly Exfoliated Epoxy/Clay Nanocomposites by 'Slurry Compounding':Process and Mechanisms", *Langmuir*, 21, 3613-3618 (2005).
20. W.P. Liu, S.V. Hoa and M. Pugh. "Augmentation of Fracture Toughness of Modified Epoxy using Nanoclay", *Canada-Japan Workshop on Composites*, Destech, August (2004).
21. T. G. Gutowski. Advanced Composites Manufacturing, John Wiley & Sons (1997).
22. S.G. Advani and E.Murat. Sozer. Processing Modeling in Composites Manufacturing, Marcel Dekker (2003).
23. S.K. Mazumdar. Composites Manufacturing (Materials, Products, and Process Engineering), CRC Press (2002).
24. G.O. Shonaike and S.G. Advani. Advanced Polymer Materials (Structure Property Relationships), CRC Press (2003).
25. M. Biron. Thermosets and Composites: Technical Information for Plastics Users, Elsevier (2004).
26. J.P.H. Sautereau, J. Verdu, and R.J.J. Williams. Thermosetting Polymers, Marcel Dekker (2002).
27. A.A. Askadskii. Physical Properties of Polymers (Prediction and Control), Gordon & Breach (1996).
28. L.H. Sperling. Polymeric Multicomponent Materials, JOHN WILEY& SONS, INC

(1997).

29. D.F. Adams, L.A. Carlsson and R.B. Pipes. Experimental Characterization of Advanced Composite Materials, CRC Press (2003).
30. S.T. Peters. Handbook of Composites, CHAPMAN&HALL (1998).
31. A.D. Pomogailo and V.N. Kestelman., Metallopolymer Nanocomposites, Springer (2005).
32. K. Friedrich, S. Fakirov and Z. Zhang. Polymer Composites (From Nano- to Macro-Scale), Springer (2005).
33. N. L. Han, S S.Suh, J.M. Yang, H. T. Hahn. "Resin film infusion of stitched stiffened composite panels", *Composites: Part A*, 34, 227-236 (2003).
34. B. Qi, J. Raju, T. Kruckenberg, R. Stanning. "A resin film infusion process for manufacture of advanced composite structures", *Composite Structure*, 47, 471-476 (1999).
35. "Resin film infusion-composites cost reducer", *Reinforced Plastics*, 44-49, February (2002).
36. J.C. Fielding, Lt. Allison Jacques. "Vacuum Infusion Processes fro Nano-Modified Aerospace Epoxy Resins", *SAMPE* (2004).
37. A.C. Caba, D. Ratazzi, R. Batra, A.C. Loos. "Verification of a Simulation Model for Resin Film Infusion of Complex Shaped Composite Structures", *Journal of Reinforced Plasitcs and Composites,* Vol. 18, No.16, 1465-1477 (1999).
38. A.C. Caba, A.C. Loos, D. Ratazzi, R. Batra. "A three-dimentional simulation model

of the resin film infusion manufacturing process", *30th international SAMPE Technical Conference,* October 20-24, 1998.

39. D. Ratna, N.R. Manoj, R. Varley. "Clay-reinforced epoxy nanocomposites," *Polymer International,* 52: 1403-1407 (2003).
40. C. Guo, C.T. Sun. "Dynamic Mode-I Crack-Propagation in a Carbon/Epoxy Composite", *Composites Science and Ttechnology*, 58, 1405-1410 (1998).
41. B.Y. Park, S.C. Kim, B. Jung. "Interlaminar Fracture Toughness of Carbon Fiber/Epoxy Composites using Short Kevlar Fiber and/or Nylon-6 Powder Reinforcement", *Polymers for Advanced Technologies*, Vol.8, 371-377 (1996).
42. R.P. Singh, M. Zhang, D. Chan. "Toughening of a brittle thermosetting polymer: effects of reinforcement particle size and volume fraction," *Journal of materials Science,* 37 (2002) 781-788.
43. K. Oguni, G. Ravichandran. "A Micromechanical Failure Model for Unidirectional Fiber Reinforced Composites", *International Journal of Solids and Structures,* 38, 7215-7233 (2003).
44. T.K. O'Brien and R.H. Martin. "Round robin testing for mode I interlaminar fracture toughness of composite materials," *Journal of composites technology and research,* Vol.15, No.4, 1993, p269-281.
45. M. Hojo, S. Mtsuda, M. Tanaka, S. Ochiai, A. Murakami. "Mode I delamination fatigue properties of interlayer-toughened CF/epoxy laminates," *Composites science and technology,* 66(2006) 665-675.

46. T.K. O'Brien, "Interlaminar fracture toughness: the long and winding road to standardization," *Composites Part B 29B*, (1998) 57-62.

47. A.C. Garg. "Failure mechanisms in toughened epoxy resins–A review," *Composites Science And Technology*, 31 (1998) 179-23.

48. P. Davies, H.H. Kausch, J.G. Wiliams, A.J. Kinloch, M.N. Charalambides, A. Pavan, D.R. Moore, R. Prediger, I. Robinson, N. Burgoyne, K. Friedrich, H. Wittich, C.A. Rebelo, A.T. Marques, F. Ramsteiner, B. Melve, M. Fischer, N. Roux, D. Martin, P. Czarnocki, D. Neville, I. Verpoest, B. Goffaux, R. Lee, K. Walls, N. Trigwell, I. K. partridge, J. Jaussaud, S. Anadersen, Y. Giraus, G. Hale, G. Mcgrath. "Round-robin interlaminar fracture testing of carbon-fibre-reinforced epoxy and PEEK composites," *Composites science and technology,* V.43, No.2, 1992, p129-136.

49. L. Chen, S.C. Wong, S. Pisharath. "Fracture properties of nanoclay-Filled Polypropylene", *Journal of Applied polymer Science,* Vol.88, 3298-3305(2003).

50. J.W. Gilman, T. Kashiwagi. "Flammability of polymer clay nanocomposites consortium : year one annual report". United States Department of Commerce, July 2000.

51. S.V. Levchik and E.D. Weil. "Thermal decomposition, combustion and flame-retardancy of epoxy resins–a review of the recent literature," *Polymer International* 53: 1901-1929 (2004).

52. A.B. Morgan, R. H. Harris, T. Kashiwagi, L.J. Chyall, J.W. Gilman. "Flammability of Polystyrene Layered Silicate (Clay) Nanocomposites: Carbonaceous Char

Formation", *Fire and Materials,* 26, 247-253 (2002).

53. S. Duquesne, C. Jama, M.Le. Bras, R. Delobel, P. Recourt, J.M. Gloaguen. "Elaboration of EVA-nanoclay systems-characterization, thermal behavior and fire performance", *Composites Science and Technology,* 63, 1141-1148 (2003).
54. J. Zhang, C.A. Wilkie. "Preparation and flammability properties of polyethylene-clay nanocomposites", *Polymer Degradation and Stability,* 80, 163-169 (2003).
55. J.F. Timmerman, B.S. Hayes, J.C. Seferis. "Nanoclay reinforcement effects on the cryogenic microcracking of carbon fiber/epoxy composites", *Composites Science and Technology*, 62, 1249-1258 (2002).
56. P. Bahadur, N.V. Sastry. Principle of Polymer Science, CRC Press (2002).
57. R.O. Ebewele. Polymer Science and Technology, CRC Press (2000).
58. B.T. Astrom. Manufacturing of Polymer Composites, Chapman & Hall (1997).
59. G.H. Michler and F.J. Balta-Calleja. Mechanical Properties of Polymers Based on Nanostructure and Morphology, Taylor & Francis (2005)
60. ASTM D5045-99. "Standard Test Method for Plane-Strain fracture Toughness and Strain Energy Release Rate of Plastic Materials", *Annual Book of ASTM Standards*, Vol 08.03, 351-359 (2002).
61. J.K. Kim and Y.W. Mai. Engineered Interfaces in Fiber Reinforced Composites, Elsevier (1998).
62. A.P. Mouritz, L.K. Jain. "Further validation of the Jain and Mai models for interlaminar frature of stitched composites", *Composites Science and Technology* 59

(1999) 1653-1662.

63. C.R. Chiang. "Prediction of the fracture toughness of fibrous composites", *Journal of materials Science* 35 (2000) 3161-3166.

64. I.M. Daniel and O. Ishai. Engineering Mechanics of Composite Materials, Oxford University Press, (1994).

65. ASTM D5528-01. "Standard Test Method for Mode I Interlaminar Fracture Toughness of Unidirectional Fiber-reinforced Polymer matrix Composites", *Annual Book of ASTM Standards*, Vol 15.03, 292-302(2002).

66. G. Pal and H. Macskasy. Plastics - Their behavior in fires, Elsevier (1991).

67. B.K. Kandola, A.R. Horrocks, P. Myler, D. Blair. "New developments in flame retardancy of glass-reinforced epoxy composites," *Journal of Applied polymer Science,* Vol. 88, 2511-2521 (2003)

Appendix

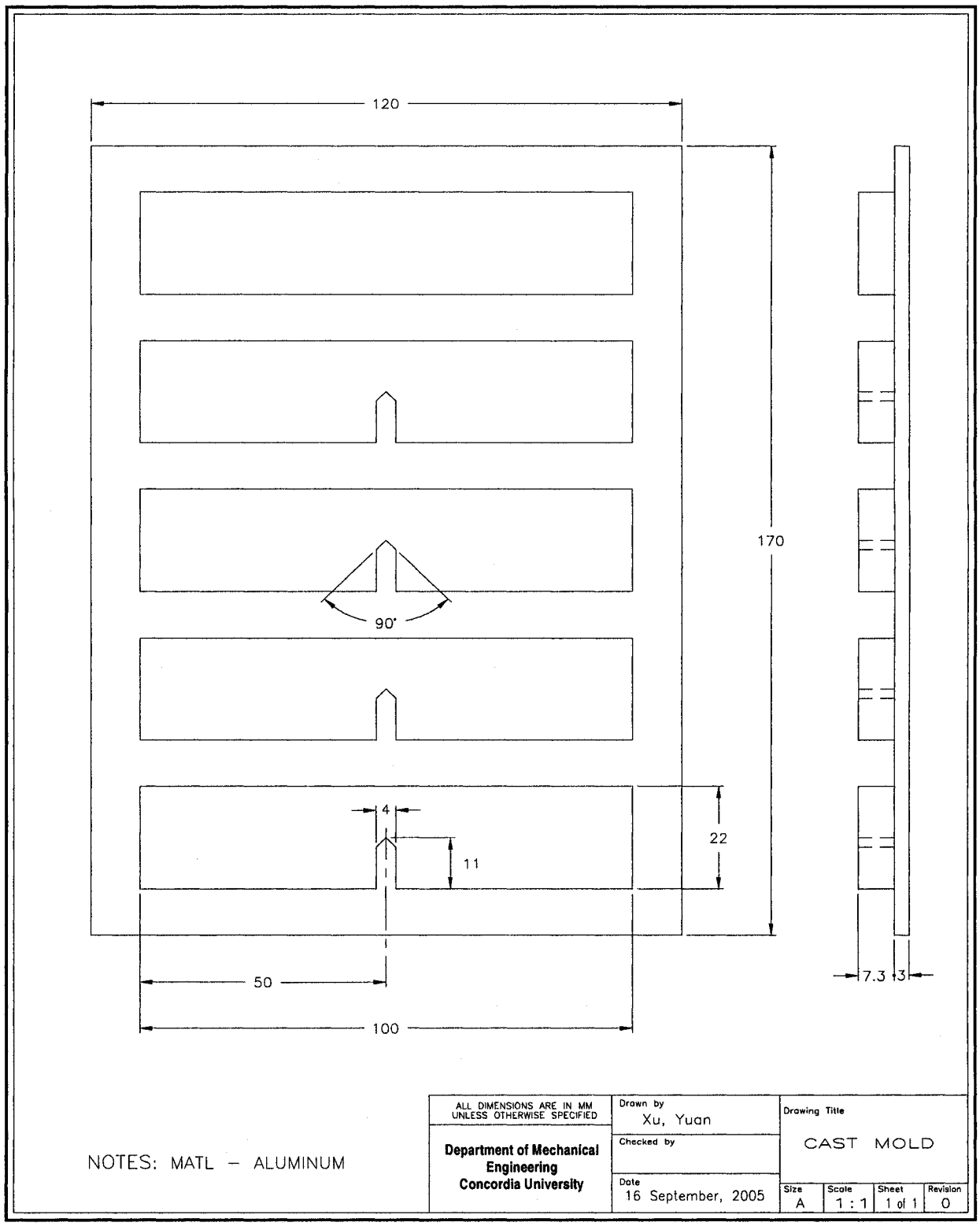
120
170
90°
4
11
22
50
100
7.3
3
NOTES: MATL – ALUMINUM
ALL DIMENSIONS ARE IN MM UNLESS OTHERWISE SPECIFIED
Department of Mechanical Engineering
Concordia University
Drawn by
Xu, Yuan
Checked by
Date
16 September, 2005
Drawing Title
CAST MOLD
Size
A
Scale
1 : 1
Sheet
1 of 1
Revision
0